

HY5 and phytochrome activity modulate shoot to root coordination during thermomorphogenesis

Christophe Gaillochet^{1*}, Yogev Burko^{1,3}, Matthieu Pierre Platre¹, Ling Zhang¹, Jan Simura⁴, Björn Willige¹, S Vinod Kumar⁵, Karin Ljung⁴, Joanne Chory^{1,3}, Wolfgang Busch^{1,2}

¹ Plant Biology Laboratory, Salk Institute for Biological Studies, 10010 N Torrey Pines Rd, La Jolla, CA 92037, USA

² Integrative Biology Laboratory, Salk Institute for Biological Studies, 10010 N Torrey Pines Rd, La Jolla, CA 92037, USA.

³ Howard Hughes Medical Institute, Salk Institute for Biological Studies, La Jolla, CA 92037, USA

⁴ Umeå Plant Science Centre, Department of Forest Genetics and Plant Physiology, Swedish University of Agricultural Sciences, SE-901 83 Umeå, Sweden

⁵ Department of Biosciences College of Life and Environmental Sciences, Stocker Road, Exeter EX4 4QD, United Kingdom

* Present address: Center for Plant Systems Biology, VIB, 9052 Ghent, Belgium

Correspondence and requests for materials should be addressed to W.B. (email:wbusch@salk.edu)

Running title:

Control of root thermomorphogenesis

Keywords:

Root development, temperature, thermomorphogenesis, phytochromes, HY5

Summary statement:

A shoot signaling-module involving HY5 and phytochromes modulates coupling between shoot and root thermomorphogenesis. Auxin biosynthesis and signaling constitute an additional regulatory axis controlling root growth response to higher temperature.

Abstract:

Temperature is one of the most impactful environmental factors to which plants adjust their growth and development. While the regulation of temperature signaling has been extensively investigated for the aerial part of plants, much less is known and understood about how roots sense and modulate their growth in response to fluctuating temperatures. Here we found that shoot and root growth responses to high ambient temperature are coordinated during early seedling development. A shoot signaling module that includes HY5, the phytochromes and the PIFs exerts a central function in coupling these growth responses and maintain auxin levels in the root. In addition to the HY5/PIF-dependent shoot module, a regulatory axis composed of auxin biosynthesis and auxin perception factors controls root responses to high ambient temperature. Together, our findings show that shoot and root developmental responses to temperature are tightly coupled during thermomorphogenesis and suggest that roots integrate energy signals with local hormonal inputs.

1 Introduction

2 Over the course of their life, plants are subjected to constant environmental fluctuations.
3 Consequently, plants have evolved tremendous developmental plasticity that allows them to
4 precisely adjust their development to environmental conditions and therefore to thrive in
5 dynamically and often unpredictably changing environments. In particular, the early stage of
6 seedling development constitutes a critical moment at which plants need to sense their
7 environment and respond quickly to fine-tune their developmental programs and successfully
8 establish themselves as autotrophic seedlings (reviewed in (Ha et al., 2017)). Not surprisingly,
9 early life stages have been shown to strongly contribute to local acclimation (reviewed in
10 (Donohue et al., 2010)).

11 Temperature is a pervasive environmental parameter influencing biological systems at all scales
12 from the rate of biochemical reactions to the timing of developmental transitions (reviewed in
13 (Penfield, 2008)). In addition, temperature shows important geographical, diurnal as well as
14 seasonal variation. Importantly, plants are equipped with sophisticated molecular machineries to
15 perceive temperature fluctuations, which allows them to sense and translate these signals into
16 appropriate developmental responses. Accordingly, raising ambient temperature leads to
17 increased elongation of the hypocotyl and root –a process called thermomorphogenesis
18 (reviewed in (Quint et al., 2016)).

19 The molecular mechanisms underlying shoot thermo-responses have been largely investigated
20 (Quint et al., 2016). In this context, the photoreceptor Phytochrome B (phyB) enables perception
21 of higher ambient temperature by switching from an active to an inactive form (Legris et al.,
22 2016). This process of phytochrome thermal reversion subsequently prevents sequestration and
23 degradation of transcription factors such as the PHYTOCHROME INTERACTING FACTORS
24 (PIFs) that can accumulate and promote the expression of downstream regulatory genes (Jung
25 et al., 2016; Kumar et al., 2012; Park et al., 2018).

26 Among the PIF clade, PIF4 acts as a central signalling hub during shoot thermomorphogenesis
27 (Quint et al., 2016; Koini et al., 2009) and recent studies showed that PIF7 also has a role in this
28 process (Chung et al., 2020; Fiorucci et al., 2020). Upon higher ambient temperature, PIF4
29 directly positively regulates the expression of a battery of genes including auxin biosynthetic
30 genes *YUCCA8* (*YUC8*) and *TRYPTOPHAN AMINOTRANSFERASE OF ARABIDOPSIS1*
31 (*TAA1*), thereby promoting an elevation of auxin levels and increased hypocotyl cell elongation
32 (Franklin et al., 2011; Sun et al., 2012). This regulatory circuit also integrates inputs from the
33 transcription factor *LONG HYPOCOTYL5* (*HY5*) that can act antagonistically to PIF4 by
34 repressing *PIF4* expression or by directly regulating key PIF4 target genes including *YUC8*
35 (Delker et al., 2014; Gangappa and Kumar, 2017). Both *HY5* and *PIF4* expression levels and
36 protein abundance are tightly regulated by a plethora of factors (reviewed in (Lau and Deng,

37 2012; Quint et al., 2016)). Among those, CONSTITUTIVE PHOTOMORPHOGENESIS
38 PROTEIN1 (COP1) and DEETIOLATED1 (DET1) trigger HY5 degradation and promote both
39 *PIF4* expression and protein stabilization (Gangappa and Kumar, 2017; Osterlund et al., 2000;
40 Saijo et al., 2003; Yanagawa et al., 2004). The collective genetic activity of *PIF4*, *HY5*, *COP1*
41 and *DET1* defines an intertwined regulatory module that acts at the interface between light and
42 temperature signalling (Delker et al., 2014; Gangappa and Kumar, 2017). Interestingly, HY5
43 protein has also been shown to translocate from the shoot to the root and to coordinate carbon
44 fixation with nitrogen uptake (Chen et al., 2016).

45 Importantly, roots can autonomously sense and respond to temperature (Bellstaedt et al., 2019),
46 which might allow them to reach deeper and cooler layers of the soil under warm surface
47 conditions (Illston and Fiebrich, 2017). However, in contrast to the shoot, the molecular
48 mechanisms underlying plant root thermo-responses have so far remained elusive. Similar to
49 the shoot, maintenance of auxin homeostasis is critical for the root response to temperature
50 (Wang et al., 2016). In line with this idea, auxin signaling increases upon perception of higher
51 ambient temperature (Hanzawa et al., 2013; Wang et al., 2016). In this context the auxin efflux
52 transporters PIN2 and PILS6 mediate auxin transport and local accumulation at the root, which
53 in turn triggers developmental response to temperature in the root (Feraru et al., 2019;
54 Hanzawa et al., 2013). Furthermore, the auxin receptors TIR1 and AFB2 are stabilized upon
55 increased ambient temperature by forming a protein complex with HEAT SHOCK PROTEIN 90
56 (HSP90) and its co-chaperone SUPPRESSOR OF G2 ALLELE SKP1 (SGT1). The
57 accumulation of TIR1 and AFB2 subsequently activates auxin signaling and mediates root
58 thermo-sensory elongation (Wang et al., 2016).

59 Although root and shoot thermomorphogenesis occur simultaneously during early seedling
60 development (Bellstaedt et al., 2019), it is still unclear whether these responses are coordinated
61 at the whole plant level. In this study, we leveraged a genetic approach combined with
62 comprehensive phenotypic analyses, transcriptional profiling and metabolic measurements to
63 further characterize the molecular circuits mediating root thermomorphogenesis. We found that
64 a shoot regulatory module including HY5, phytochromes and PIFs can also regulate the root
65 growth response upon perception of higher ambient temperature, demonstrating that shoot and
66 root growth responses are coupled during early seedling development. Furthermore, we show
67 that an additional regulatory axis composed of auxin biosynthesis and perception genes is
68 required during root thermomorphogenesis and propose that the relative abundance of auxin
69 and its downstream signaling activity in the shoot and in the root are critical to coordinately
70 control growth response to temperature in these organs.

71

72 Results

73

74 *HY5* controls the root thermo-response

75 The impact of increased temperature on plant development has been extensively investigated
76 (reviewed in (Quint et al., 2016)), however it is still unclear whether a core regulatory network
77 governs temperature sensing and signalling in multiple developmental contexts and whether
78 these responses are coordinated across multiple organs. To assess how ambient temperature
79 modulates root development, we grew plants at 21°C and analyzed their growth until three days
80 after transfer at either 21°C or 27°C. In line with previous reports (Feraru et al., 2019; Martins et
81 al., 2017; Wang et al., 2016), wild type plants grown at 27°C displayed an increased primary
82 root growth compared to plants kept at 21°C (Fig. 1A,B). Having established this experimental
83 set up to analyze the root response to temperature shifts, we went on to further characterize the
84 genetic mechanisms underlying this process.

85 The transcription factor *HY5* is a key regulator of shoot thermomorphogenesis, while at the
86 same time regulates root development and hormonal signaling pathways (reviewed in
87 (Gangappa and Botto, 2016)). Thus, we hypothesized that *HY5* could regulate the root
88 response to increased ambient temperature. We analyzed the relative root growth of *hy5* mutant
89 and wild type plants grown at 21°C and 27°C (Fig. 1A-D) and in line with our hypothesis, four
90 different allelic versions of *hy5* mutants displayed reduced root growth response to temperature
91 compared to wild type. While wild type plants increased root growth by 80 to 120%, *hy5* mutants
92 displayed an increase of only 20 to 40% (Fig. 1A-D). This reduced response was also observed
93 under a different growth condition with reduced light intensity (see material and methods; source
94 data file) as well as when roots were grown in the dark or on medium not supplemented with
95 sucrose (Fig. S1A-C), indicating that the reduced response observed in *hy5* was not dependent
96 on light or nutrient conditions. To test whether this reduced response was also associated with
97 changes in root apical meristem activity, we measured the dynamics of the root meristem size
98 after temperature shift. Interestingly, *hy5* mutants displayed a lower relative root meristem size
99 at all time points analyzed –from 24 hours to 72 hours after temperature shift– as well as
100 showed an earlier onset of cell elongation. This indicates that their meristem is hypersensitive to
101 increased ambient temperature compared to wild type plants (Fig. 1E,F; Fig. S1D). Together,
102 these data demonstrate that *HY5* is required to mediate root responses to temperature.

103 While analyzing the root phenotypes of *hy5* mutants, we observed that plants with a lower root
104 growth frequently displayed longer hypocotyls than plants with a higher root growth, suggesting
105 that shoot and root responses to temperature could be functionally connected. To test this
106 observation, we simultaneously measured hypocotyl and root growth on individual plants and
107 calculated the relative hypocotyl or root growth. Raising ambient temperature strongly promoted

108 hypocotyl growth while decreasing root growth response in the *hy5* mutant (Fig. S1E),
109 supporting the idea that these two processes could be coordinated during early seedling
110 development.

111

112 Phytochromes and PIF activity regulate the root response to higher ambient temperature

113 The phenotypic relation between hypocotyl and root growth response in the *hy5* mutant
114 suggested that additional regulators of shoot thermomorphogenesis might also modulate the
115 root growth response. Previous studies had demonstrated a critical role of PHYB to sense
116 temperature in the shoot and to mediate hypocotyl growth (Jung et al., 2016; Legris et al., 2016),
117 leading us to hypothesize that the phytochromes might also regulate root thermo-responses.
118 Accordingly, both *phyA* and *phyB* single mutant plants displayed a reduction in the root
119 response to temperature compared to wild type. This difference was further enhanced in *phyAB*
120 double mutants, showing that *phyA* and *phyB* co-regulate this process (Fig. 2A,B, Fig. S1F).
121 The lower root growth in *phyAB* was also associated with a decreased relative root meristem
122 size, demonstrating that root meristematic activity was hypersensitive to increased ambient
123 temperature, similarly to what we observed in *hy5* mutant plants (Fig. 2C,D; Fig. S1D).
124 Collectively, these data demonstrate that in addition to their function in the shoot, the
125 phytochromes are also required for root thermomorphogenesis.

126 Phytochromes mediate the phosphorylation of downstream factors including the PIFs, which are
127 then targeted for degradation (Lorrain et al., 2008). As PIF4 functionally interacts with HY5
128 during shoot thermomorphogenesis (Delker et al., 2014; Gangappa and Kumar, 2017), we
129 reasoned that PIF4 might also modulate root responses to temperature downstream of the
130 phytochromes. Thus, we tested whether PIF4 and other PIF family members could control the
131 root growth response to temperature. Similarly to previous studies (Martins et al., 2017), *pif4*
132 mutants did not show an impaired root response (Fig. 2E,F). Moreover, simultaneously
133 interfering with the function of multiple PIFs such as *PIF1*, *PIF3*, *PIF4*, *PIF5* and *PIF7* in *pifq* or
134 *pif7 pifq* mutants had no effect on the root response compared to wild type, indicating that the
135 PIFs were not required to regulate this process (Fig. 2E,F; Fig. S1G). Although the loss-of-
136 function mutants did not display impaired root response to higher temperature, we reasoned
137 that because phytochromes are negative regulators of PIFs, PIF activity might be increased in
138 phytochrome mutants, and that in turn might contribute to the reduction of the root thermo-
139 response in *phyAB* mutants. Thus, we next tested whether promoting PIF function could be
140 sufficient to modulate root growth response. In line with this idea, the gain-of-function
141 *pPIF4:PIF4-FLAG* mutant line (PIF4OX; Gangappa and Kumar, 2017) showed a significant
142 reduction in the root response to higher temperature (Fig. 2G), demonstrating that while PIF4
143 function is not required, it is indeed sufficient to modulate this developmental response. As PIF

144 activity is promoted in phytochrome mutants (Park et al., 2018, 2004), our results further
145 suggest that increased PIF4 activity in the *phyAB* could lead to a reduction of the root thermo-
146 response.

147

148 HY5-PIF activity co-regulate root thermomorphogenesis

149 Having shown that HY5 or phytochromes/PIF activity can modulate shoot and root responses to
150 temperature, we next hypothesized that HY5 and PIFs could co-regulate this process. To test
151 this idea, we first impaired HY5 function together with DET1 and COP1, which are regulators of
152 *PIF4* expression and the hypocotyl response to temperature (Fig. S2A; Gangappa and Kumar,
153 2017)). In accordance with a previous report (Gangappa and Kumar, 2017), both *hy5 det1* and
154 *hy5 cop1* double mutants suppressed the enhanced hypocotyl response of *hy5* mutants (Fig.
155 3A,B). Interestingly, these lines also displayed a significant increase in root growth temperature
156 response compared to *hy5* (Fig. 3C). The genetic interaction of *HY5* and *COP1* was highly
157 significantly dependent on temperature (ANOVA: p-value= 1.85×10^{-6}), while the genetic
158 interaction of *HY5* and *DET1* was only marginally significant (ANOVA: p-value=0.0553). Overall,
159 these results demonstrated that impairing *DET1* and *COP1* function can partially rescue root
160 growth in response to higher ambient temperature. Importantly, neither *det1* nor *cop1* single
161 mutants displayed an increased root growth response to temperature, suggesting that the
162 genetic interaction between *HY5*, *DET1* or *COP1* is critical to modulate root
163 thermomorphogenesis (Fig. 3C). To directly test whether *HY5* and PIFs could co-regulate this
164 process, we next simultaneously interfered with *HY5* and PIF function using the *hy5 pifQ*
165 quintuple mutant and analyzed growth responses to elevated temperature (Fig. 3D-F).
166 Consistent with this idea, both hypocotyl and root growth responses were significantly rescued
167 compared to *hy5* mutants, demonstrating that *HY5* and PIF pathways functionally interact to
168 regulate shoot and root responses to temperature (Fig. 3D-F). These results demonstrate that
169 the activity of a shoot signaling module including *HY5* and *PIF* genes mediates root response to
170 temperature.

171 Taken together, our phenotypic analyses showed that enhanced shoot growth response was
172 associated with a decreased root response to temperature. We have observed a similar trend
173 when wild type plants were grown in dark and shifted to higher ambient temperature (Fig.
174 S2B,C). These results suggested that shoot and root thermomorphogenesis could be
175 quantitatively negatively correlated. To test this idea, we combined measurements of hypocotyl
176 and root growth of individual plants for nine different genotypes (wild type, *hy5-221*, *hy5*, *hy5-*
177 *215*, *hy5 pifQ*, *hy5 cop1*, *hy5 det1*, *phyAB* and *PIF4OX*) as well as for wild type and *hy5-221*
178 mutant under a different light environment. We then analyzed the relation between hypocotyl
179 and root growth rate at 21°C, 27°C or the relation between their normalized growth (Fig. 3G ;

180 Fig. S2D-I). Remarkably, we observed that at 27°C, individual genotypes formed distinct groups
181 with root growth rate decreasing as the hypocotyl growth increased, supporting the idea that
182 these traits could be negatively correlated (Fig. 3G; Fig. S2D). We next applied a linear
183 regression model and observed a negative correlation between the root and the hypocotyl
184 growth rate at 27°C ($R^2=0.365$) (Fig. 3H). We have also observed this negative correlation under
185 the second light environment ($R^2=0.623$) (Fig. S2E) indicating that root growth rate negatively
186 correlates with hypocotyl growth rate at 27°C. Interestingly, we did not observe this relation at
187 21°C ($R^2=0.064$) or when analyzing temperature responses ($R^2=0.035$) (Fig. S2F-I), indicating
188 that this hypocotyl-root growth correlation is specific to higher ambient temperature conditions.
189 Together, these results show that upon increased ambient temperature, the HY5-PIF module is
190 required to balance hypocotyl with root growth responses and further suggest that a
191 developmental trade-off governs hypocotyl and root growth response at higher ambient
192 temperature.

193

194 A shoot to root developmental trade-off in response to higher ambient temperature

195 The observation that shoot and the root thermomorphogenesis were negatively correlated was
196 intriguing and prompted us to test whether modulating shoot thermo-response was sufficient to
197 impact root growth. To investigate this idea, we used a genetic chimera approach by taking
198 advantage of a HA-YFP-HA-HY5 fusion protein (DoF-HY5) that showed restricted cell-to-cell
199 movement and aimed at driving its expression specifically in the shoot of *hy5* mutants using
200 *CAB3* or *CER6* promoters (Burko et al, 2020b; Procko et al., 2016). In line with previous studies
201 (Chen et al., 2016; Procko et al., 2016), we detected strong accumulation of DoF-HY5 in leaves,
202 petioles and at weaker level in hypocotyls for both constructs, confirming that our *CAB3* and
203 *CER6* promoters were driving expression in the shoot (Fig. S3A-F; Burko et al, 2020b). While
204 we detected DoF-HY5 accumulation in the root of the *pCER6:DOF-HY5* line, we did not detect
205 fluorescence signal in the root of the *pCAB3:DOF-HY5* lines, indicating that expression driven
206 from the *CAB3* promoter was specific to the shoot and that our tagged version of HY5 was not
207 able to move from the shoot to the root (Fig. 4A,C; Fig. S3A-F). To further confirm these
208 observations, we assessed the accumulation of DoF-HY5 fusion protein either in the root or in
209 the shoot using immunoblotting with a HY5 or a HA antibody (Fig. 4D,E). Consistent with our
210 microscopy observations, we observed that DoF-HY5 protein accumulated in the shoot of
211 *pCAB3:DOF-HY5* lines whereas the detected protein levels were similar to *hy5* mutant in the
212 root or were accumulating ubiquitously in the *pCER6:DOF-HY5* line (Fig. 4D,E). This provided
213 us with valuable genetic material to further test whether HY5 local activity in the shoot could
214 regulate the root response to temperature.

215 We went on to analyze the functionality of the DoF-HY5 fusion protein by measuring hypocotyl
216 and root growth upon response to increased ambient temperature in the *pCER6:DOF-HY5* line.
217 Although *hy5* displayed an increased relative hypocotyl growth and a reduced root growth
218 response, these responses were rescued to levels similar to wild type in the *pCER6:DOF-HY5*
219 line, demonstrating that the DoF-HY5 fusion protein was functional (Fig. S3G-I). These results
220 next prompted us to investigate the local function of HY5 in the shoot during temperature
221 response by analyzing the *pCAB3:DOF-HY5* chimera rescue lines (Fig. 4F,G). In line with DoF-
222 HY5 accumulation in the shoot, both *pCAB3:DOF-HY5* lines displayed a partial rescue of the
223 relative hypocotyl growth observed in *hy5* (Fig. 4F). Strikingly, these two independent lines also
224 showed a significant rescue of the root growth response compared to *hy5*, demonstrating that
225 HY5 function in the shoot was sufficient to modulate root growth response to temperature (Fig.
226 4G).

227 However, the partial rescue of these lines also suggested that HY5 function could be required
228 locally for root thermomorphogenesis. To test this idea, we removed the shoot of seedlings and
229 assessed the root growth response upon temperature shift on these isolated roots. While root
230 elongation in isolated roots of wild type plants was lower than in intact plants, their relative
231 responses to the temperature shift were similar (Fig. S3K-M, Supplementary data). The root
232 growth response in whole seedlings and isolated roots of *hy5* mutants was lower than that of
233 wild type, suggesting that HY5 function is indeed also required locally in the root (Fig. S3L). In
234 contrast to *hy5* mutants, the relative response was fully rescued in isolated roots of *phyAB*
235 mutants, suggesting that the phytochromes act mainly in the shoot during
236 thermomorphogenesis (Fig. S3M). Together, these results reveal that modulating shoot
237 thermomorphogenesis by local HY5 rescue is sufficient to regulate root growth, but that local
238 root action of HY5 is required for the full root growth temperature response.

239

240 Transcriptional change of metabolic genes in response to temperature

241 Having shown that a developmental trade-off quantitatively couples shoot and root
242 thermomorphogenesis, we wanted to further delineate the regulatory mechanisms underlying
243 this process. To this end, we used a genome-wide approach and profiled the transcriptomes of
244 isolated shoots and roots after a short (4 hours) or a more prolonged (18 hours) temperature
245 treatment using RNAseq.

246 We first asked whether a core regulatory network could mediate responses to temperature in
247 the shoot and in the root. To strengthen our approach and to alleviate the influence of the
248 genotypes on the response, we compared the transcriptional changes in wild type, *hy5* and
249 *phyAB* plants. Using this method, we identified 327 genes in the shoot and in the root that were
250 temperature regulated in all genotypes for the early time point while we found that 550 and 904

251 genes were commonly regulated at the late time point (Fig. 5A,B; Fig. S4A,B). Consistent with
252 the temperature treatment imposed onto the plants, the shared regulatory signatures were
253 associated with heat response (“response to heat”, “response to hydrogen peroxide” and
254 “response to high light intensity”) (Fig. 5A; Fig. S4A,B). We also observed contrasting regulatory
255 responses in the shoot and root, which were mainly related to metabolism. In particular, we
256 detected a significant enrichment for members of the glucosinolate biosynthetic among genes
257 specifically responding in the root, whereas we observed that flavonoid biosynthesis genes were
258 enriched in the shoot (Fig. 5A,B; Fig. S4A,B). Moreover, we observed a greater proportion of
259 genes involved in sucrose transport in the root and sucrose response in the shoot, suggesting
260 that increased ambient temperature modulates energy metabolism (Fig. 5B, Fig. S4A,B).
261 Together, these results show that in addition to common core regulatory signatures, shoots and
262 roots display specific responses to elevated temperature, with roots differentially re-adjusting
263 their metabolism in response to higher temperature.

264 To further characterize the regulatory function of HY5 and phytochromes during root
265 thermomorphogenesis, we next identified genes misregulated in *hy5* and *phyAB* compared to
266 wild type at 27°C (Fig. 5C). Strikingly, we observed significant overlap (hypergeometric test;
267 $p < 0.001$) in the sets of genes that were upregulated or downregulated in *hy5* and *phyAB* mutant
268 roots or shoots at both time points (Fig. S4C,D). This overlap supports our previous genetic
269 analyses and demonstrates that HY5 and phytochromes regulate a set of common genes in the
270 root (Fig. 5C, Fig. S4C). Among the co-regulated genes, we identified known HY5 target genes
271 – such as *HY5 HOMOLOG (HYH)*, *SUPPRESSOR OF PHYA (SPA)* gene family and *FHY1-*
272 *LIKE (FHL)*– as well as known light signaling genes, which confirmed the quality of our dataset
273 (Fig. S4E;(Burko et al., 2020; Ciolfi et al., 2013; Lee et al., 2007; Li et al., 2010)). Importantly,
274 we also detected an enrichment for misregulated genes involved in the generation of precursor
275 metabolites, suggesting that the metabolic status was altered in *hy5* and in *phyAB* mutant roots
276 ($p = 2.6e-14$; Fig. 5C). Accordingly, all genes belonging to the GO category “generation of
277 precursor metabolites and energy precursor” were significantly downregulated either in *hy5* or
278 *phyAB* at both time points, indicating that HY5 and phytochrome activities are required for the
279 expression of energy metabolism genes in the root ($n = 35/35$, Fig. 5D). These results also show
280 that the reduced root growth response observed in *hy5* and *phyAB* mutants correlates with a
281 substantial downregulation of genes involved in the chemical reactions and pathways resulting
282 in the formation of substances from which energy is derived or genes involved in releasing
283 energy from these metabolites. Taken together, the analysis of transcriptional responses
284 suggests that HY5 and phytochrome activity regulate root growth at higher temperature by
285 modulating energy metabolism.

286

287 Auxin perception, signalling and biosynthesis are involved in root thermomorphogenesis

288 Having shown that HY5 and phytochromes are required for the expression of energy precursor
289 genes in the root, we next wanted to investigate whether other signals could regulate root
290 thermomorphogenesis downstream of the HY5-PIF module. Some reports have demonstrated
291 that auxin transport and signaling are required for the root response to higher ambient
292 temperature (Feraru et al., 2019; Hanzawa et al., 2013; Wang et al., 2016), however these
293 regulatory interactions have also been challenged and debated (Martins et al., 2017). This
294 prompted us to first confirm the function of auxin homeostasis in our root growth assays.

295 Shifting plants from 21°C to 27°C led to increased auxin signaling as shown by the increased
296 signal of the *pDR5v2:3xYFP-NLS* transcriptional reporter at the root tip and increased *IAA29*
297 gene expression (Fig. S5A-C, (Wang et al., 2016)). Genetically interfering with the auxin
298 receptors TIR1 and AFB2 in *tir1*, *afb2* and *tir1 afb2* mutant also led to a slight but significant
299 reduction when considering the root growth response to temperature (Fig. 6A). However, we
300 note that when considering root growth rates without normalizing, the single knockouts were not
301 significantly responding to temperature and the genetic interaction of *TIR1* and *AFB2* was
302 interacting with temperature only marginally significant (two-way ANOVA for
303 *AFB1:TIR1:temperature* interaction P-value=0.0967) . To complement these data, we impaired
304 another branch of auxin signaling by interfering with TMKs function, which are membrane
305 localized receptor like kinases involved in the perception of auxin independently of the TIR/AFB
306 system (Cao et al., 2019; Xu et al., 2014). Like suggested by the *TIR/AFB* related mutants, we
307 found a reduced root elongation in *tmk1,4* compared to wild type during the root temperature
308 response (Fig. 6B). Together, these results confirmed that auxin perception and signaling are
309 required for root thermomorphogenesis.

310 We next hypothesized that auxin biosynthesis and the control of the hormone level at the root
311 might also modulate root thermomorphogenesis. Thus, we examined the function of auxin
312 biosynthesis by genetically interfering with *YUC* gene activity in the *yuc3,5,7,8,9* (*yucQ*)
313 quintuple mutant. Accordingly, *yucQ* displayed a reduced root growth response compared to
314 wild type, demonstrating that auxin biosynthesis through the activity of the YUCs is also
315 required for root elongation upon higher ambient temperature (Fig. 6C). Together, these data
316 demonstrate that auxin biosynthesis is required for root thermomorphogenesis, and further
317 suggest that auxin perception and signaling plays a role in it.

318

319 HY5 and phytochromes regulate auxin homeostasis at the root

320 Having confirmed the function of auxin signaling during root thermomorphogenesis, we next
321 asked whether HY5 and phytochromes could regulate this hormonal pathway. In our root
322 transcriptome, we analyzed the overlap between genes misregulated in *hy5* or *phyAB* at 27°C

323 and auxin responsive genes in the root as obtained from RNA-seq after 6 hours of indole 3-
324 acetic acid (IAA) treatment (Omelyanchuk et al., 2017). Interestingly, we found a significant
325 overlap of genes that were transcriptionally responding to IAA treatment and misregulated in
326 *hy5* and *phyAB* at both early and late time points (Fig. 6D, Fig. S6E). We also found that a
327 significant proportion of genes whose transcriptional response to temperature was differentially
328 regulated in *hy5* or *phyAB* mutants were also responding to auxin in the root (Fig. S6F).
329 Together these results demonstrated that HY5 and phytochromes activities converged with the
330 auxin regulatory network and further suggested that these factors might control auxin
331 homeostasis during root thermomorphogenesis.

332 To further examine this idea, we assessed the state of the auxin metabolic pathway by
333 measuring the concentration of IAA and its precursors in roots of wild type, *hy5* and *phyAB*
334 mutants 12 hours after a temperature shift. Surprisingly, we did not observe a change in total
335 auxin level after temperature shift in wild type roots, suggesting that a change in total auxin level
336 is not required for root thermomorphogenesis, unlike what has been reported for the shoot (Fig.
337 5E;(Gray et al., 1998)). While we observed a slight decrease in IAA levels as well as some of
338 the auxin precursors in *hy5* and *phyAB* roots compared to wild type demonstrating that HY5 and
339 phytochromes are required to maintain IAA levels in the root independently of temperature (Fig.
340 6E, Fig. S5G-H), the interaction of genotypes with temperature was not statistically significant
341 when conducting a two-way ANOVA (Supplementary source data). When comparing the ratio of
342 root IAA levels, we observed a decrease in the relative IAA level in *hy5* and *phyAB* mutants
343 compared to wild type upon increased ambient temperature, indicating that the dynamics of
344 auxin accumulation in the root might be impaired upon loss of HY5 and phytochrome activity
345 (Fig. 6F). Together these results show that HY5 and phytochrome are required to maintain auxin
346 levels, but that further data will be required to thoroughly test the role of *hy5* and *phyAB*
347 dependent auxin levels in root thermomorphogenesis.

348

349

351

352 In this study, we investigated the regulatory mechanisms controlling root thermomorphogenesis.
353 Using a genetic approach combined with phenotypic analyses, we find that a regulatory module
354 –including HY5 and phytochromes– modulates the shoot to root growth coordination of
355 responses to higher temperature. In addition, we gain insight on the function of auxin signaling
356 pathway and its connection with HY5 and phytochromes during root thermomorphogenesis (Fig.
357 7). Together, our findings highlight that a developmental trade-off governs shoot and root growth
358 responses and further suggests that roots integrate energy signals with hormonal inputs during
359 thermomorphogenesis.

360 We showed that HY5 and the phytochromes are required for the root response to temperature.
361 In line with published reports, interfering with PIF activity did not lead to impaired root growth
362 responses to temperature, which previously led to the conclusion that PIFs were not regulating
363 root responses to temperature (Martins et al., 2017). However, we observe that a PIF4 gain-of-
364 function phenocopies the *hy5* and *phyAB* mutant phenotypes, showing that PIF4 is sufficient to
365 regulate root thermomorphogenesis. Furthermore, HY5 acts antagonistically to PIF4 at the
366 promoter of multiple target genes and interfering with HY5 function could enhance PIF4-
367 mediated gene regulation (Gangappa and Kumar, 2017). Accordingly, shoot and root
368 phenotypes in *hy5* mutants are suppressed by dampening *PIF* expression, demonstrating that
369 *HY5* genetically interacts with *PIFs* during shoot and root thermomorphogenesis. Thus, our
370 results support a model where PIF4 acts downstream of the phytochromes and functionally
371 converges with HY5 to regulate root thermomorphogenesis. Future experiments interfering with
372 phytochromes and PIFs function in higher order mutants will be important to further dissect the
373 function of this regulatory circuit during thermomorphogenesis.

374 In this context, *HY5* also genetically interacts with *COP1* and *DET1* as shown by the
375 suppression of *hy5* phenotypes in *hy5 det1* and *hy5 cop1*. Interestingly, while the *det1-1* mutant
376 responds similarly to control plants, *cop1-4* shows decreased root growth in response to
377 temperature. Moreover, while the genetic interaction of *COP1* and *HY5* is statistically highly
378 significant, the *DET1 HY5* genetic interaction with temperature is only marginally significant.
379 Taken together, these results are intriguing since *DET1* and *COP1* act together in order to
380 promote *HY5* degradation (reviewed in (Lau and Deng, 2012)). Thus, our results also suggest
381 that *COP1* can signal independently from *HY5* during root thermomorphogenesis.

382 Our finding that a shoot regulatory module can control hypocotyl growth response and can
383 concomitantly modulate root growth raises interesting questions as to how these two processes
384 are coordinated. Our current data suggest two putative mechanisms that could act in parallel to
385 coordinate shoot with root thermomorphogenesis.

386 First, we observe that a reduced root growth response is associated with a strong promotion of
387 hypocotyl growth. Such increase in growth is promoted by the temperature shift and could
388 impact the availability of elements such as water as well as have indirect effect on root
389 metabolism. Accordingly, our data suggest that temperature responses are tightly connected
390 with the energy metabolism. The observed negative correlation between hypocotyl and root
391 growth responses and the associated downregulation of metabolic precursor genes that play a
392 role in chemical reactions and pathways from which energy is released indicate these two
393 processes could be coordinated by a limitation of metabolic resources that are required during
394 enhanced hypocotyl growth. This hypothesis is consistent with classical studies on biomass
395 allocation between shoots and roots (Shibley and Meziane, 2002; Thornley, 1972). In this
396 context, one possible relevant energy signal could be sucrose, which is produced in the shoot
397 through photosynthesis and has been shown to act as a long-distance signal to promote root
398 growth (Kircher and Schopfer, 2012). Interestingly we found in our genome-wide expression
399 analysis of root responses to temperature that a significant proportion of genes involved in
400 sucrose transport was enriched, suggesting that changes in sugar availability could regulate
401 shoot-to-root growth coordination upon increased ambient temperature. In addition, HY5-PIF4
402 have been shown to directly regulate the expression of photosynthetic genes and consequently
403 the production of chlorophyll content in young seedlings. Accordingly, *hy5* mutants display lower
404 chlorophyll content than wild type at 27°C (Toledo-Ortiz et al., 2014), which could have a direct
405 impact on the production of photosynthesis-derived sucrose and consequently on root growth.
406 Given that *hy5* mutant still displayed a reduced root response to increased ambient temperature
407 in medium that was not supplemented with sucrose (Fig. S1C), we believe that external sucrose
408 would have limited impact on this process. Together these data suggest that shoot growth could
409 influence the availability of energy signals and in turn modulate root growth response upon
410 increased ambient temperature. To uncouple growth mechanism from energy balance, it would
411 be interesting to analyze root growth response to temperature upon overexpression of
412 expansins in the shoot (Cosgrove, 2000).

413 In parallel to this pathway, another important signal could be the phytohormone auxin. Previous
414 studies have shown that auxin transport and signaling regulate root growth upon shift at higher
415 temperature (Feraru et al., 2019; Hanzawa et al., 2013; Wang et al., 2016), while the
416 brassinosteroid pathway regulate this process upon long term exposure (Martins et al., 2017).
417 Furthermore both studies from Feraru *et al.* and Wang *et al.* shifted plants to 29°C which could
418 also be perceived as a stress by the plants, thereby possibly confounding root response to
419 higher ambient temperature with temperature stress pathway (Bielach et al., 2017). These
420 studies highlight the important function of auxin in controlling various environmental fluctuations
421 (Kazan, 2013; Zhao, 2018). By conducting our temperature shifts to 27°C, we have now

422 confirmed that auxin perception and signaling are required for root response to higher ambient
423 temperature. We also obtained genetic evidence for the requirement of auxin biosynthesis for
424 the root growth response to elevated temperature, suggesting that the control of auxin levels is
425 critical to regulate root thermomorphogenesis. Our measurements of auxin levels show that *hy5*
426 and phytochrome mutants display lower auxin levels at 21°C and at 27°C than wild type.
427 However, while the levels seem to mildly decrease upon increased ambient temperature in
428 these mutants, these changes are not statistically significant from wild type with our limited
429 experimental replication at a single time point. Given our genetic evidence that suggests that
430 auxin signaling is required for root thermomorphogenesis and has a permissive role rather than
431 an inductive role, it is possible that auxin levels might be controlled in a more complex and
432 dynamic manner. Moreover, auxin signaling output is tightly connected to its transport within and
433 across tissues (reviewed in (Benjamins and Scheres, 2008). For instance, during shoot
434 responses to temperature, auxin is produced in the cotyledons and transported to the hypocotyl
435 to promote cell elongation (Bellstaedt et al., 2019). Furthermore, the modulation of auxin long-
436 distance transport from the shoot to the root can regulate root developmental responses to
437 environmental light conditions (Sassi et al., 2012). As the molecular mechanisms controlling the
438 shoot-to-root auxin transport during thermomorphogenesis remains elusive, it will be critical to
439 further investigate the dynamics of auxin production, signaling and transport as well as to how it
440 is coordinated between shoot and root.

441 Together with our findings, these hypotheses open new avenues to further characterize the
442 communication between shoot and root, which could have important implications for plant
443 growth and biomass allocation upon environmental challenges. Studies have commonly used
444 micro-grafting experiments to investigate long distance signaling between the shoot and the root
445 (Chen et al., 2006, 2016). Given that we analyzed growth response to temperature at early
446 seedling stage, this strategy remains technically challenging as the impact of sectioning on the
447 growth response might override the effect of the genetic backgrounds used as scion. Instead we
448 have used domain-specific rescue approach (Hacham et al., 2011; Kang et al., 2017) by driving
449 a tagged version of HY5 under a shoot-specific promoter. In line with the specificity of the shoot
450 expression, we did not detect fluorescent signal, nor HY5 protein accumulation in the root by
451 immuno-blotting. Although these experimental methods cannot fully exclude that traces of HY5
452 protein are still present, the levels would be considerably lower than the wild type and unlikely to
453 have strong impact on the observed phenotype. The use of large tags fused to HY5 such as
454 3xYFP could further immobilize the protein and could be used in combination with organ specific
455 promoters to probe the HY5 domain-specific function. To complement the chimera approach, we
456 have used a mechanical approach by removing shoots and have observed that HY5 function
457 might be locally required in the root for thermomorphogenesis while phytochrome might act

458 mainly from the shoot. This observation could be further tested using shoot-specific or root-
459 specific genetics with tools such as the CAB3 or the INORGANIC PHOSPHATE
460 TRANSPORTER 1-1 (PHT1:1) promoters (Procko et al., 2016; Vijaybhaskar et al., 2008) could
461 be valuable to further elucidate how the shoot and the root communicate during
462 thermomorphogenesis.

463 Based on our results, we propose a model where roots integrate systemic signals modulated by
464 a shoot module including HY5, phytochromes with more locally acting auxin signaling during
465 thermomorphogenesis (Fig. 7). The integration of signals that are relayed from the shoot as well
466 as more local ones in the root could constitute a flexible system to adapt growth in response to
467 changes in air temperature perceived in the shoot while at the same time tuning growth locally
468 by modulating hormonal homeostasis. Thus, it will be important in the future to further
469 understand to what extent these two signaling pathways interact and how they are coupled at
470 the temporal level.

471

472 Material and methods

473

474 Plant material and growth conditions

475 In this study we used the following published lines: *phyAB* (Zheng et al., 2013), *hy5* (Jia et al.,
476 2014), *hy5-221*, *hy5-215*, *hy5-1* (Oyama et al., 1997), *phyA-211* (Reed et al., 1994), *phyB-9*
477 (Reed et al., 1993), *pif4-101* (Lorrain et al., 2008), *pif1,3,4,5 (pifQ)*(Leivar et al., 2008), PIF4-OX
478 (pPIF4:PIF4-FLAG)(Gangappa and Kumar, 2017), *hy5 pifQ* (Jia et al., 2014), *det1-1* (Pepper et
479 al., 1994), *cop1-4* (McNellis et al., 1994), *hy5 det1* (Gangappa and Kumar, 2017), *hy5 cop1*
480 (Rolauuffs et al., 2012), *tir1-1*, *afb2-3*, *tir afb2* (Parry et al., 2009), *tmk1 tmk4* (Dai et al., 2013),
481 *yucca3,5,7,8,9 (yucQ)* (Chen et al., 2014), DR5v2 (Liao et al., 2015). CAB3, CER6 promoters
482 were previously described (Procko et al. 2016) and the DoF (HA-YFP-HA) tag was described in
483 (Burger et al. 2017). HY5 rescue lines were generated by inserting *pCAB3:HA-YFP-HA-HY5*
484 and *pCER6:HA-YFP-HA-HY5* in the *hy5* background (Lian et al., 2011) as described in (Burko
485 et al, 2020b).

486 When not specified, plants were grown in long day conditions (16/8h) in walk-in growth
487 chambers (Convion, Winnipeg, Manitoba, Canada) at 21°C or 27°C, 60% humidity, at 146 PAR
488 (see source data for light spectra). During nighttime, temperature was decreased to 15°C and
489 21°C respectively. In our growth condition 2, plants were grown in reach-in growth chambers at
490 60% humidity, 122 PAR (see source data for light spectra), temperature was kept constant at
491 either 21°C or 27°C. Environmental conditions were established and monitored with commercial
492 software (Valoya, Helsinki, Finland).

493 Plants were cultivated on plates containing ½ Murashige Skoog (Caisson, Smithfield, UT, USA),
494 1%MES (Acros Organic, Hampton, NH, USA), 1% sucrose (Fisher Bioreagents, Hampton, NH,
495 USA) and 0.8% Agar powder (Caisson, Smithfield, UT, USA). For temperature shift experiments,
496 plants were germinated and grown until 3 days after germination at 21°C to synchronize their
497 development. On the third day, plants were shifted at ZT1-3 at 27°C and grown for 3 additional
498 days at 21°C or 27°C.

499 For dark-grown seedlings the plates were left in the light for 24 hours at 21°C, then isolated from
500 light using aluminum foil and grown at 21°C for an additional two days. After three days, half of
501 the plates moved to 27°C. After 24 hours, half of the plates from 21°C or 27°C scanned, then
502 after 72 hours, the rest of the plates were scanned.

503 Roots grown on plates in the dark were isolated from light using metal combs that contained
504 holes and plates were wrapped with aluminum foil.

505 Shoot sectioning was performed by cutting at the apex of the hypocotyl to prevent damage of
506 the root. Sections were done 3 days after germination and were then transferred at 21°C or
507 27°C.

508

509

510

511 Root measurements and analysis

512 Root images were acquired using a multiplex scanning system as described in (Slovak et al.,
513 2014). Images were processed using the Fiji software (<https://fiji.sc/>). Root and hypocotyl
514 lengths were measured at 3DAG (before temperature shift) and at 6DAG. Growth rate were
515 obtained by subtracting the length at 6DAG and 3DAG. Normalized growth was calculated by
516 dividing root growth rate at 27°C by the average growth rate at 21°C. Raw values for individual
517 temperatures can be found in the source data file.

518 For the time course analysis of normalized root growth, plates were scanned at 0, 12, 24, 48, 72
519 hours after temperature shift. Images were stacked with Image J and root length was measured
520 at individual time points.

521 Cumulative root meristem cell size was conducted on Fiji using the Cell-O-Tape plugin (French
522 et al., 2012)

523 Statistical analysis was performed using Excel (Microsoft, Redmond, WA, USA) or R software
524 (<https://www.r-project.org/>). Linear regression was performed using the lm function in R and
525 graph displayed with ggplot2 (<https://www.r-project.org/>) (codes are available upon request).

526 Confocal pictures were acquired on a Zeiss 710 inverted microscope (Zeiss, Oberkochen,
527 Germany) or on Zeiss CSU Spinning Disk Confocal Microscope (Salk Biophotonics Core).
528 Pictures were processed using Fiji software (<https://fiji.sc/>). Root meristem size was measured
529 from the quiescent center to the first cortical cell that is twice as long as wide as was previously
530 described (Feraru et al., 2019).

531 Dot plots were generated using the plots of data online tool (Postma and Goedhart, 2019).

532

533 Immunoblotting

534 Western blots were performed as described in (Li et al., 2012) with minor modifications. 25 roots
535 and 20 shoots were harvested at 6DAG and extracted in 2X loading buffer (36µl bME+1ml 4x
536 loading buffer). Loading buffer was added to roots (70µl) and shoots (140µl) and then boiled
537 for 5 min. Bis-tris gel 4-12% (Invitrogen, Carlsbad, CA, USA) and semi-dry transfer (Pierce G2
538 Fast Blotter, Thermo Scientific, Waltham, MA, USA) were used. Primary antibodies used were
539 αHA-HRP 1:2000 (12013819001 Roche), αHY5(N) 1:5000 (R1245-1b ABicode), αActin
540 1:30,000 (A0408 Sigma).

541

542 Gene expression analysis

543 Biological triplicates were analysed. Total RNA was extracted from roots or shoot of plants 6
544 DAG using RNA easy kit (Qiagen, Hilden, Germany). RNA was treated with DNase using the
545 Turbo DNA-free kit (Invitrogen, Carlsbad, CA, USA) and further purified on columns from the
546 RNA easy kit.

547 Next generation sequencing (NGS) library was generated using the TruSeq Stranded mRNA
548 library prep kits (Illumina, San Diego, CA, USA). Libraries were sequenced on HiSeq2500
549 (Illumina, San Diego, CA, USA) as single read 50bases. Raw reads can be found at GEO under
550 the number: GSE138133.

551 NGS analysis was performed using Tophat2 for mapping reads on the Arabidopsis genome
552 (TAIR10) (Kim et al., 2013, p. 2), HT-seq for counting reads (Anders et al., 2014) and EdgeR for
553 quantifying differential expression (Robinson et al., 2009). We set a threshold for differentially
554 expressed genes (Fold change (FC) >2 or FC<-2, FDR<0.01). Genotype x Environment
555 interaction analysis was performed using linear model and type II ANOVA in R (codes are
556 available upon request).

557 Gene ontology analysis was performed using AgriGOv2 online tool (Tian et al., 2017). Venn
558 diagrams were generated with the VIB online tool
559 (<http://bioinformatics.psb.ugent.be/webtools/Venn/>).

560

561 Auxin measurements

562 For auxin measurement, plants were shifted at ZT1-3 at 27°C, grown at 21°C or 27°C and
563 harvested at ZT 13-15.

564 The extraction, purification and the LC-MS analysis of endogenous IAA, its precursors and
565 metabolites were carried out according to (Novák et al., 2012). Briefly, approx. 10 mg of frozen
566 material per sample was homogenized using a bead mill (27 hz, 10 min, 4°C; MixerMill, Retsch
567 GmbH, Haan, Germany) and extracted in 1 ml of 50 mM sodium phosphate buffer containing 1%
568 sodium diethyldithiocarbamate and the mixture of ¹³C₆- or deuterium-labeled internal standards.
569 After centrifugation (14000 RPM, 15 min, 4°C), the supernatant was divided in two aliquots, the
570 first aliquot was derivatized using cysteamine (0.25 M; pH 8; 1h; room temperature; Sigma-
571 Aldrich), the second aliquot was immediately further processed as following. The pH of sample
572 was adjusted to 2.5 by 1 M HCl and applied on preconditioned solid-phase extraction column
573 Oasis HLB (30 mg 1 cc, Waters Inc., Milford, MA, USA). After sample application, the column
574 was rinsed with 2 ml 5% methanol. Compounds of interest were then eluted with 2 ml 80%
575 methanol. Derivatized fraction was purified alike. Mass spectrometry analysis and quantification
576 were performed by an LC-MS/MS system comprising of a 1290 Infinity Binary LC System
577 coupled to a 6490 Triple Quad LC/MS System with Jet Stream and Dual Ion Funnel
578 technologies (Agilent Technologies, Santa Clara, CA, USA).

579 Raw measurements for individual temperatures can be found in the source data file.

580

581 Competing interests

582 The authors declare no competing interests

583

584 Acknowledgements

585 We would like to thank Yvon Jaillais (ENS, Lyon, France), Mark Estelle (UCSD, La Jolla, USA),
586 Yunde Zhao (UCSD, La Jolla, USA), and Adam Seluzicki (Salk Institute, La Jolla, USA) for
587 kindly sharing published mutant plant lines with us. We would also like to thank members of the
588 Busch laboratory for critically reading the manuscript. This study was funded by the National
589 Institute of General Medical Sciences of the National Institutes of Health (grant number
590 R01GM127759 to W.B.) and start-up funds from the Salk Institute for Biological Studies. J.C. is
591 investigator of the Howard Hughes Medical Institute. This study was supported by the HHS NIH
592 National Institute of General Medical Sciences (grant 5R35GM122604-02_05 to J.C.), the
593 Howard Hughes Medical Institute (to J. C.), the European Molecular Biology Organization (grant
594 ALTF 785-2013 to Y.B.), the United States-Israel Binational Agricultural Research and
595 Development Fund (grant FI-488-13 to Y.B), the Human Frontier Science Program
596 (LT000222/2013-L to B.W). K.L. and J.S. acknowledge the Swedish research councils
597 VINNOVA, VR and the Knut and Alice Wallenberg Foundation (KAW). They also thank the
598 Swedish Metabolomics Centre (<http://www.swedishmetabolomicscentre.se/>) for access to
599 instrumentation.

References

- Anders, S., Pyl, P.T., Huber, W.,** (2014). HTSeq—a Python framework to work with high-throughput sequencing data. *Bioinformatics* 31, 166–169. <https://doi.org/10.1093/bioinformatics/btu638>
- Bellstaedt, J., Trenner, J., Lippmann, R., Poeschl, Y., Zhang, X., Friml, J., Quint, M., Delker, C.,** (2019). A Mobile Auxin Signal Connects Temperature Sensing in Cotyledons with Growth Responses in Hypocotyls. *Plant Physiol.* 180, 757. <https://doi.org/10.1104/pp.18.01377>
- Benjamins, R., Scheres, B.,** (2008). Auxin: The Looping Star in Plant Development. *Annu. Rev. Plant Biol.* 59, 443–465. <https://doi.org/10.1146/annurev.arplant.58.032806.103805>
- Bielach, A., Hrtyan, M., Tognetti, V.B.,** (2017). Plants under Stress: Involvement of Auxin and Cytokinin. *INTERNATIONAL JOURNAL OF MOLECULAR SCIENCES* 18. <https://doi.org/10.3390/ijms18071427>
- Burko, Y., Seluzicki, A., Zander, M., Pedmale, U.V., Ecker, J.R., Chory, J.,** (2020). Chimeric Activators and Repressors Define HY5 Activity and Reveal a Light-Regulated Feedback Mechanism. *Plant Cell* 32, 967. <https://doi.org/10.1105/tpc.19.00772>
- Burko, Y., Gailloch, C., Seluzicki, A., Chory, J., Busch, W.,** (2020b). Local HY5 Activity Mediates Hypocotyl Growth and Shoot-to-Root Communication. *Plant Commun.* 100078. <https://doi.org/10.1016/j.xplc.2020.100078>
- Cao, M., Chen, R., Li, P., Yu, Y., Zheng, R., Ge, D., Zheng, W., Wang, X., Gu, Y., Gelová, Z., Friml, J., Zhang, H., Liu, R., He, J., Xu, T.,** (2019). TMK1-mediated auxin signalling regulates differential growth of the apical hook. *Nature* 568, 240–243. <https://doi.org/10.1038/s41586-019-1069-7>
- Chen, A., Komives, E.A., Schroeder, J.I.,** (2006). An Improved Grafting Technique for Mature Arabidopsis Plants Demonstrates Long-Distance Shoot-to-Root Transport of Phytochelatin in Arabidopsis. *Plant Physiol.* 141, 108. <https://doi.org/10.1104/pp.105.072637>
- Chen, Q., Dai, X., De-Paoli, H., Cheng, Y., Takebayashi, Y., Kasahara, H., Kamiya, Y., Zhao, Y.,** (2014). Auxin Overproduction in Shoots Cannot Rescue Auxin Deficiencies in Arabidopsis Roots. *Plant Cell Physiol.* 55, 1072–1079. <https://doi.org/10.1093/pcp/pcu039>
- Chen, X., Yao, Q., Gao, X., Jiang, C., Harberd, N.P., Fu, X.,** (2016). Shoot-to-Root Mobile Transcription Factor HY5 Coordinates Plant Carbon and Nitrogen Acquisition. *Curr. Biol.* 26, 640–646. <https://doi.org/10.1016/j.cub.2015.12.066>
- Chung, B.Y.W., Balcerowicz, M., Di Antonio, M., Jaeger, K.E., Geng, F., Franaszek, K., Marriott, P., Brierley, I., Firth, A.E., Wigge, P.A.,** (2020). An RNA thermoswitch regulates daytime growth in Arabidopsis. *Nat. Plants* 6, 522–532. <https://doi.org/10.1038/s41477-020-0633-3>
- Ciolfi, A., Sessa, G., Sassi, M., Possenti, M., Salvucci, S., Carabelli, M., Morelli, G., Ruberti, I.,** (2013). Dynamics of the Shade-Avoidance Response in Arabidopsis. *Plant Physiol.* 163, 331–353. <https://doi.org/10.1104/pp.113.221549>
- Cosgrove, D.J.,** (2000). Loosening of plant cell walls by expansins. *Nature* 407, 321–326. <https://doi.org/10.1038/35030000>

- Dai, N., Wang, W., Patterson, S.E., Bleecker, A.B.,** (2013). The TMK Subfamily of Receptor-Like Kinases in Arabidopsis Display an Essential Role in Growth and a Reduced Sensitivity to Auxin. *PLOS ONE* 8, 1–12. <https://doi.org/10.1371/journal.pone.0060990>
- Delker, C., Sonntag, L., James, G.V., Janitza, P., Ibañez, C., Ziermann, H., Peterson, T., Denk, K., Mull, S., Ziegler, J., Davis, S.J., Schneeberger, K., Quint, M.,** (2014). The DET1-COP1-HY5 Pathway Constitutes a Multipurpose Signaling Module Regulating Plant Photomorphogenesis and Thermomorphogenesis. *Cell Rep.* 9, 1983–1989. <https://doi.org/10.1016/j.celrep.2014.11.043>
- Donohue, K., Rubio de Casas, R., Burghardt, L., Kovach, K., Willis, C.G.,** (2010). Germination, Postgermination Adaptation, and Species Ecological Ranges. *Annu. Rev. Ecol. Evol. Syst.* 41, 293–319. <https://doi.org/10.1146/annurev-ecolsys-102209-144715>
- Feraru, E., Feraru, M.I., Barbez, E., Waidmann, S., Sun, L., Gaidora, A., Kleine-Vehn, J.,** (2019). PILS6 is a temperature-sensitive regulator of nuclear auxin input and organ growth in Arabidopsis thaliana. *Proc. Natl. Acad. Sci.* 116, 3893. <https://doi.org/10.1073/pnas.1814015116>
- Fiorucci, A.-S., Galvão, V.C., Ince, Y.Ç., Boccaccini, A., Goyal, A., Allenbach Petrolati, L., Trevisan, M., Fankhauser, C.,** (2020). PHYTOCHROME INTERACTING FACTOR 7 is important for early responses to elevated temperature in Arabidopsis seedlings. *New Phytol.* 226, 50–58. <https://doi.org/10.1111/nph.16316>
- Franklin, K.A., Lee, S.H., Patel, D., Kumar, S.V., Spartz, A.K., Gu, C., Ye, S., Yu, P., Breen, G., Cohen, J.D., Wigge, P.A., Gray, W.M.,** (2011). PHYTOCHROME-INTERACTING FACTOR 4 (PIF4) regulates auxin biosynthesis at high temperature. *Proc. Natl. Acad. Sci.* 108, 20231–20235. <https://doi.org/10.1073/pnas.1110682108>
- French, A.P., Wilson, M.H., Kenobi, K., Dietrich, D., Voß, U., Ubeda-Tomás, S., Pridmore, T.P., Wells, D.M.,** (2012). Identifying biological landmarks using a novel cell measuring image analysis tool: Cell-o-Tape. *Plant Methods* 8, 7. <https://doi.org/10.1186/1746-4811-8-7>
- Gangappa, S.N., Botto, J.F.,** (2016). The Multifaceted Roles of HY5 in Plant Growth and Development. *Mol. Plant* 9, 1353–1365. <https://doi.org/10.1016/j.molp.2016.07.002>
- Gangappa, S.N., Kumar, S.V.,** (2017). DET1 and HY5 Control PIF4-Mediated Thermosensory Elongation Growth through Distinct Mechanisms. *Cell Rep.* 18, 344–351. <https://doi.org/10.1016/j.celrep.2016.12.046>
- Gray, W.M., Östin, A., Sandberg, G., Romano, C.P., Estelle, M.,** (1998). High temperature promotes auxin-mediated hypocotyl elongation in *Arabidopsis*. *Proc Natl Acad Sci USA* 95, 7197. <https://doi.org/10.1073/pnas.95.12.7197>
- Ha, J.-H., Han, S.-H., Lee, H.-J., Park, C.-M.,** (2017). Environmental Adaptation of the Heterotrophic-to-Autotrophic Transition: The Developmental Plasticity of Seedling Establishment. *Crit. Rev. Plant Sci.* 36, 128–137. <https://doi.org/10.1080/07352689.2017.1355661>
- Hacham, Y., Holland, N., Butterfield, C., Ubeda-Tomas, S., Bennett, M.J., Chory, J., Savaldi-Goldstein, S.,** (2011). Brassinosteroid perception in the epidermis controls root meristem size. *Development* 138, 839. <https://doi.org/10.1242/dev.061804>

- Hanzawa, T., Shibasaki, K., Numata, T., Kawamura, Y., Gaude, T., Rahman, A.,** (2013). Cellular Auxin Homeostasis under High Temperature Is Regulated through a SORTING NEXIN1-Dependent Endosomal Trafficking Pathway. *Plant Cell* 25, 3424–3433. <https://doi.org/10.1105/tpc.113.115881>
- Hoecker, U.,** (2017). The activities of the E3 ubiquitin ligase COP1/SPA, a key repressor in light signaling. *Curr. Opin. Plant Biol.* 37, 63–69. <https://doi.org/10.1016/j.pbi.2017.03.015>
- Illston, B.G., Fiebrich, C.A.,** (2017). Horizontal and vertical variability of observed soil temperatures. *Geosci. Data J.* 4, 40–46. <https://doi.org/10.1002/gdj3.47>
- Jia, K.-P., Luo, Q., He, S.-B., Lu, X.-D., Yang, H.-Q.,** (2014). Strigolactone-Regulated Hypocotyl Elongation Is Dependent on Cryptochrome and Phytochrome Signaling Pathways in Arabidopsis. *Mol. Plant* 7, 528–540. <https://doi.org/10.1093/mp/sst093>
- Jung, J.-H., Domijan, M., Klose, C., Biswas, S., Ezer, D., Gao, M., Khattak, A.K., Box, M.S., Charoensawan, V., Cortijo, S., Kumar, M., Grant, A., Locke, J.C.W., Schäfer, E., Jaeger, K.E., Wigge, P.A.,** (2016). Phytochromes function as thermosensors inseparability. *Science* 354, 886. <https://doi.org/10.1126/science.aaf6005>
- Kang, Y.H., Breda, A., Hardtke, C.S.,** (2017). Brassinosteroid signaling directs formative cell divisions and protophloem differentiation in *Arabidopsis* root meristems. *Development* 144, 272. <https://doi.org/10.1242/dev.145623>
- Kazan, K.,** (2013). Auxin and the integration of environmental signals into plant root development. *Annals of Botany* 112, 1655–1665. <https://doi.org/10.1093/aob/mct229>
- Kim, D., Perteza, G., Trapnell, C., Pimentel, H., Kelley, R., Salzberg, S.L.,** (2013). TopHat2: accurate alignment of transcriptomes in the presence of insertions, deletions and gene fusions. *Genome Biol.* 14, R36. <https://doi.org/10.1186/gb-2013-14-4-r36>
- Kircher, S., Schopfer, P.,** (2012). Photosynthetic sucrose acts as cotyledon-derived long-distance signal to control root growth during early seedling development in Arabidopsis. *Proc. Natl. Acad. Sci.* 109, 11217. <https://doi.org/10.1073/pnas.1203746109>
- Koini, M.A., Alvey, L., Allen, T., Tilley, C.A., Harberd, N.P., Whitelam, G.C., Franklin, K.A.,** (2009). High Temperature-Mediated Adaptations in Plant Architecture Require the bHLH Transcription Factor PIF4. *Curr. Biol.* 19, 408–413. <https://doi.org/10.1016/j.cub.2009.01.046>
- Kumar, S.V., Lucyshyn, D., Jaeger, K.E., Alós, E., Alvey, E., Harberd, N.P., Wigge, P.A.,** (2012). Transcription factor PIF4 controls the thermosensory activation of flowering. *Nature* 484, 242–245. <https://doi.org/10.1038/nature10928>
- Lau, O.S., Deng, X.W.,** (2012). The photomorphogenic repressors COP1 and DET1: 20 years later. *Trends Plant Sci.* 17, 584–593. <https://doi.org/10.1016/j.tplants.2012.05.004>
- Lee, J., He, K., Stolc, V., Lee, H., Figueroa, P., Gao, Y., Tongprasit, W., Zhao, H., Lee, I., Deng, X.W.,** (2007). Analysis of Transcription Factor HY5 Genomic Binding Sites Revealed Its Hierarchical Role in Light Regulation of Development. *Plant Cell* 19, 731. <https://doi.org/10.1105/tpc.106.047688>
- Legris, M., Klose, C., Burgie, E.S., Rojas, C.C.R., Neme, M., Hiltbrunner, A., Wigge, P.A., Schäfer, E., Vierstra, R.D., Casal, J.J.,** (2016). Phytochrome B integrates light and temperature signals in Arabidopsis. *Science* 354, 897. <https://doi.org/10.1126/science.aaf5656>

- Leivar, P., Monte, E., Oka, Y., Liu, T., Carle, C., Castillon, A., Huq, E., Quail, P.H.,** (2008). Multiple Phytochrome-Interacting bHLH Transcription Factors Repress Premature Seedling Photomorphogenesis in Darkness. *Curr. Biol.* 18, 1815–1823.
<https://doi.org/10.1016/j.cub.2008.10.058>
- Li, J., Li, G., Gao, S., Martinez, C., He, G., Zhou, Z., Huang, X., Lee, J.-H., Zhang, H., Shen, Y., Wang, H., Deng, X.W.,** (2010). Arabidopsis Transcription Factor ELONGATED HYPOCOTYL5 Plays a Role in the Feedback Regulation of Phytochrome A Signaling. *Plant Cell* 22, 3634–3649.
<https://doi.org/10.1105/tpc.110.075788>
- Li, L., Ljung, K., Breton, G., Schmitz, R.J., Pruneda-Paz, J., Cowing-Zitron, C., Cole, B.J., Ivans, L.J., Pedmale, U.V., Jung, H.-S., Ecker, J.R., Kay, S.A., Chory, J.,** (2012). Linking photoreceptor excitation to changes in plant architecture. *Genes Dev.* 26, 785–790.
<https://doi.org/10.1101/gad.187849.112>
- Lian, H.-L., He, S.-B., Zhang, Y.-C., Zhu, D.-M., Zhang, J.-Y., Jia, K.-P., Sun, S.-X., Li, L., Yang, H.-Q.,** (2011). Blue-light-dependent interaction of cryptochrome 1 with SPA1 defines a dynamic signaling mechanism. *Genes Dev.* 25, 1023–1028. <https://doi.org/10.1101/gad.2025111>
- Liao, C.-Y., Smet, W., Brunoud, G., Yoshida, S., Vernoux, T., Weijers, D.,** (2015). Reporters for sensitive and quantitative measurement of auxin response. *Nat. Methods* 12, 207.
- Lorrain, S., Allen, T., Duek, P.D., Whitelam, G.C., Fankhauser, C.,** (2008). Phytochrome-mediated inhibition of shade avoidance involves degradation of growth-promoting bHLH transcription factors. *Plant J.* 53, 312–323. <https://doi.org/10.1111/j.1365-313X.2007.03341.x>
- Martins, S., Montiel-Jorda, A., Cayrel, A., Huguet, S., Roux, C.P.-L., Ljung, K., Vert, G.,** (2017). Brassinosteroid signaling-dependent root responses to prolonged elevated ambient temperature. *Nat. Commun.* 8, 309. <https://doi.org/10.1038/s41467-017-00355-4>
- McNellis, T.W., von Arnim, A.G., Araki, T., Komeda, Y., Miséra, S., Deng, X.W.,** (1994). Genetic and molecular analysis of an allelic series of cop1 mutants suggests functional roles for the multiple protein domains. *Plant Cell* 6, 487. <https://doi.org/10.1105/tpc.6.4.487>
- Novák, O., Hényková, E., Sairanen, I., Kowalczyk, M., Pospíšil, T., Ljung, K.,** (2012). Tissue-specific profiling of the Arabidopsis thaliana auxin metabolome. *Plant J.* 72, 523–536.
<https://doi.org/10.1111/j.1365-313X.2012.05085.x>
- Omelyanchuk, N.A., Wiebe, D.S., Novikova, D.D., Levitsky, V.G., Klimova, N., Gorelova, V., Weinholdt, C., Vasiliev, G.V., Zemlyanskaya, E.V., Kolchanov, N.A., Kochetov, A.V., Grosse, I., Mironova, V.V.,** (2017). Auxin regulates functional gene groups in a fold-change-specific manner in Arabidopsis thaliana roots. *Sci. Rep.* 7, 2489. <https://doi.org/10.1038/s41598-017-02476-8>
- Osterlund, M.T., Hardtke, C.S., Wei, N., Deng, X.W.,** (2000). Targeted destabilization of HY5 during light-regulated development of Arabidopsis. *Nature* 405, 462–466.
<https://doi.org/10.1038/35013076>
- Oyama, T., Shimura, Y., Okada, K.,** (1997). The Arabidopsis HY5 gene encodes a bZIP protein that regulates stimulus-induced development of root and hypocotyl. *Genes Dev.* 11, 2983–2995.
<https://doi.org/10.1101/gad.11.22.2983>

- Park, E., Kim, J., Lee, Y., Shin, J., Oh, E., Chung, W.-I., Liu, J.R., Choi, G.,** (2004). Degradation of Phytochrome Interacting Factor 3 in Phytochrome-Mediated Light Signaling. *Plant Cell Physiol.* 45, 968–975. <https://doi.org/10.1093/pcp/pch125>
- Park, E., Kim, Y., Choi, G.,** (2018). Phytochrome B Requires PIF Degradation and Sequestration to Induce Light Responses across a Wide Range of Light Conditions. *Plant Cell* 30, 1277. <https://doi.org/10.1105/tpc.17.00913>
- Parry, G., Calderon-Villalobos, L.I., Prigge, M., Peret, B., Dharmasiri, S., Itoh, H., Lechner, E., Gray, W.M., Bennett, M., Estelle, M.,** (2009). Complex regulation of the TIR1/AFB family of auxin receptors. *Proc. Natl. Acad. Sci.* 106, 22540. <https://doi.org/10.1073/pnas.0911967106>
- Penfield, S.,** (2008). Temperature perception and signal transduction in plants. *New Phytol.* 179, 615–628. <https://doi.org/10.1111/j.1469-8137.2008.02478.x>
- Pepper, A., Delaney, T., Washburnt, T., Poole, D., Chory, J.,** (1994). DET1, a negative regulator of light-mediated development and gene expression in arabidopsis, encodes a novel nuclear-localized protein. *Cell* 78, 109–116. [https://doi.org/10.1016/0092-8674\(94\)90577-0](https://doi.org/10.1016/0092-8674(94)90577-0)
- Postma, M., Goedhart, J.,** (2019). PlotsOfData—A web app for visualizing data together with their summaries. *PLOS Biol.* 17, e3000202. <https://doi.org/10.1371/journal.pbio.3000202>
- Procko, C., Burko, Y., Jaillais, Y., Ljung, K., Long, J.A., Chory, J.,** (2016). The epidermis coordinates auxin-induced stem growth in response to shade. *Genes Dev.* 30, 1529–1541. <https://doi.org/10.1101/gad.283234.116>
- Quint, M., Delker, C., Franklin, K.A., Wigge, P.A., Halliday, K.J., van Zanten, M.,** (2016). Molecular and genetic control of plant thermomorphogenesis. *Nat. Plants* 2, 15190. <https://doi.org/10.1038/nplants.2015.190>
- Reed, J.W., Nagatani, A., Elich, T.D., Fagan, M., Chory, J.,** (1994). Phytochrome A and Phytochrome B Have Overlapping but Distinct Functions in Arabidopsis Development. *Plant Physiol.* 104, 1139. <https://doi.org/10.1104/pp.104.4.1139>
- Reed, J.W., Nagpal, P., Poole, D.S., Furuya, M., Chory, J.,** (1993). Mutations in the gene for the red/far-red light receptor phytochrome B alter cell elongation and physiological responses throughout Arabidopsis development. *Plant Cell* 5, 147. <https://doi.org/10.1105/tpc.5.2.147>
- Robinson, M.D., McCarthy, D.J., Smyth, G.K.,** (2009). edgeR: a Bioconductor package for differential expression analysis of digital gene expression data. *Bioinformatics* 26, 139–140. <https://doi.org/10.1093/bioinformatics/btp616>
- Rolauffs, S., Fackendahl, P., Sahm, J., Fiene, G., Hoecker, U.,** (2012). Arabidopsis *COP1* and *SPA* Genes Are Essential for Plant Elongation But Not for Acceleration of Flowering Time in Response to a Low Red Light to Far-Red Light Ratio. *Plant Physiol.* 160, 2015–2027. <https://doi.org/10.1104/pp.112.207233>
- Saijo, Y., Sullivan, J.A., Wang, H., Yang, J., Shen, Y., Rubio, V., Ma, L., Hoecker, U., Deng, X.W.,** (2003). The COP1–SPA1 interaction defines a critical step in phytochrome A-mediated regulation of HY5 activity. *Genes Dev.* 17, 2642–2647. <https://doi.org/10.1101/gad.1122903>

- Salisbury, F.J., Hall, A., Grierson, C.S., Halliday, K.J.,** (2007). Phytochrome coordinates Arabidopsis shoot and root development. *Plant J.* 50, 429–438. <https://doi.org/10.1111/j.1365-313X.2007.03059.x>
- Sassi, M., Lu, Y., Zhang, Y., Wang, J., Dhonukshe, P., Bliilou, I., Dai, M., Li, J., Gong, X., Jaillais, Y., Yu, X., Traas, J., Ruberti, I., Wang, H., Scheres, B., Vernoux, T., Xu, J.,** (2012). COP1 mediates the coordination of root and shoot growth by light through modulation of PIN1- and PIN2-dependent auxin transport in Arabidopsis. *Development* 139, 3402. <https://doi.org/10.1242/dev.078212>
- Shiple, B., Meziane, D.,** (2002). The balanced-growth hypothesis and the allometry of leaf and root biomass allocation. *Funct. Ecol.* 16, 326–331. <https://doi.org/10.1046/j.1365-2435.2002.00626.x>
- Slovak, R., Göschl, C., Su, X., Shimotani, K., Shiina, T., Busch, W.,** (2014). A Scalable Open-Source Pipeline for Large-Scale Root Phenotyping of Arabidopsis. *Plant Cell* 26, 2390. <https://doi.org/10.1105/tpc.114.124032>
- Sun, J., Qi, L., Li, Y., Chu, J., Li, C.,** (2012). PIF4–Mediated Activation of YUCCA8 Expression Integrates Temperature into the Auxin Pathway in Regulating Arabidopsis Hypocotyl Growth. *PLoS Genet.* 8, e1002594. <https://doi.org/10.1371/journal.pgen.1002594>
- Thornley, J.H.M.,** (1972). A Balanced Quantitative Model for Root: Shoot Ratios in Vegetative Plants. *Ann. Bot.* 36, 431–441. <https://doi.org/10.1093/oxfordjournals.aob.a084602>
- Tian, T., Liu, Y., Yan, H., You, Q., Yi, X., Du, Z., Xu, W., Su, Z.,** (2017). agriGO v2.0: a GO analysis toolkit for the agricultural community, 2017 update. *Nucleic Acids Res.* 45, W122–W129. <https://doi.org/10.1093/nar/gkx382>
- Toledo-Ortiz, G., Johansson, H., Lee, K.P., Bou-Torrent, J., Stewart, K., Steel, G., Rodríguez-Concepción, M., Halliday, K.J.,** (2014). The HY5-PIF Regulatory Module Coordinates Light and Temperature Control of Photosynthetic Gene Transcription. *PLOS Genet.* 10, 1–14. <https://doi.org/10.1371/journal.pgen.1004416>
- Van Gelderen, K., Kang, C., Paalman, R., Keuskamp, D., Hayes, S., Pierik, R.,** (2018). Far-Red Light Detection in the Shoot Regulates Lateral Root Development through the HY5 Transcription Factor. *Plant Cell* 30, 101. <https://doi.org/10.1105/tpc.17.00771>
- Vijaybhaskar, V., Subbiah, V., Kaur, J., Vijayakumari, P., Siddiqi, I.,** (2008). Identification of a root-specific glycosyltransferase from Arabidopsis and characterization of its promoter. *J. Biosci.* 33, 185–193. <https://doi.org/10.1007/s12038-008-0036-5>
- Wang, R., Zhang, Y., Kieffer, M., Yu, H., Kepinski, S., Estelle, M.,** (2016). HSP90 regulates temperature-dependent seedling growth in Arabidopsis by stabilizing the auxin co-receptor F-box protein TIR1. *Nat. Commun.* 7, 10269. <https://doi.org/10.1038/ncomms10269>
- Xiong, Y., McCormack, M., Li, L., Hall, Q., Xiang, C., Sheen, J.,** (2013). Glucose–TOR signalling reprograms the transcriptome and activates meristems. *Nature* 496, 181.
- Xu, T., Dai, N., Chen, J., Nagawa, S., Cao, M., Li, H., Zhou, Z., Chen, X., De Rycke, R., Rakusová, H., Wang, W., Jones, A.M., Friml, J., Patterson, S.E., Bleecker, A.B., Yang, Z.,** (2014). Cell Surface ABP1-TMK Auxin-Sensing Complex Activates ROP GTPase Signaling. *Science* 343, 1025. <https://doi.org/10.1126/science.1245125>

- Yanagawa, Y., Sullivan, J.A., Komatsu, S., Gusmaroli, G., Suzuki, G., Yin, J., Ishibashi, T., Saijo, Y., Rubio, V., Kimura, S., Wang, J., Deng, X.W.,** (2004). Arabidopsis COP10 forms a complex with DDB1 and DET1 in vivo and enhances the activity of ubiquitin conjugating enzymes. *Genes Dev.* 18, 2172–2181. <https://doi.org/10.1101/gad.1229504>
- Zhao, Y.,** (2018). Essential Roles of Local Auxin Biosynthesis in Plant Development and in Adaptation to Environmental Changes. *Annu. Rev. Plant Biol.* 69, 417–435. <https://doi.org/10.1146/annurev-arplant-042817-040226>
- Zheng, X., Wu, S., Zhai, H., Zhou, P., Song, M., Su, L., Xi, Y., Li, Z., Cai, Y., Meng, F., Yang, L., Wang, H., Yang, J.,** (2013). Arabidopsis Phytochrome B Promotes SPA1 Nuclear Accumulation to Repress Photomorphogenesis under Far-Red Light. *Plant Cell* 25, 115. <https://doi.org/10.1105/tpc.112.1070>

Figure Legends

Figure 1: HY5 mediates the root response to higher ambient temperature

(A) Wild type and *hy5* allelic mutant seedling plants 6DAG and 3 days after transfer at 21°C or 27°C. (B-D), Normalized root growth (27°C/21°C) in wild type, *hy5*, *hy5-221*, *hy5-1* and *hy5-215*. (E) Root meristem in wild type and *hy5-221* 5DAG and 2 days after transfer at 21°C or 27°C. Asterisks mark the root transition zone. (F) Normalized root meristem size (27°C/21°C) in wild type and *hy5-22* at 24, 48 and 72 hours after temperature shift. Statistics: n indicates the number of individual seedlings measured. Measured seedlings were obtained in one (F) or two (B,C,D) independent replications of the experiment. One-way ANOVA, Tukey HSD post-hoc test $P < 0.05$ (A). Student's t-test (C,D,F). Red bar represents the mean (B,C,D,F). Scale bar: 5mm (A), 100µm (E).

Figure 2: Phytochrome signaling regulates the root response to higher ambient temperature

(A) Wild type (WT) and *phyAB* mutant seedlings 6DAG and 3 days after transfer at 21°C or 27°C. (B) Normalized root growth (27°C/21°C) in wild type and *phyAB*. (C) Root meristem in wild type and *phyAB*, 5DAG 2 days after transfer at 21°C or 27°C. Asterisk marks the root transition zone. (D) Normalized root meristem size (27°C/21°C) in wild type and *phyAB*, 48 and 72 hours after temperature shift. (E) Wild type, *pif4*, *pifQ* and PIF4 OX mutant seedlings 6DAG and 3 days after transfer at 21°C or 27°C. (F-G) Normalized root growth (27°C/21°C) in wild type, *pif4*, *pifQ* (F) and PIF4 OX (G). Statistics: n indicates the number of individual seedlings measured. Measured seedlings were obtained in one (F) or two (B,D,G) independent replications of the experiment. One-way ANOVA, Tukey HSD post-hoc test $P < 0.05$ (F). Student t-test (B,D,G). Red bar represents the mean (B,D,F,G). Scale bar: 5mm (A,E), 100µm (C).

Figure 3: HY5-PIF module regulates the root response to temperature.

(A) Wild type, *hy5*, *hy5 det1* and *hy5 cop1* mutant seedlings 6DAG and 3 days after transfer at 21°C or 27°C. (B-C) Normalized hypocotyl (B) and root growth (C) (27°C/21°C) in wild type, *cop1*, *det1*, *hy5*, *hy5 det1* and *hy5 cop1*. (D) Wild type, *pifQ*, *hy5* and *hy5 pifQ* mutant seedlings 6DAG and 3 days after transfer at 21°C or 27°C. (E-F) Normalized hypocotyl (E) and root growth (F) (27°C/21°C) in wild type, *pifQ*, *hy5-215* and *hy5 pifQ*. (G-H) Relation between root and hypocotyl growth rate at 27°C as shown with measurements on individual wild type (n=23), *hy5-221* (n=24), *phyAB* (n=43), PIF4OX (n=22), *hy5* (n=22), *hy5 det1* (n=20), *hy5 cop1* (n=22), *hy5-215* (n=23), *hy5 pifQ* (n=22) plants (G) and after non-parametric regression analysis (H). Statistics: n indicates the number of individual seedlings measured. Measured seedlings were obtained in one (G,H) or three (B,C,E,F) independent replications of the experiment. One-way ANOVA, Tukey HSD post-hoc test $P < 0.05$ (C,F). One way ANOVA after log10 transformation (B,E), linear regression method, Pearson correlation (H). Red bar represents the mean (B,C,E,F). Scale bar: 5mm (A,D).

Figure 4: Shoot response to temperature is sufficient to modulate root growth response

(A-C) Brightfield or false color view of wild type seedlings 6DAG (A) and two independent lines of *hy5* carrying *pCAB3:DOF-HY5* (B,C). (D-E) Immunoblotting of shoot (D) or root tissues (E) in wild type (WT), *hy5*, two independent lines of *hy5* carrying *pCAB3:DOF-HY5*, *hy5* carrying *pCER6:DOF-HY5* and *pCAB3:DOF-HY5* lines at 27°C. DoF-HY5 protein was detected using HA or HY5 antibodies. Amido black staining and actin antibody were used as controls. (F) Normalized hypocotyl growth (27°C/21°C) in wild type, *hy5* and *pCAB3:DOF-HY5* rescue lines. (G) Normalized root growth (27°C/21°C) in wild type, *hy5* and *pCAB3:DOF-HY5* rescue lines. Statistics: n indicates the number of individual seedlings measured. Measured seedlings were obtained in two (D-G) or three (A-C) independent replications of the experiment. One-way ANOVA, Tukey HSD post-hoc test $P < 0.05$ (F,G). Red bar represents the mean (F,G). Scale bar: 100µm (A-C).

Figure 5: Genome-wide analysis of root response to temperature.

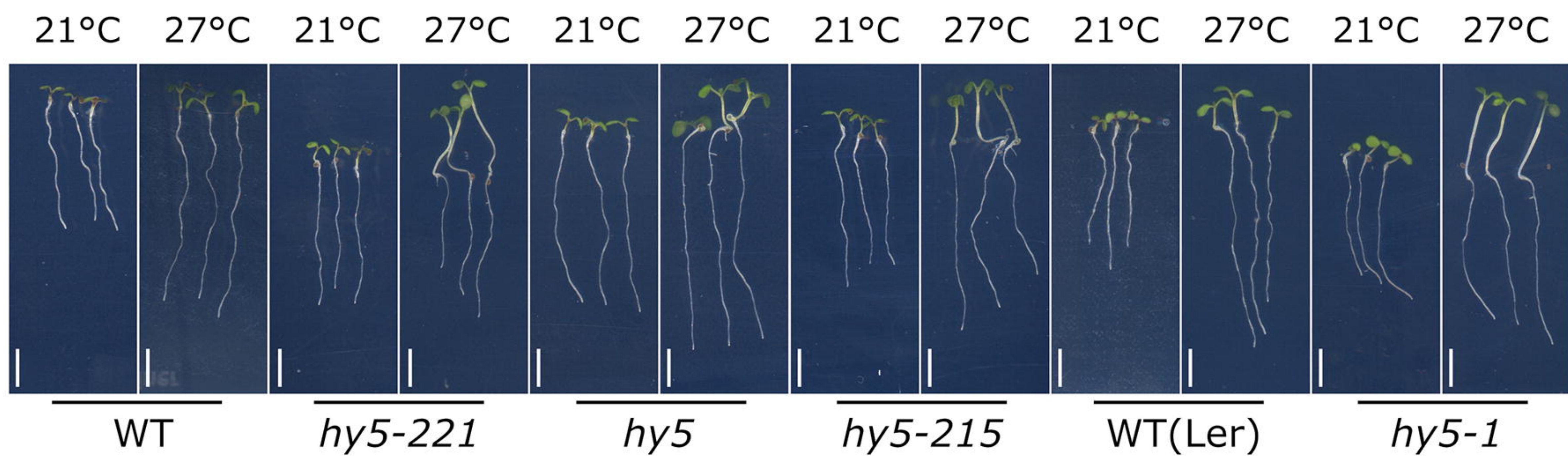
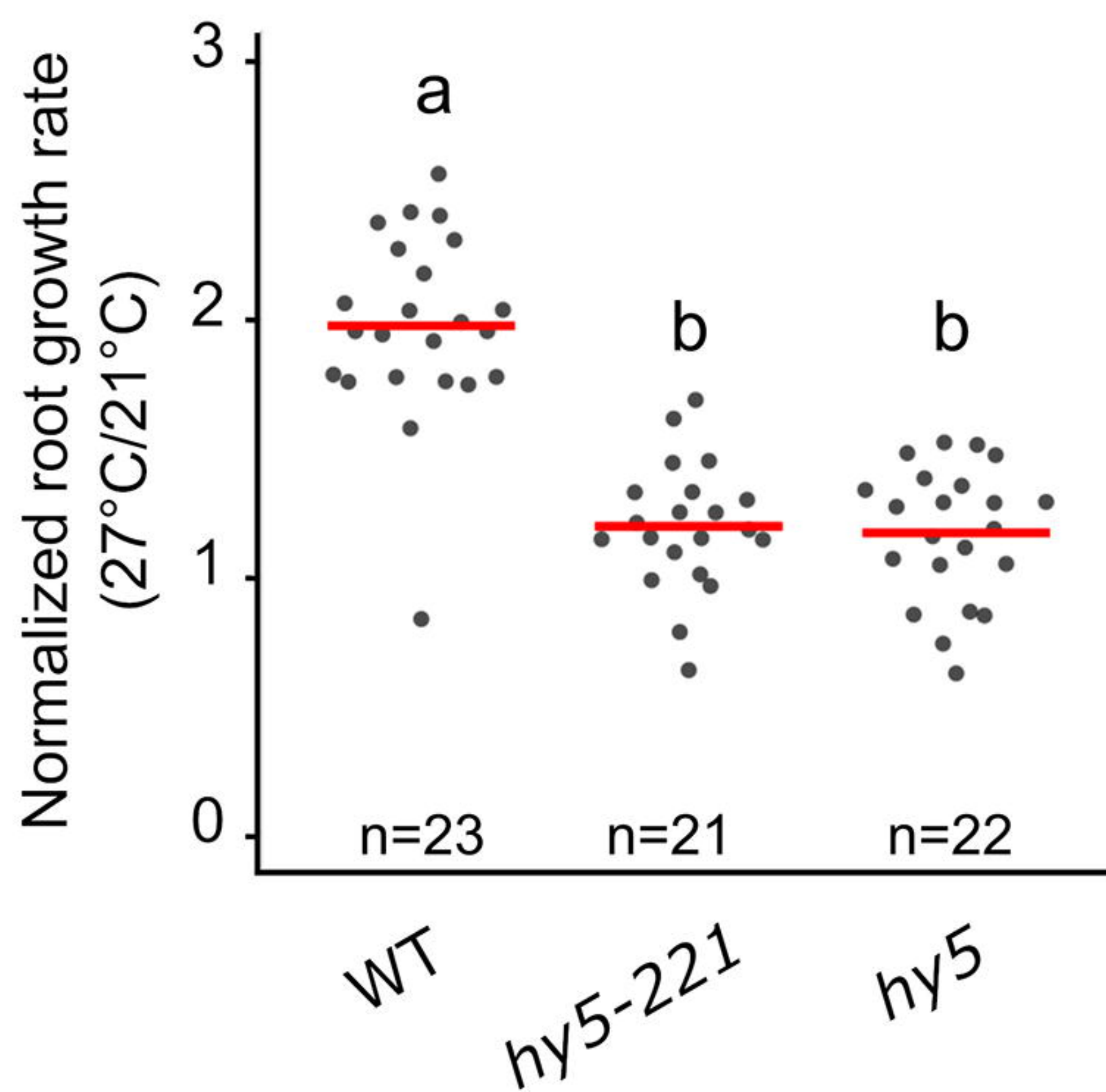
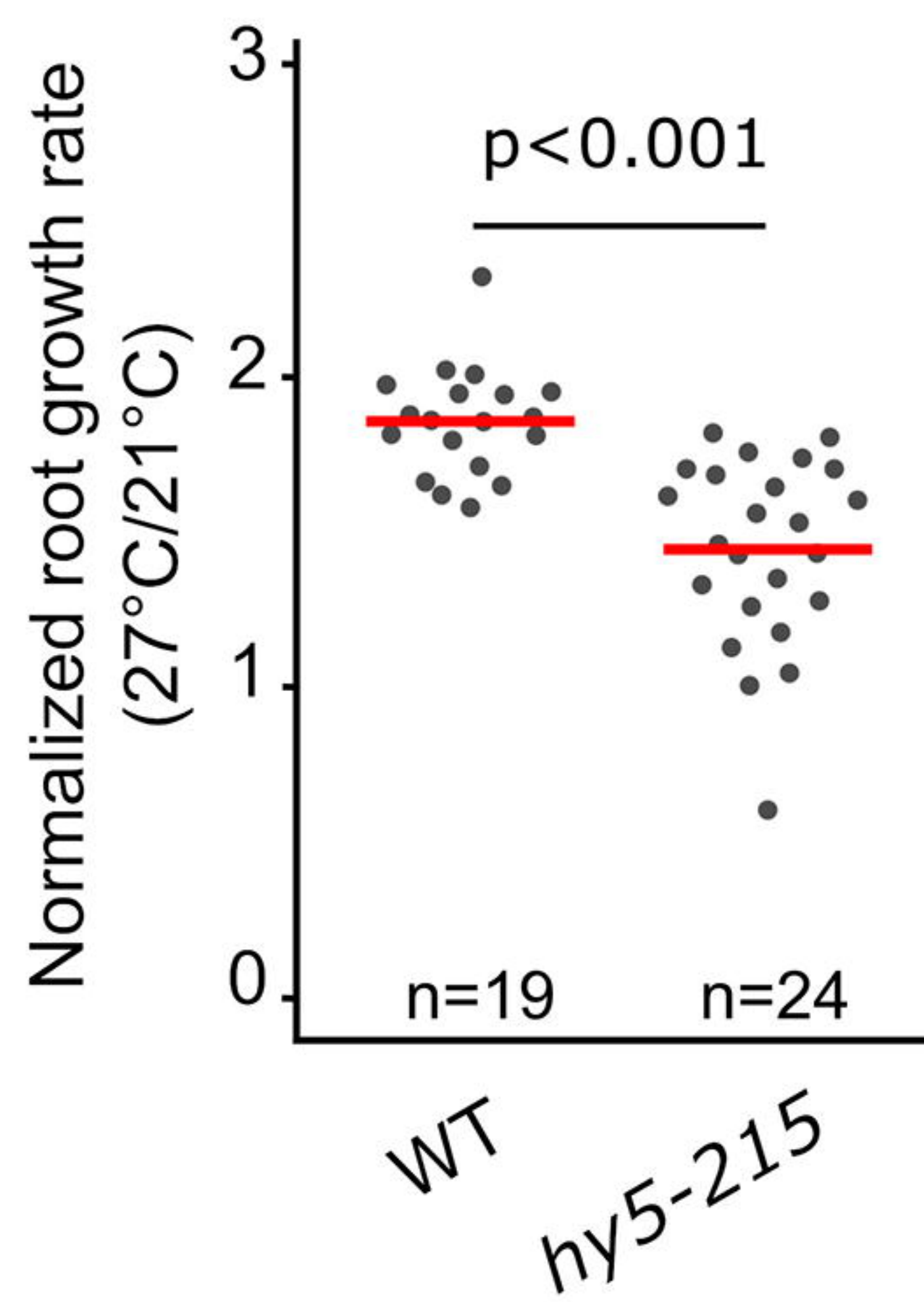
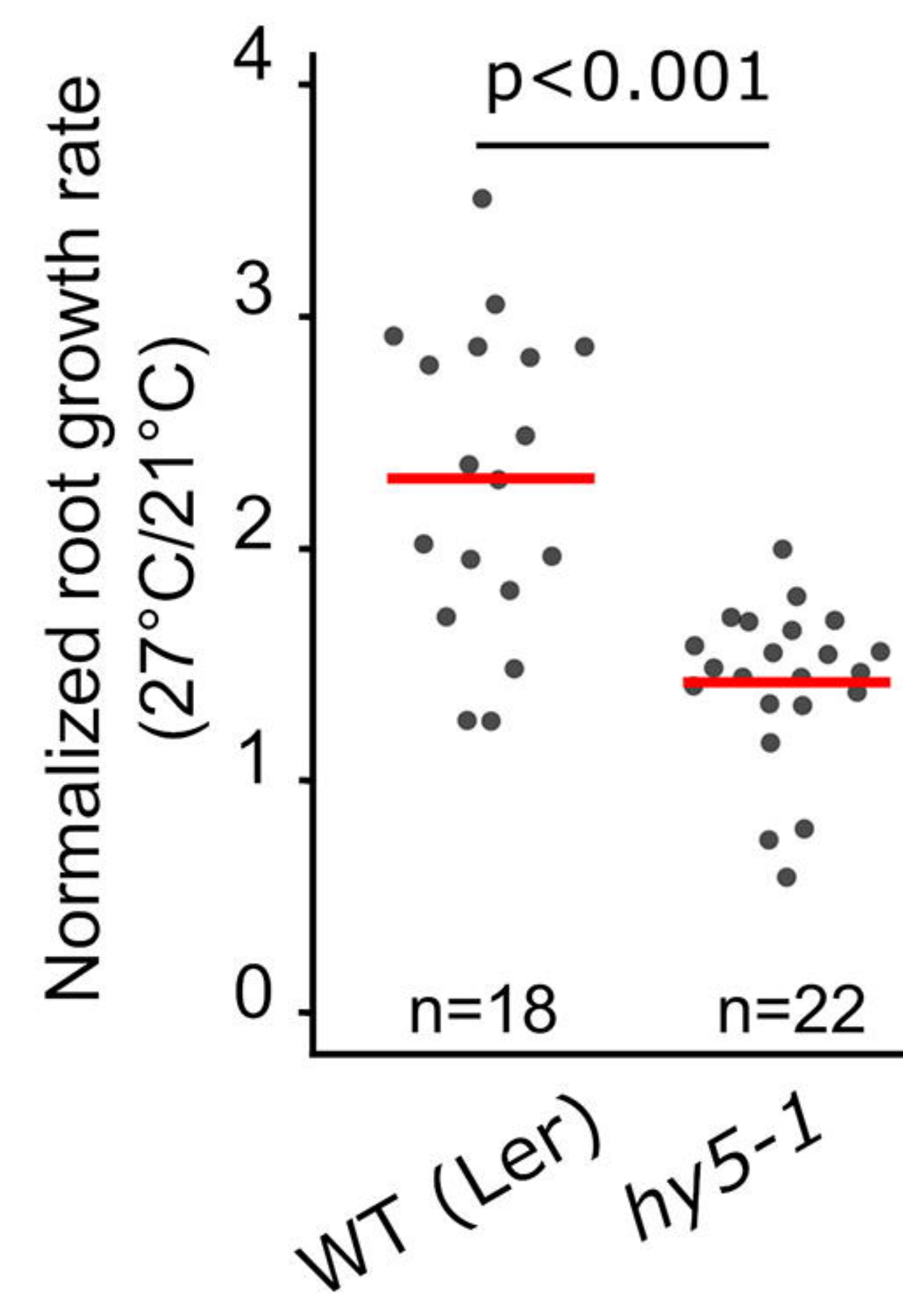
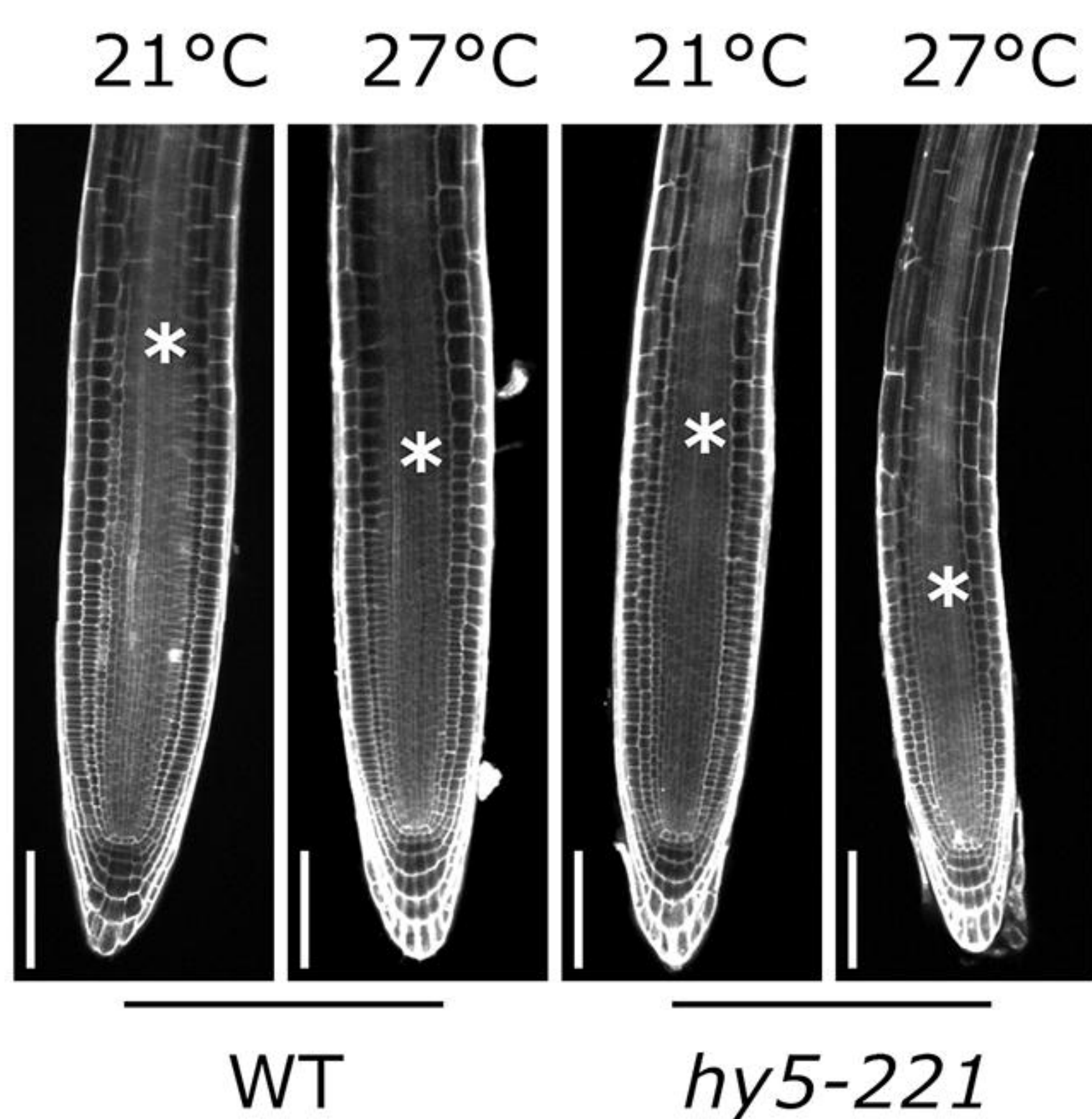
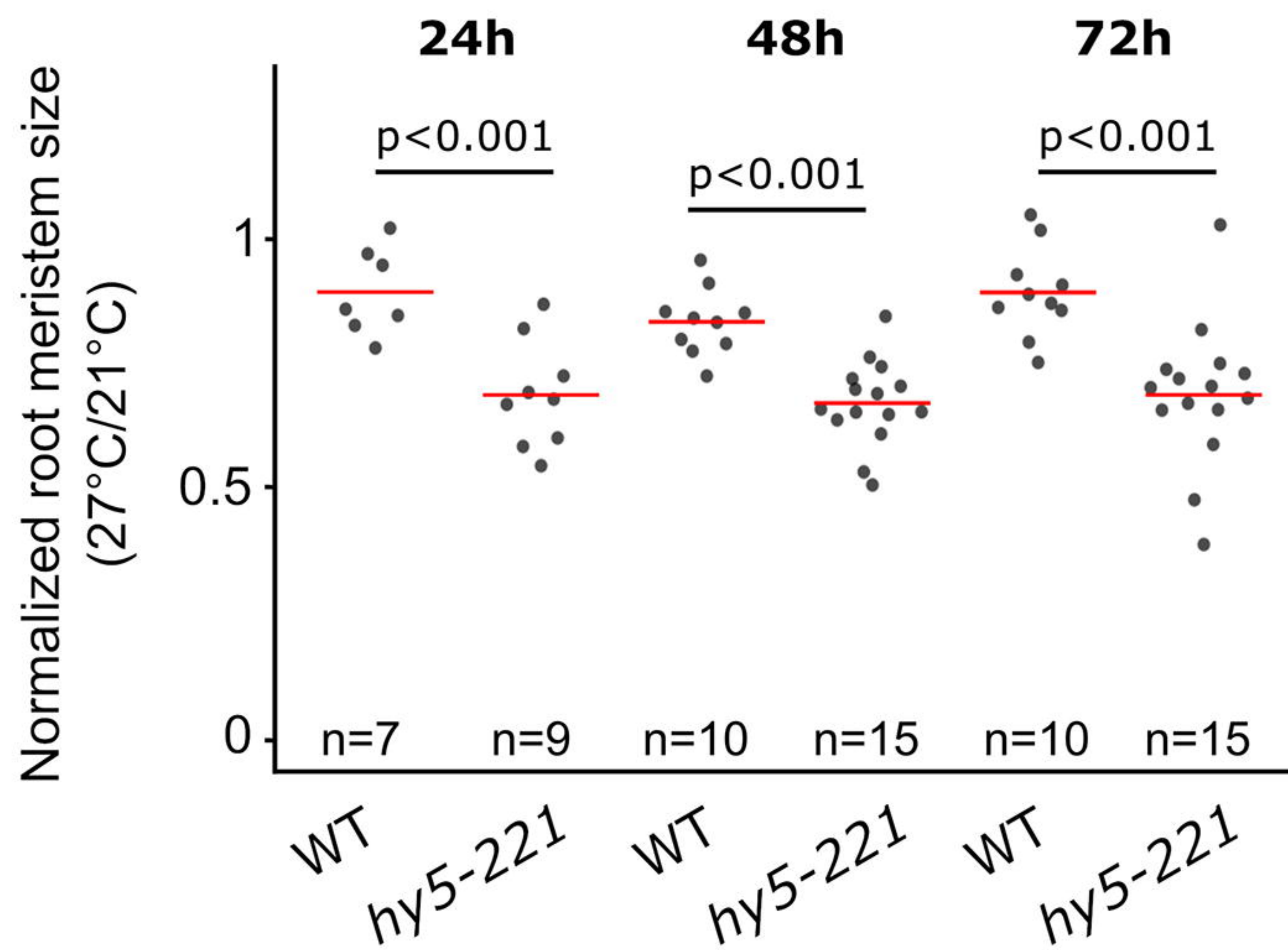
(A-B) Genes regulated 4 hours (A) or 18 hours (B) after temperature shift in wild type, *hy5* and *phyAB* roots. Gene ontologies (GO) characterize the biological processes enriched among the temperature-regulated genes that are shared between wild type, *hy5* and *phyAB*. (C) Overlapping misregulated genes in *hy5* and *phyAB* roots at 27°C. (D) Differentially regulated genes belonging to the GO category “Generation of precursor metabolites and energy genes” in *hy5* and *phyAB* roots at 27°C. Statistics: biological triplicate are analyzed; p-value as calculated with AgrigoV2 (A-C).

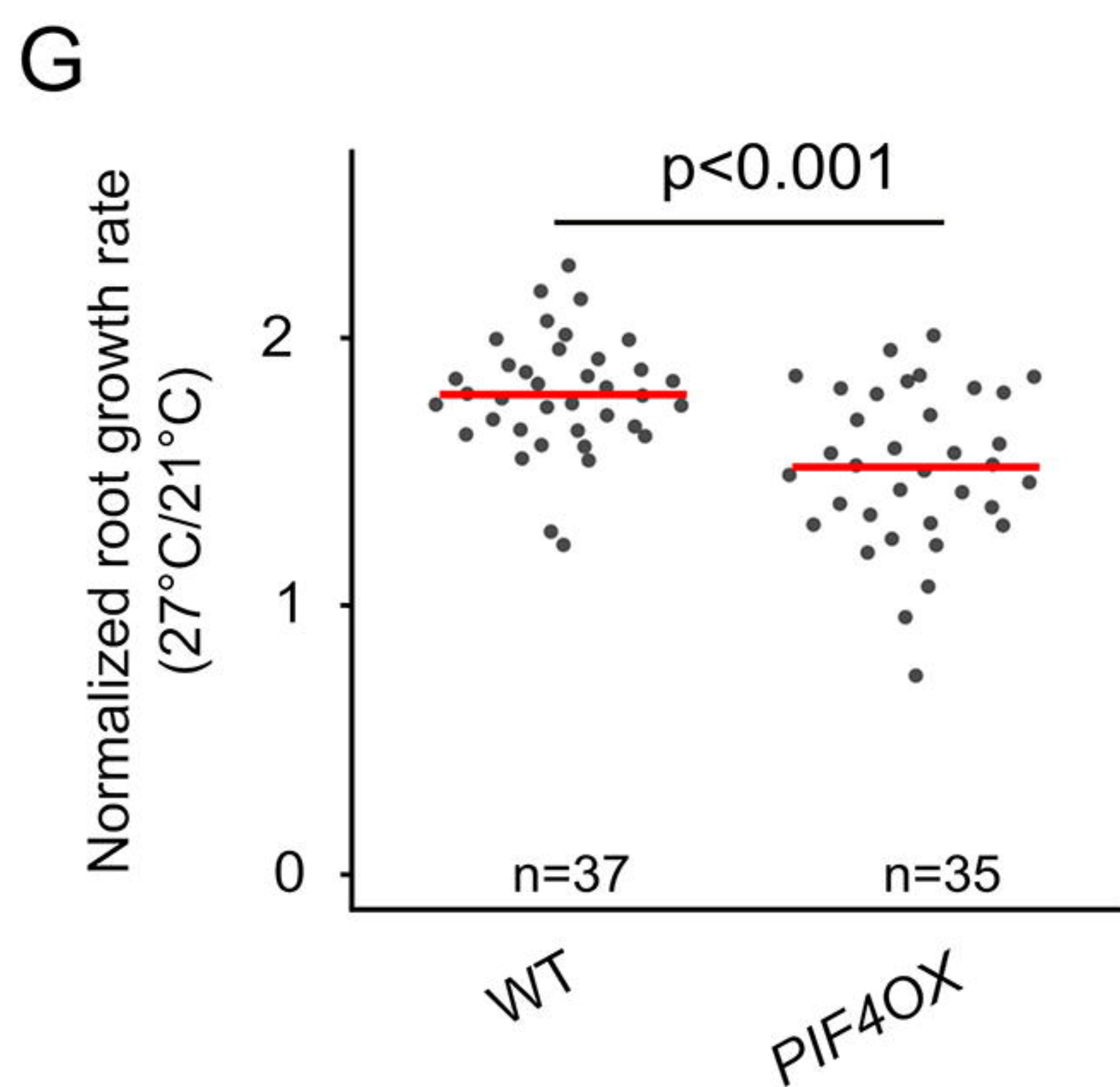
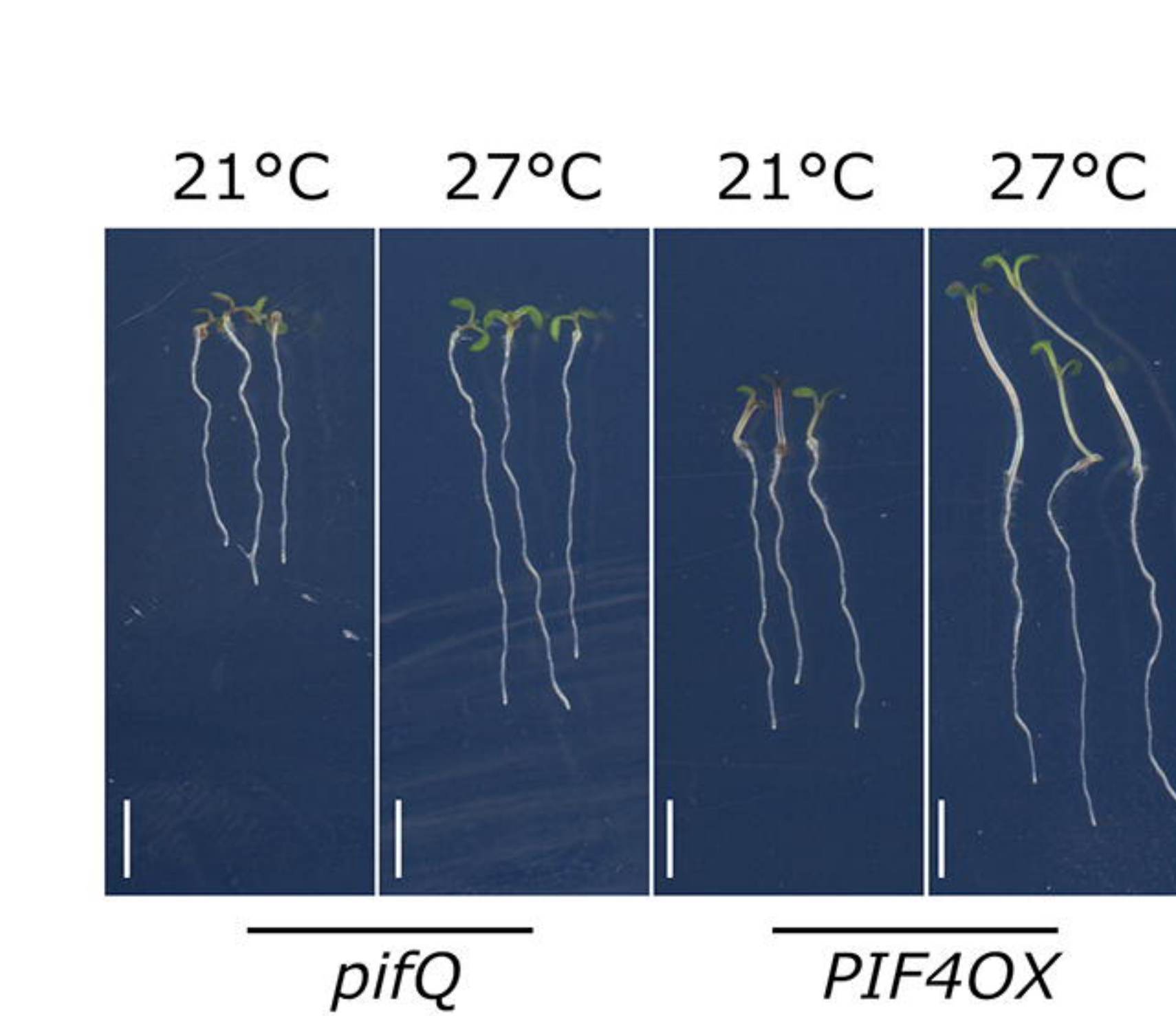
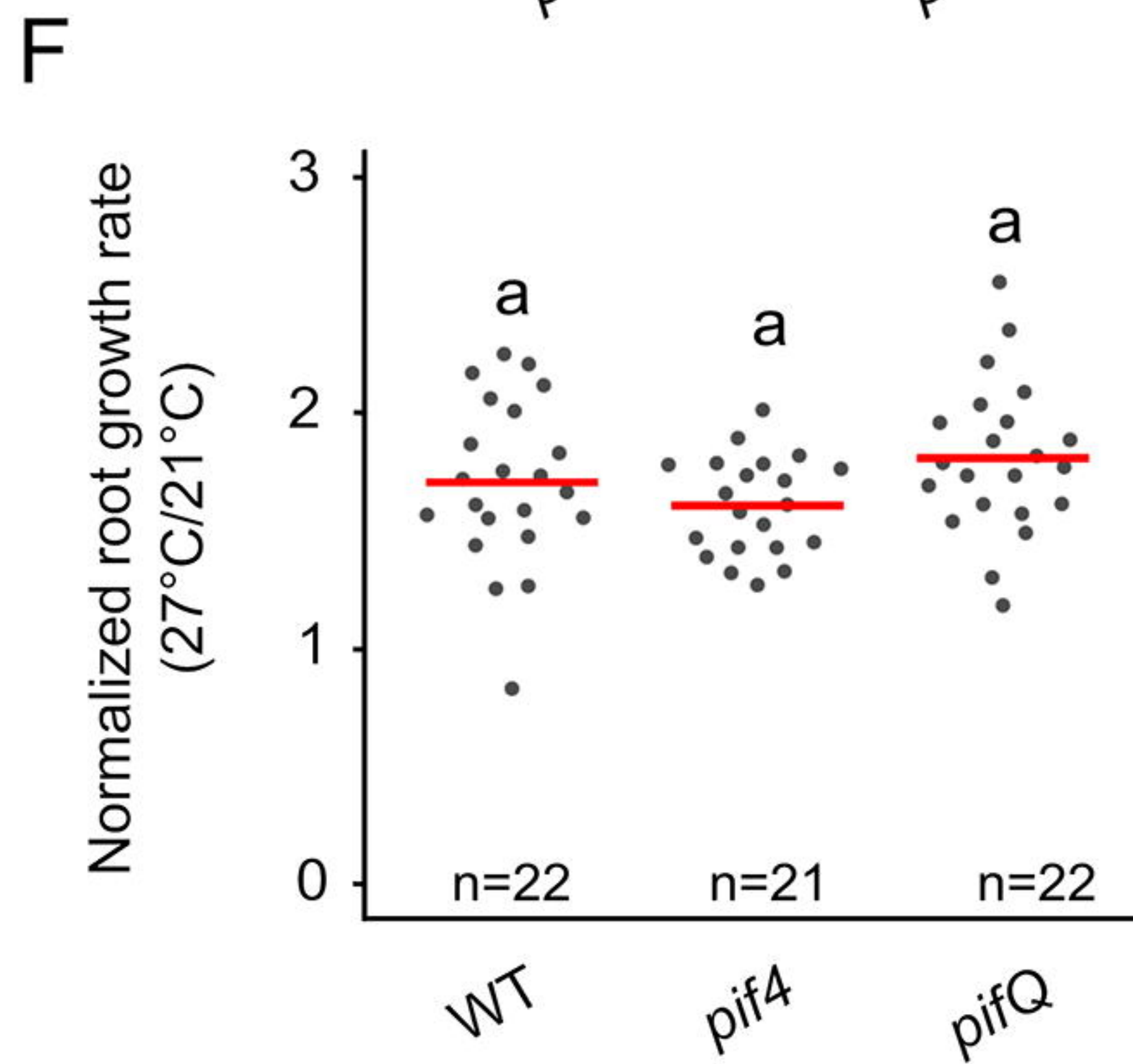
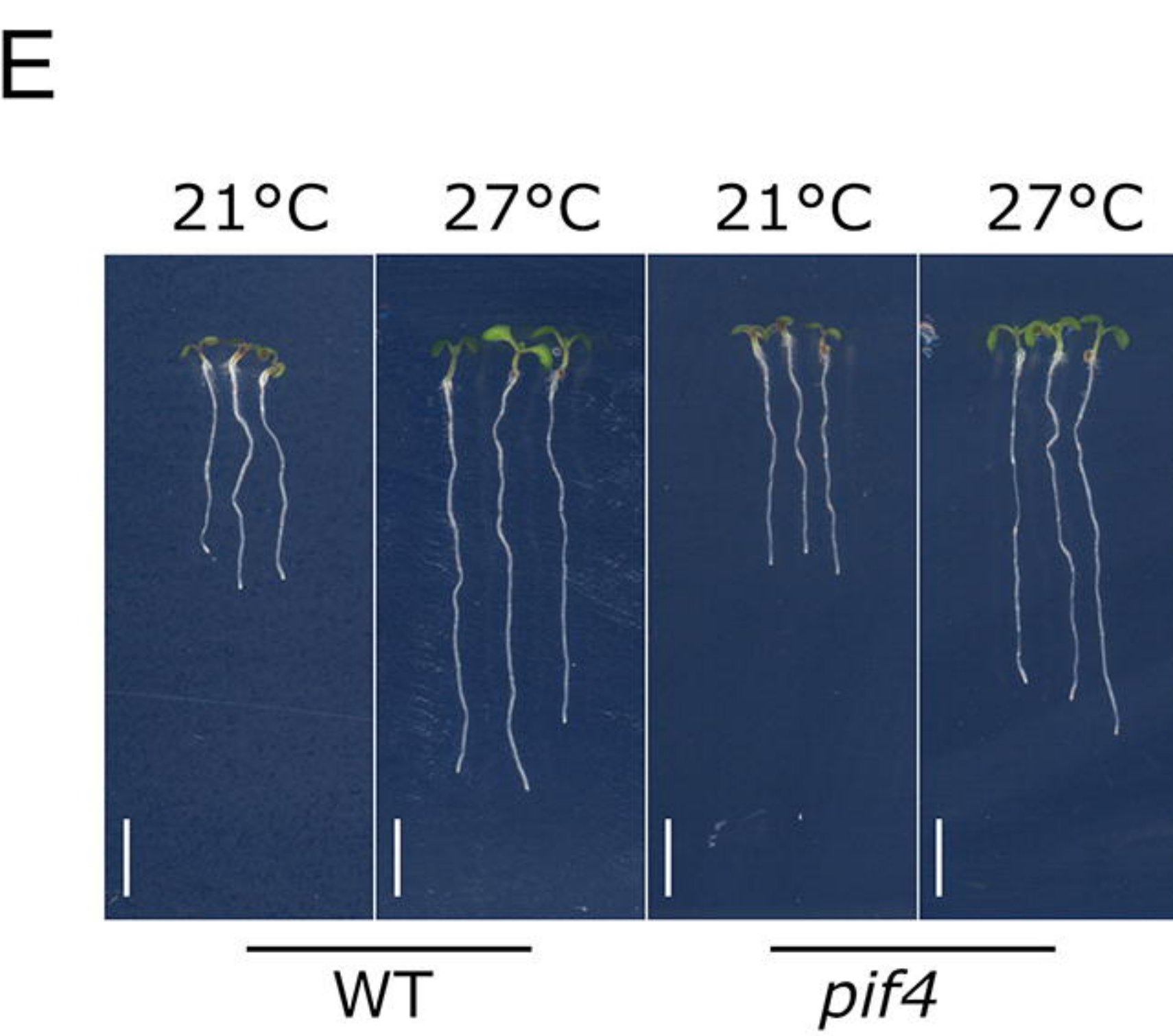
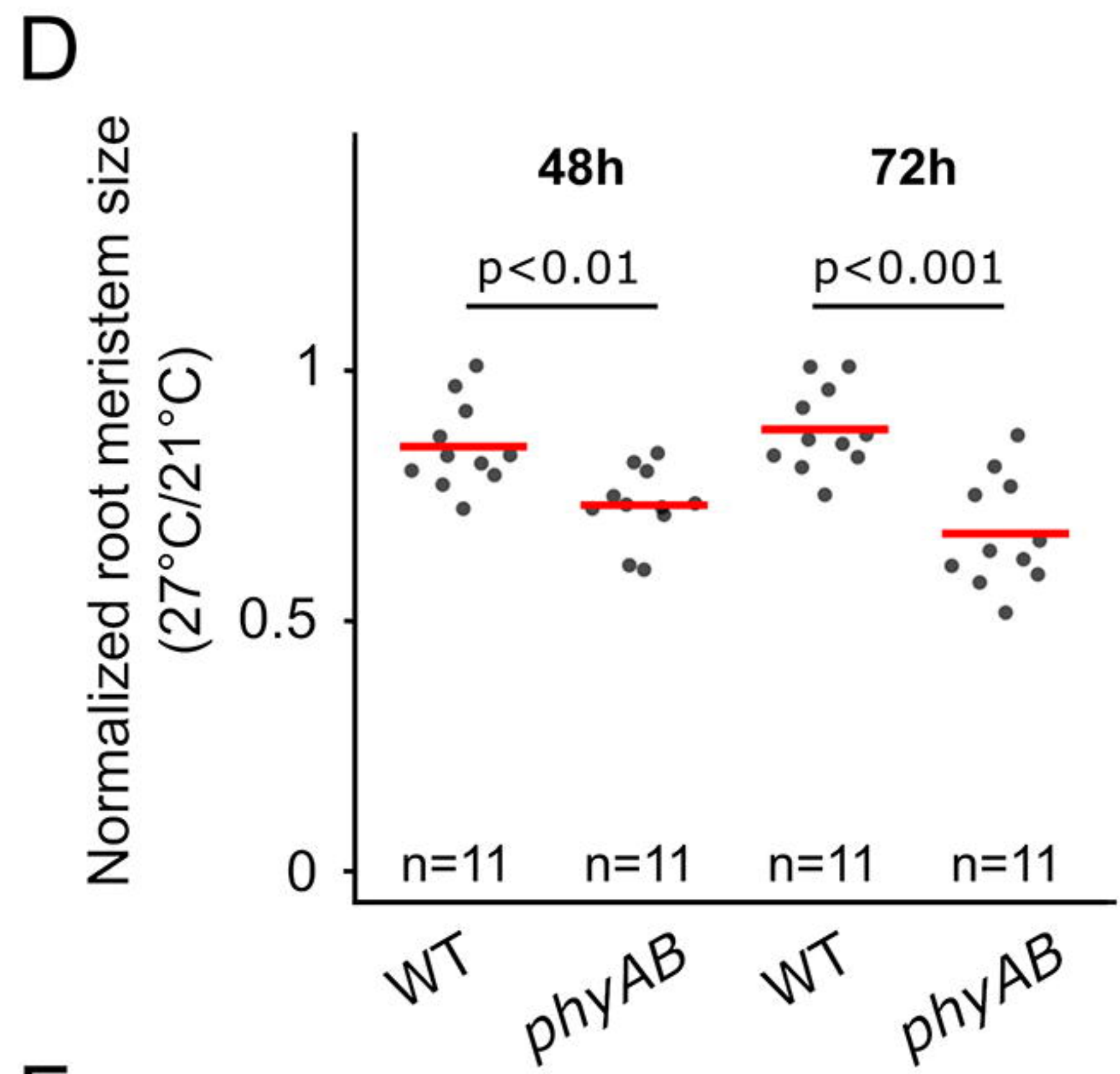
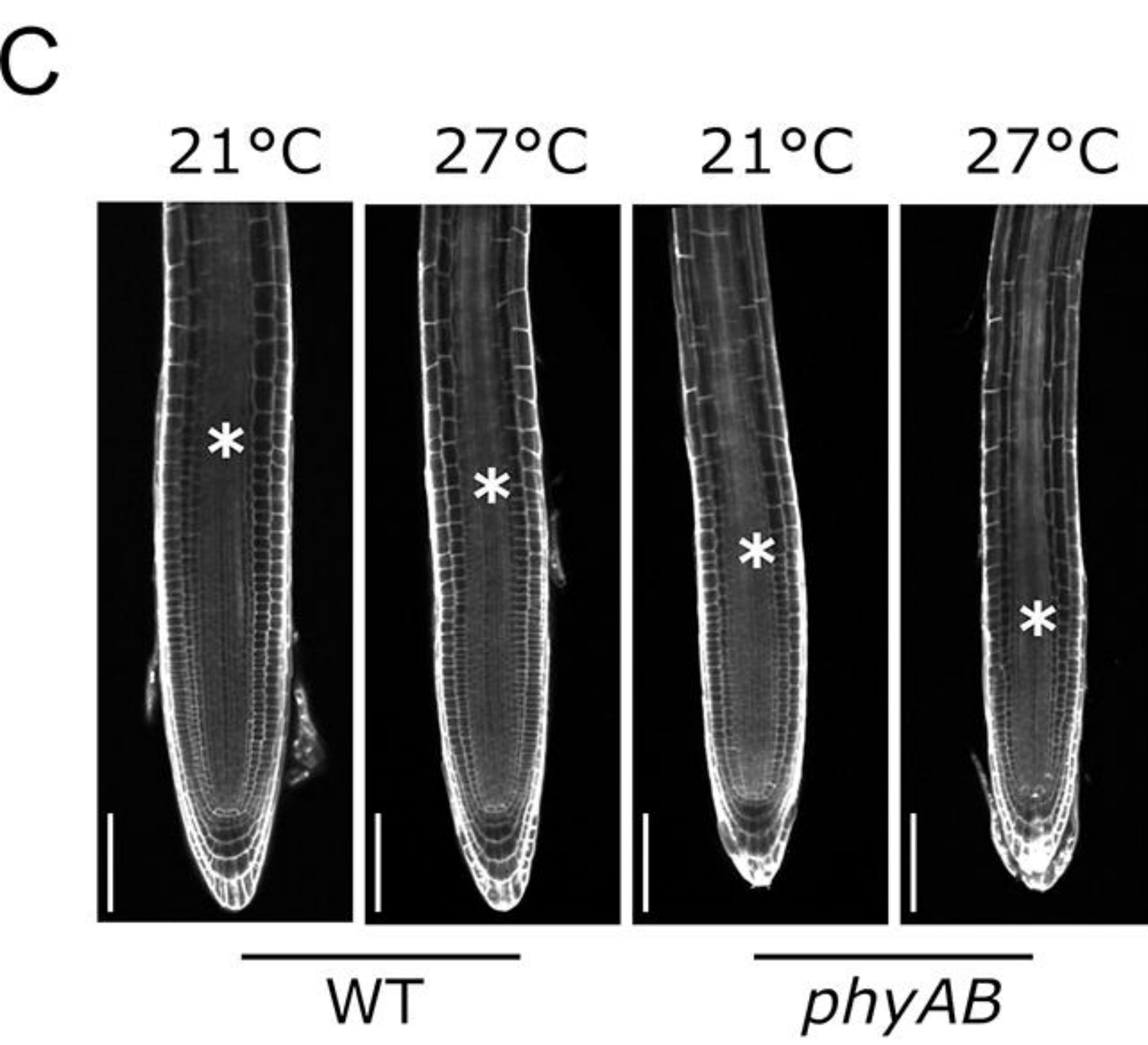
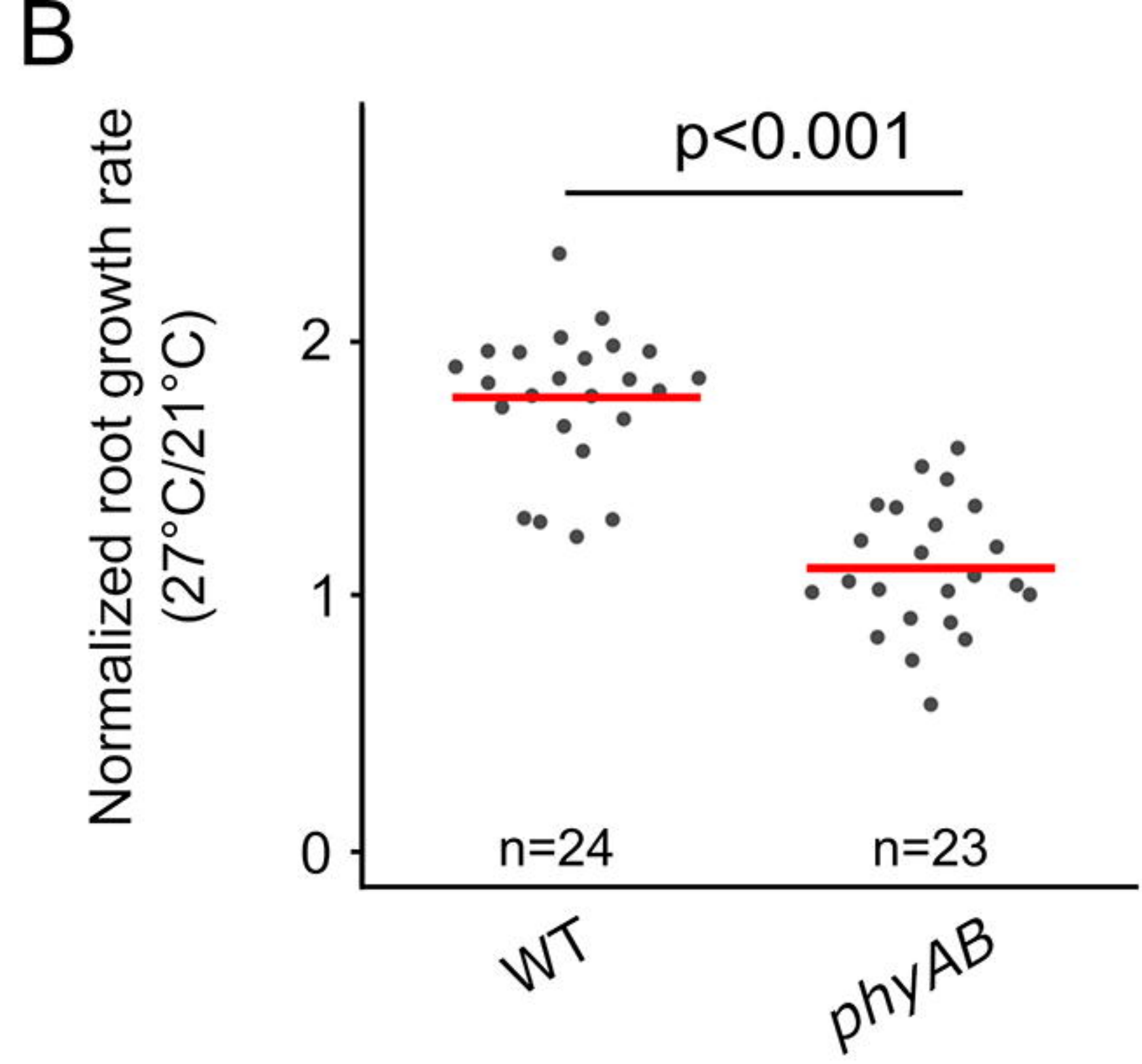
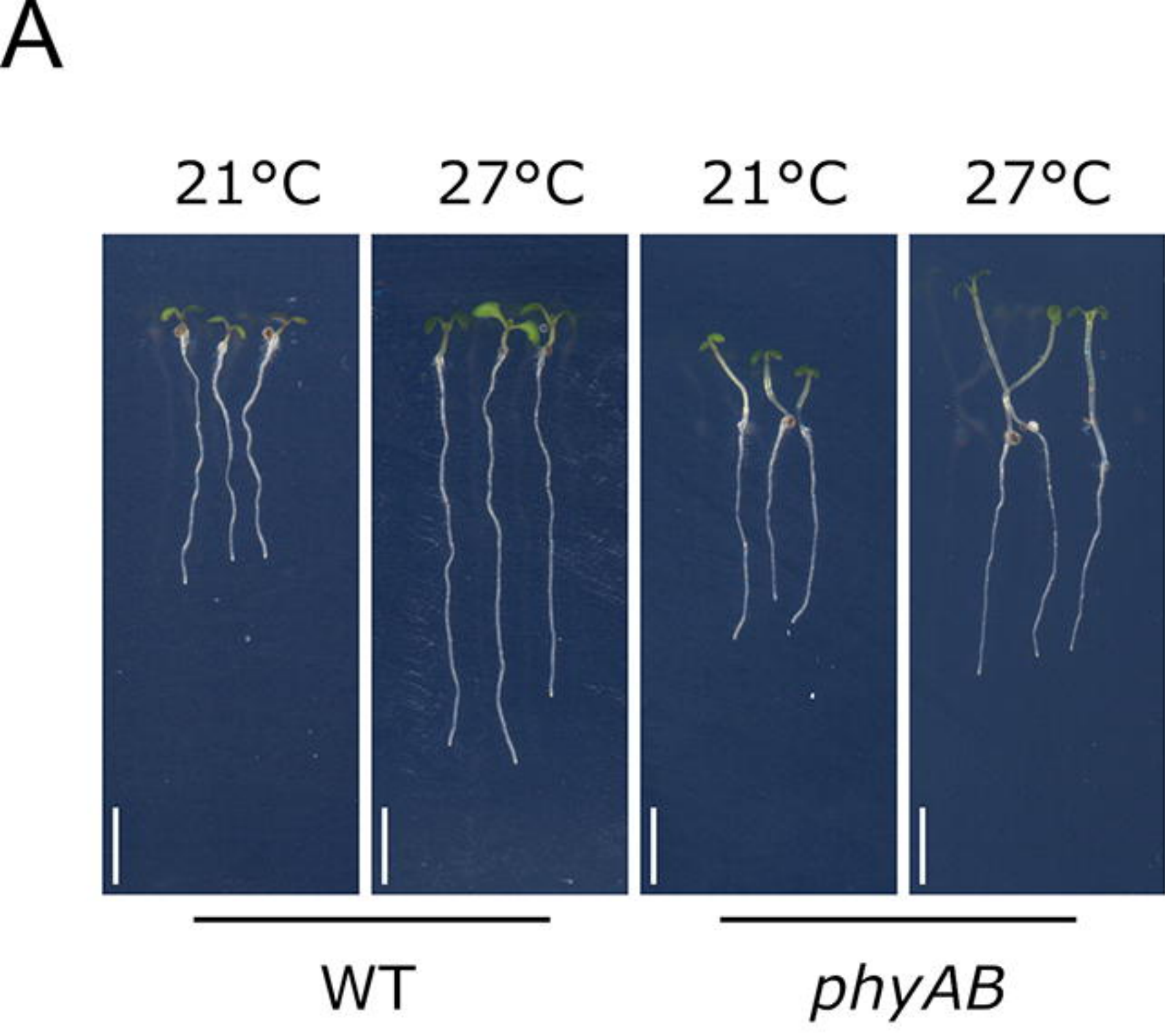
Figure 6: Auxin homeostasis regulates root thermomorphogenesis

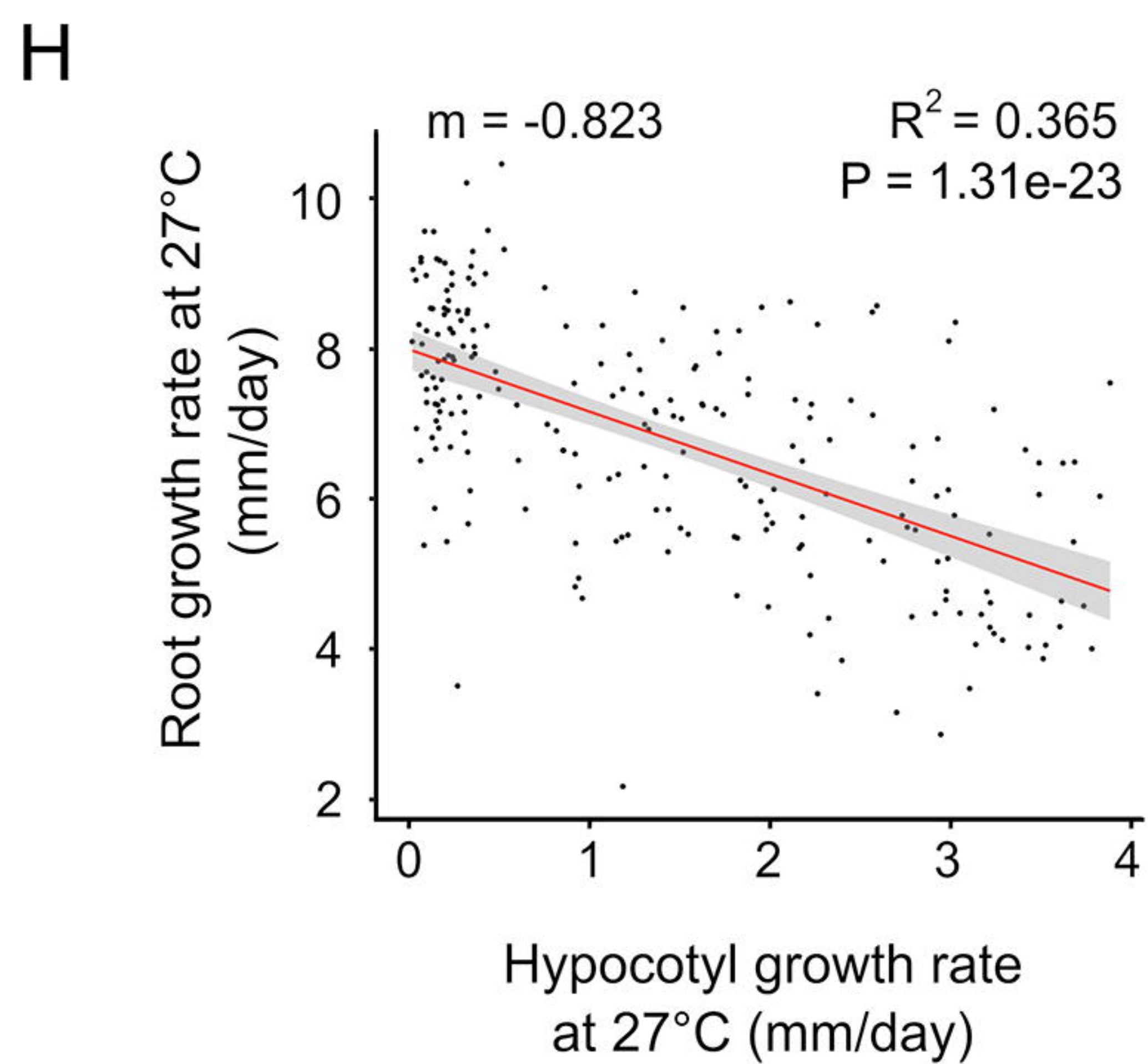
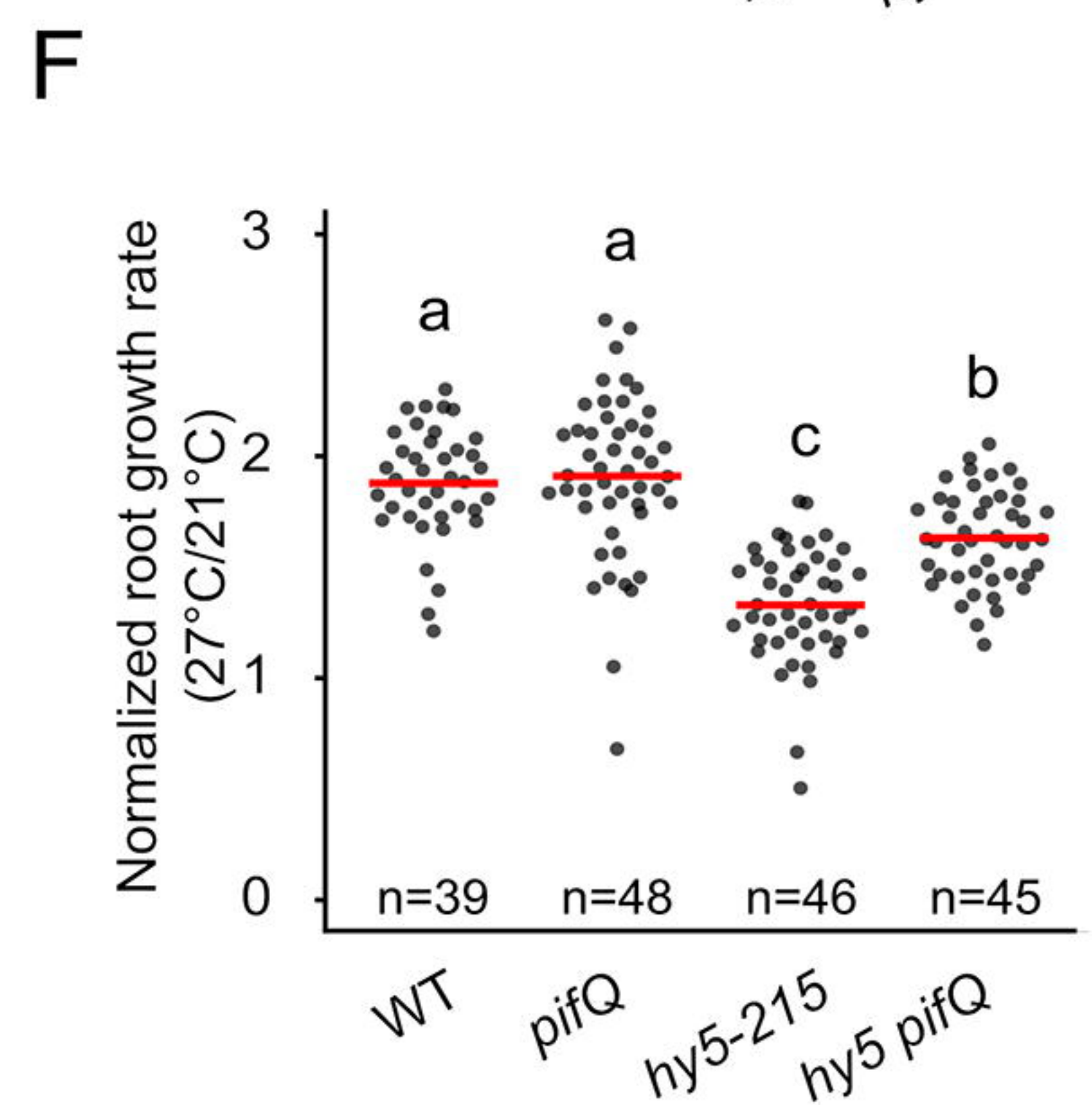
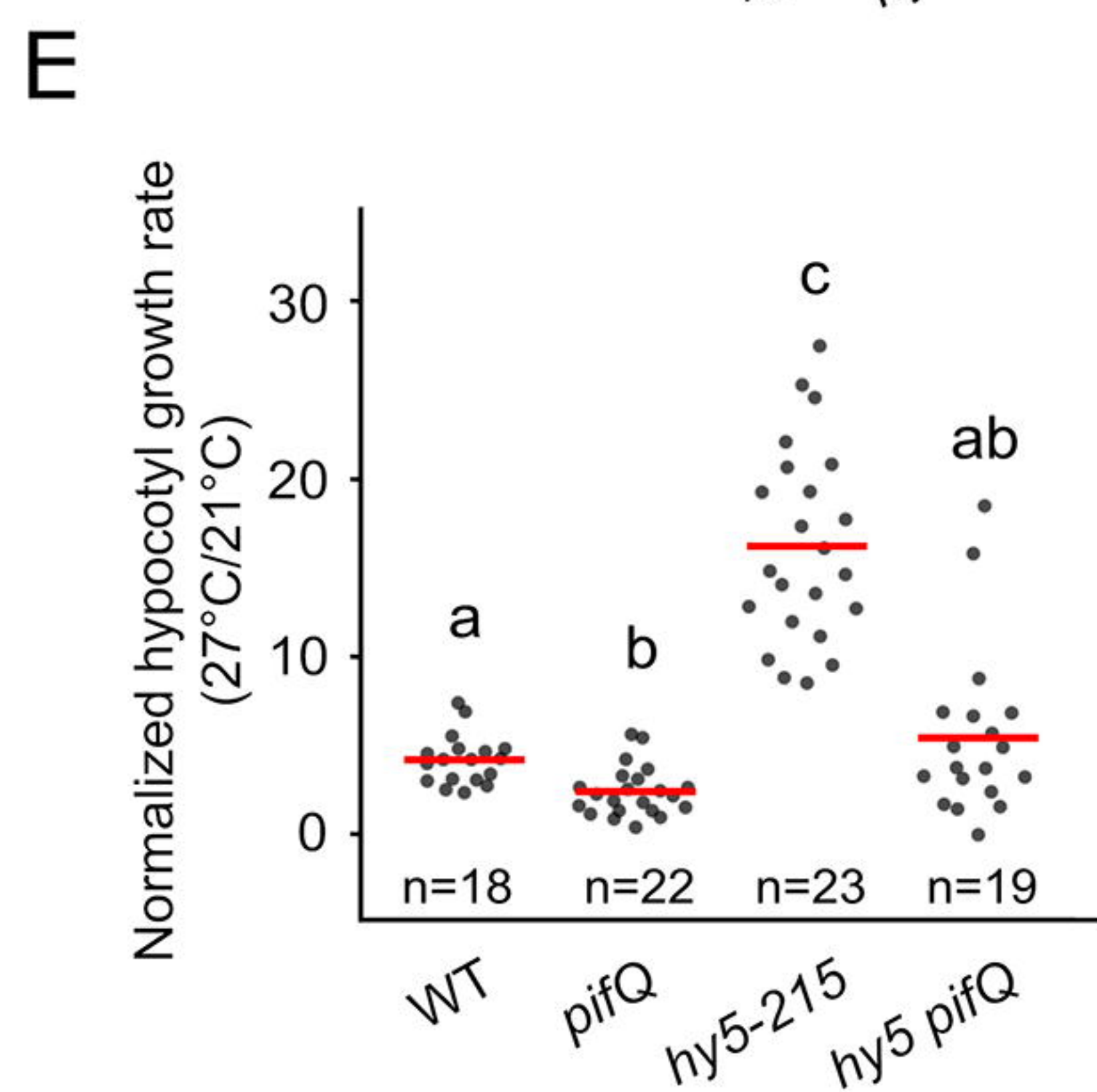
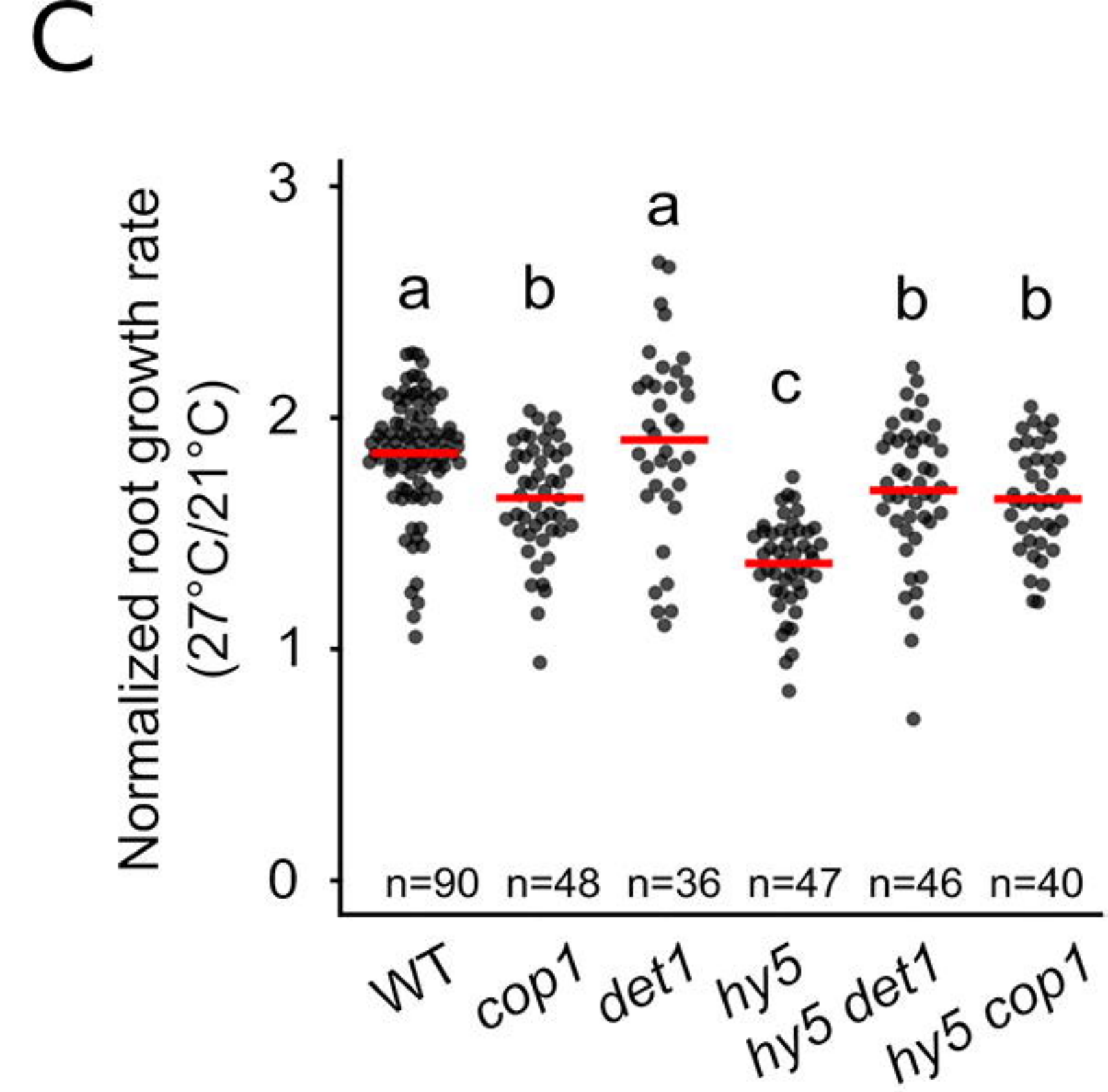
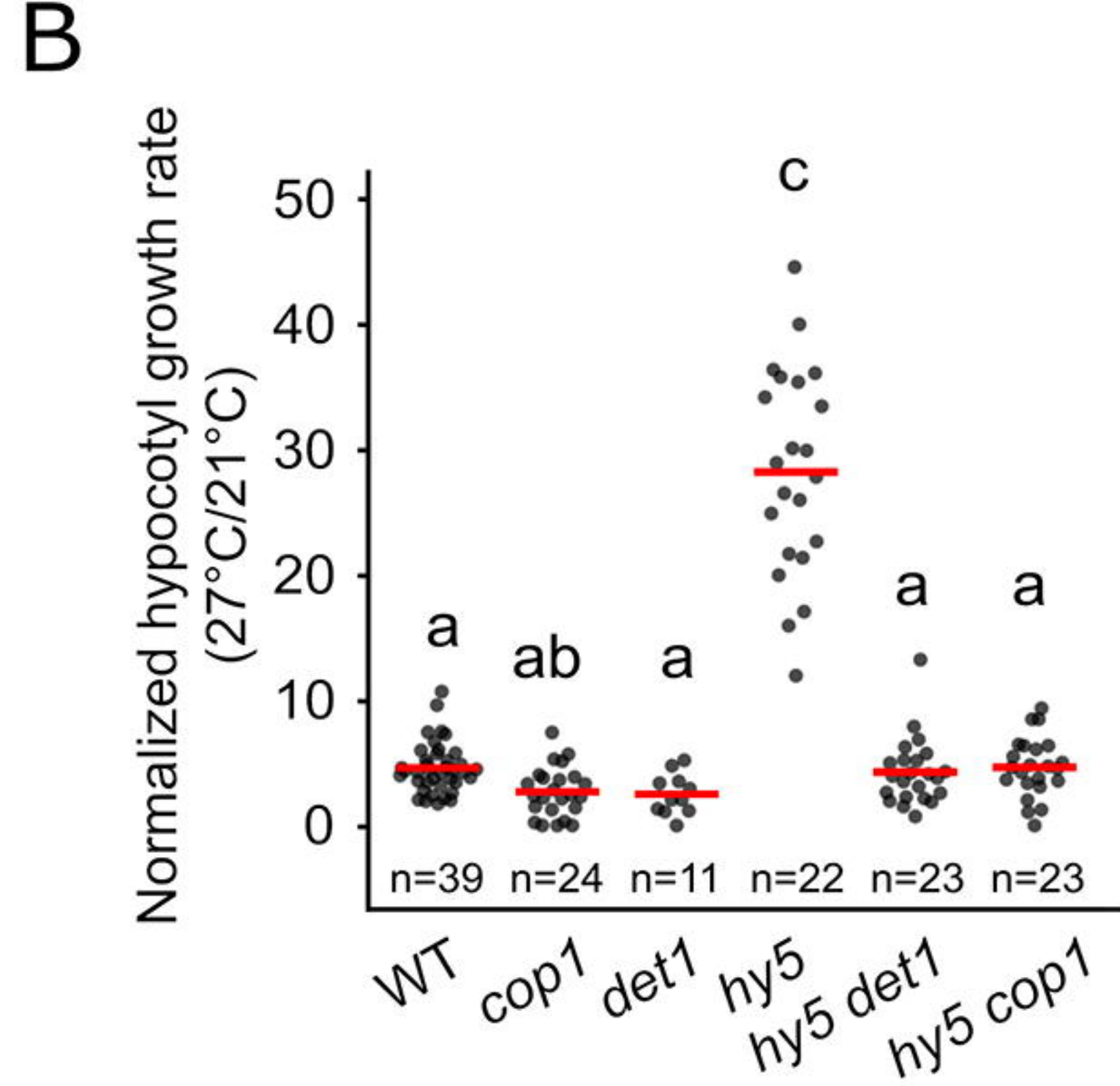
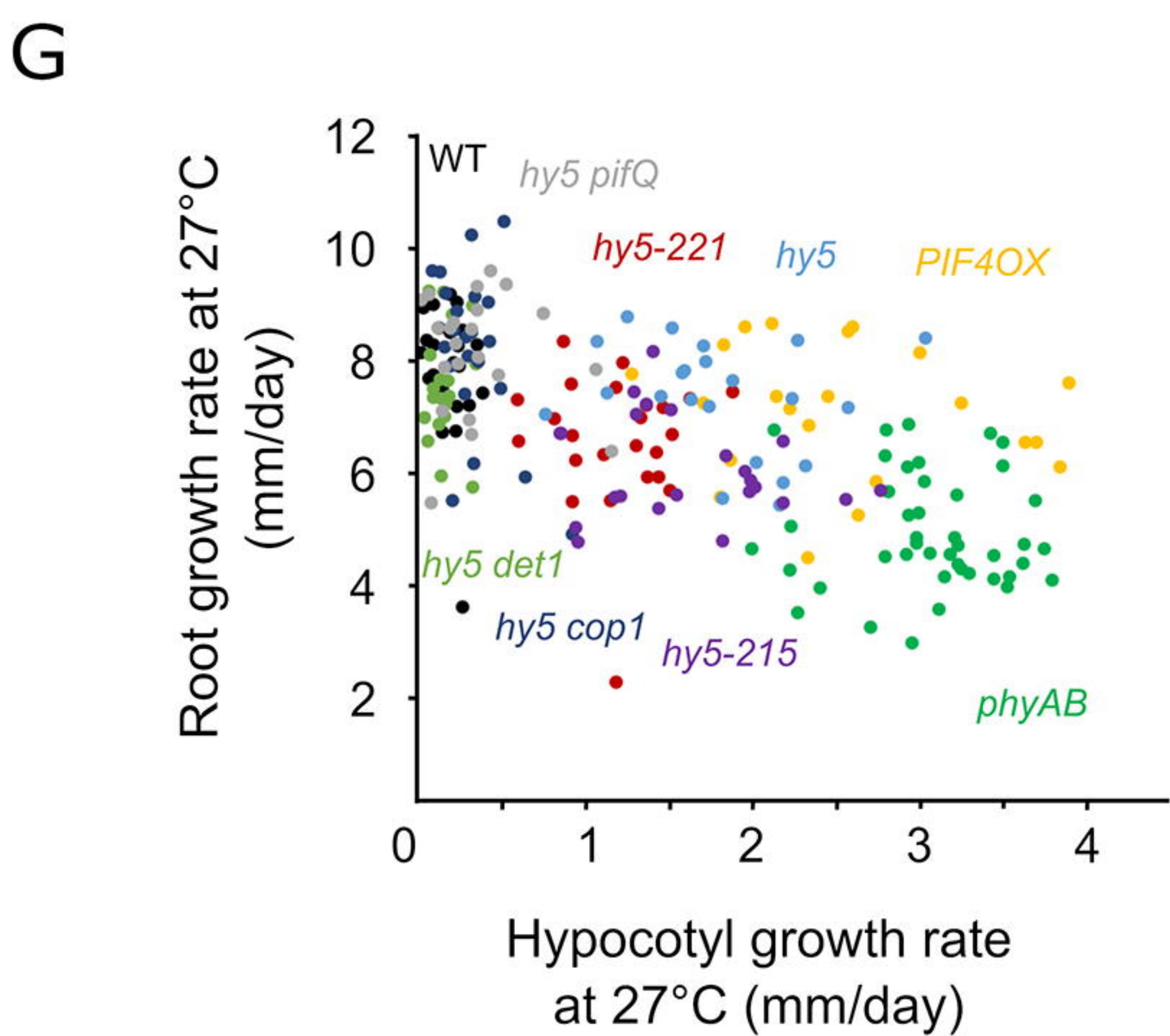
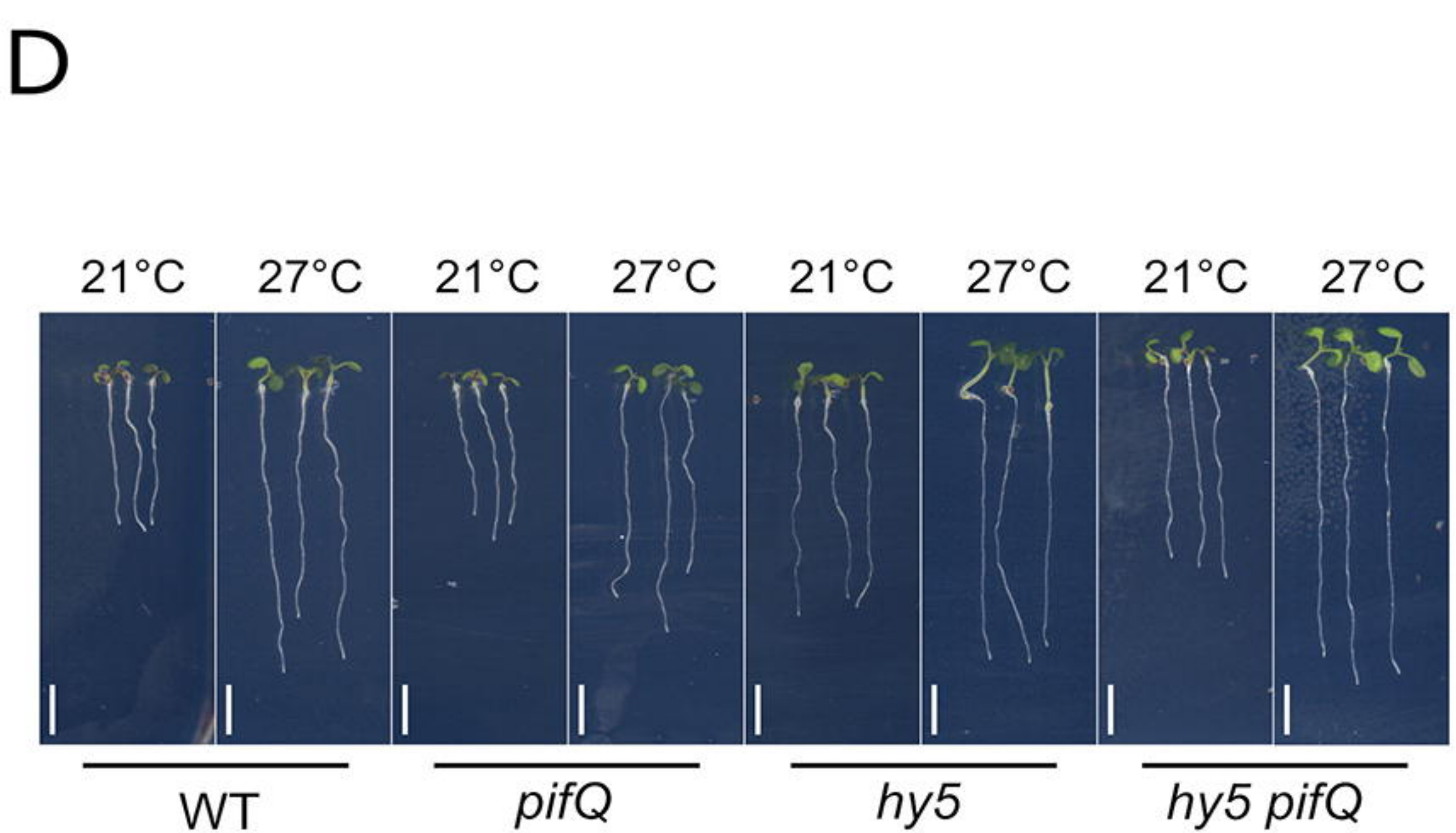
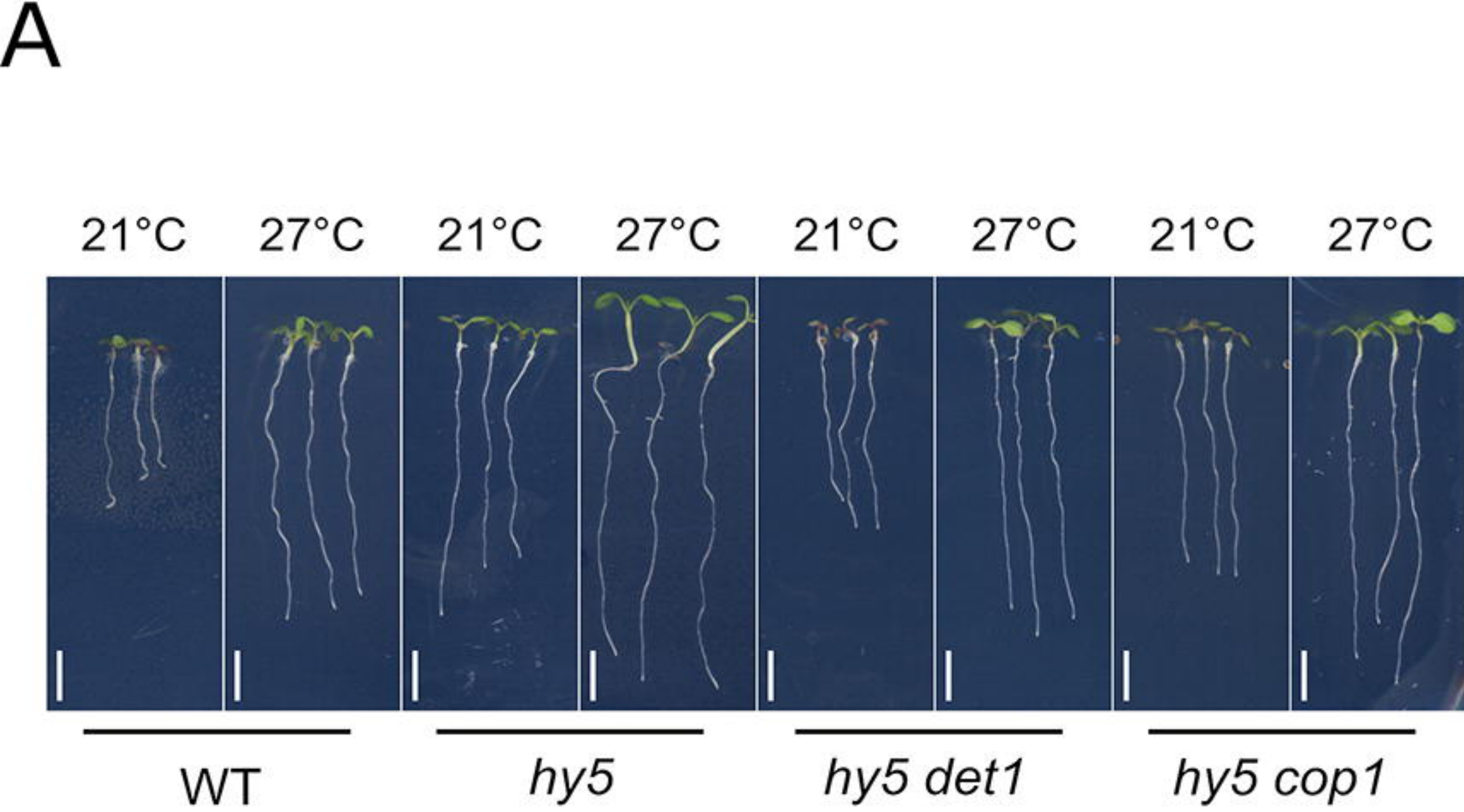
(A-C) Normalized root growth (27°C/21°C) in wild type, *tir1*, *afb2*, *tir1 afb2* (A), *tmk1,4* (B), *yucQ* (C) . (D) Differentially regulated genes in *hy5* and *phyAB* roots at 27°C that are auxin responsive according to (Omelyanchuk et al., 2017), 18 hours after temperature shift. (E) IAA concentration (pmol / g of fresh weight (FW)) in roots of seedlings 6DAG, 12 hours after transfer at 21°C or 27°C ($n > 3$). (F) Relative IAA content in root compared to shoot tissues of seedlings 6DAG, 12 hours after transfer at 21°C or 27°C ($n > 3$). Statistics: n indicates the number of individual seedlings measured (A-C) or the number of biological replicates (E,F). Measured seedlings were obtained in three (A-C) independent replications of the experiment. One-way ANOVA, Tukey HSD post-hoc test $p < 0.05$ (A,E). Student's t-test (B,C). Hypergeometric test (D). One-way ANOVA, Student-Newmann Keuls's post hoc test $p < 0.05$ (F). Red bar represents the mean (A-C).

Figure 7: A genetic model for organ growth coordination during plant thermomorphogenesis

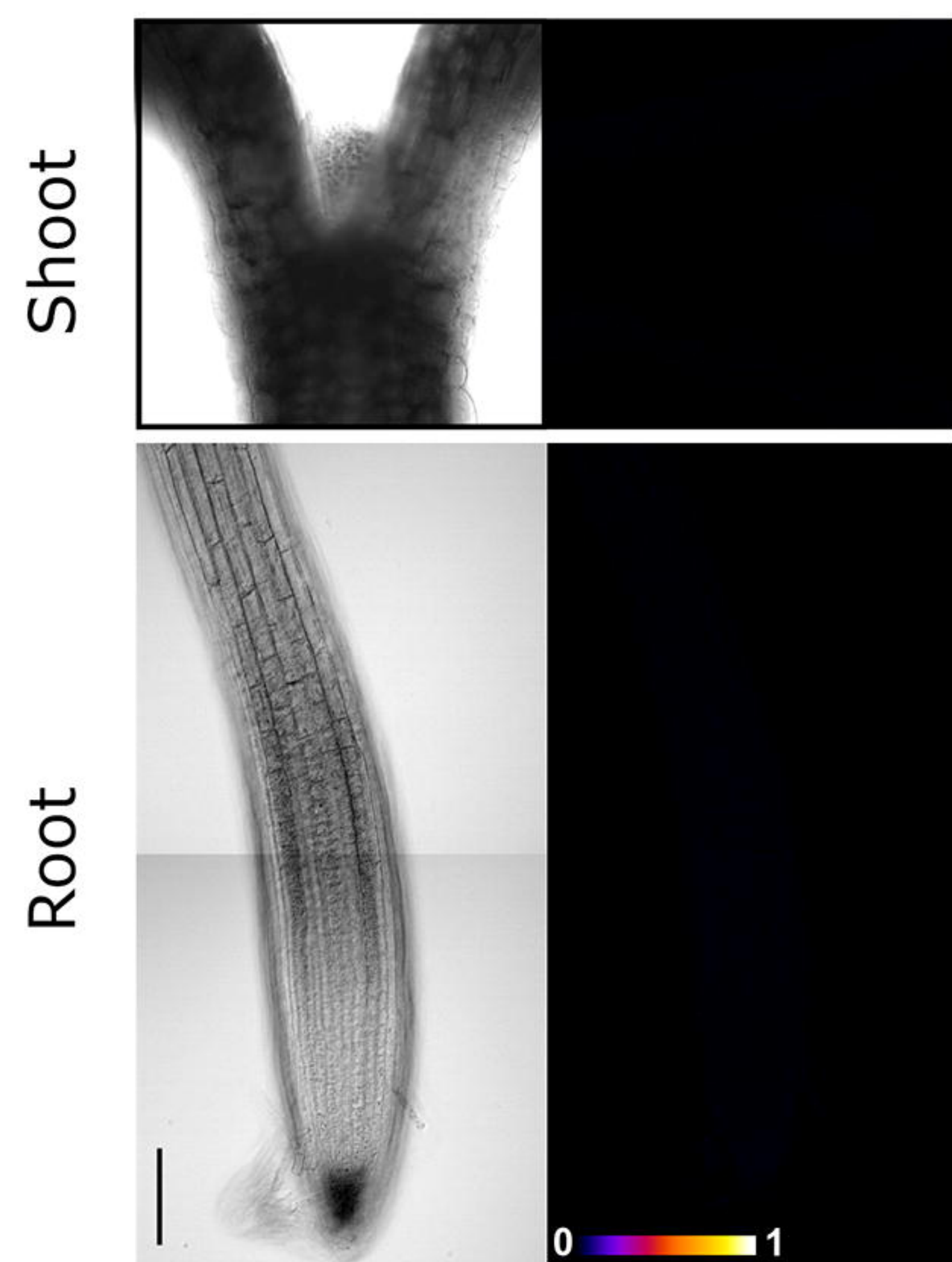
Model of root thermosensory response. Roots integrate regulatory signals coming from the shoot through the activity of phytochromes and HY5 with auxin signals mediated by biosynthetic genes (YUC) and signaling (TIR, AFB, TMK).

A**B****C****D****E****F**



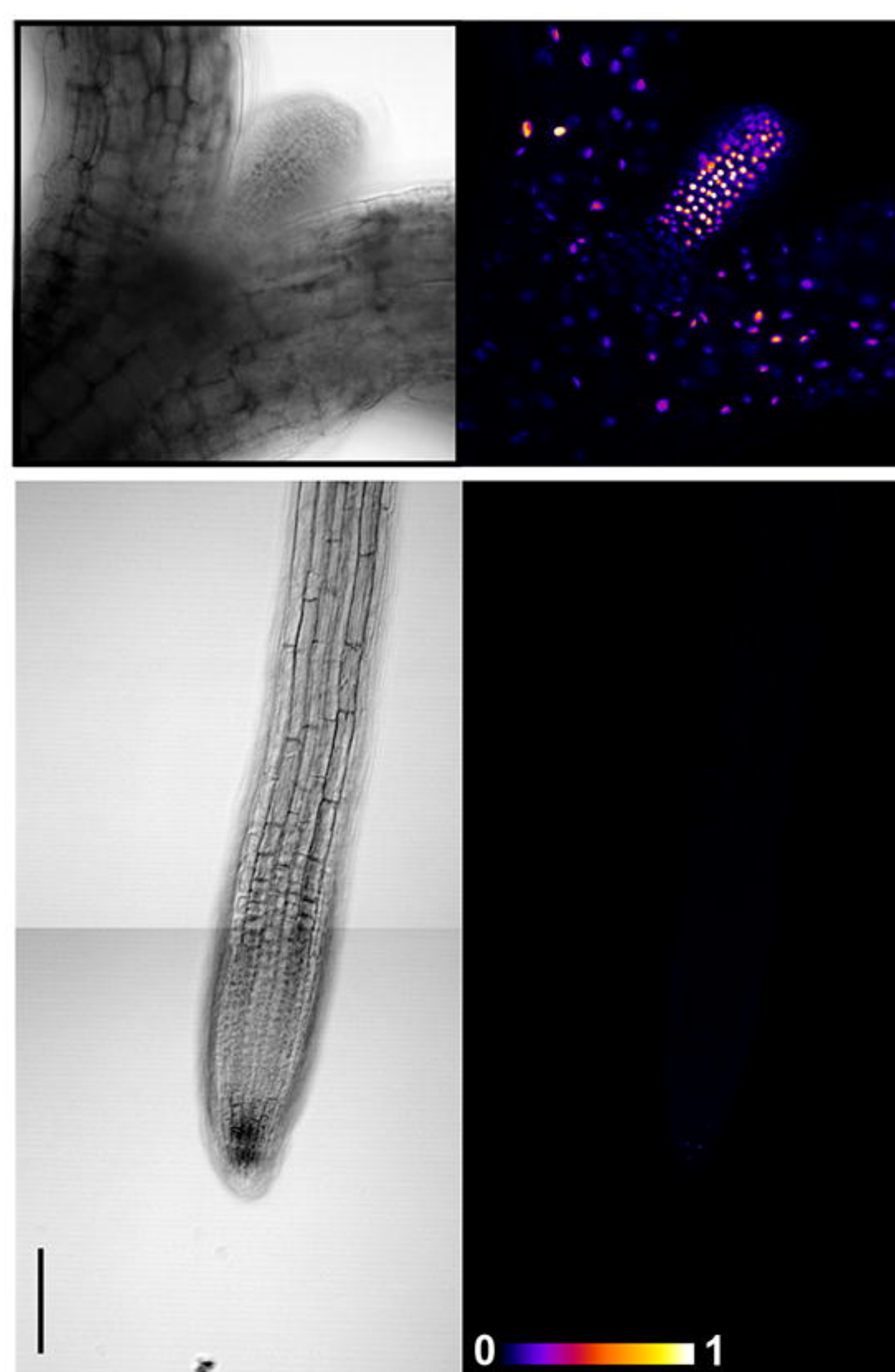


A

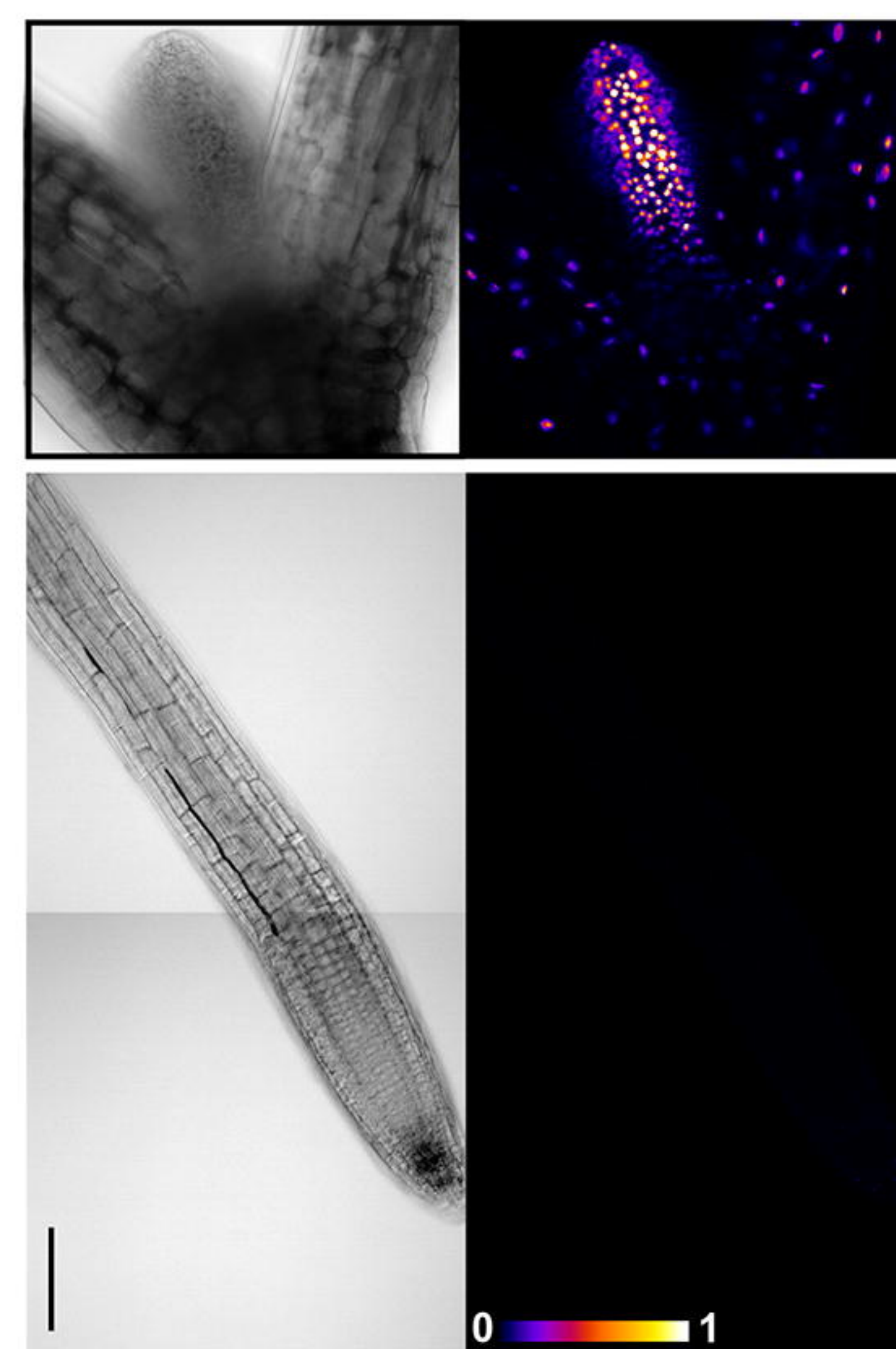


WT

B

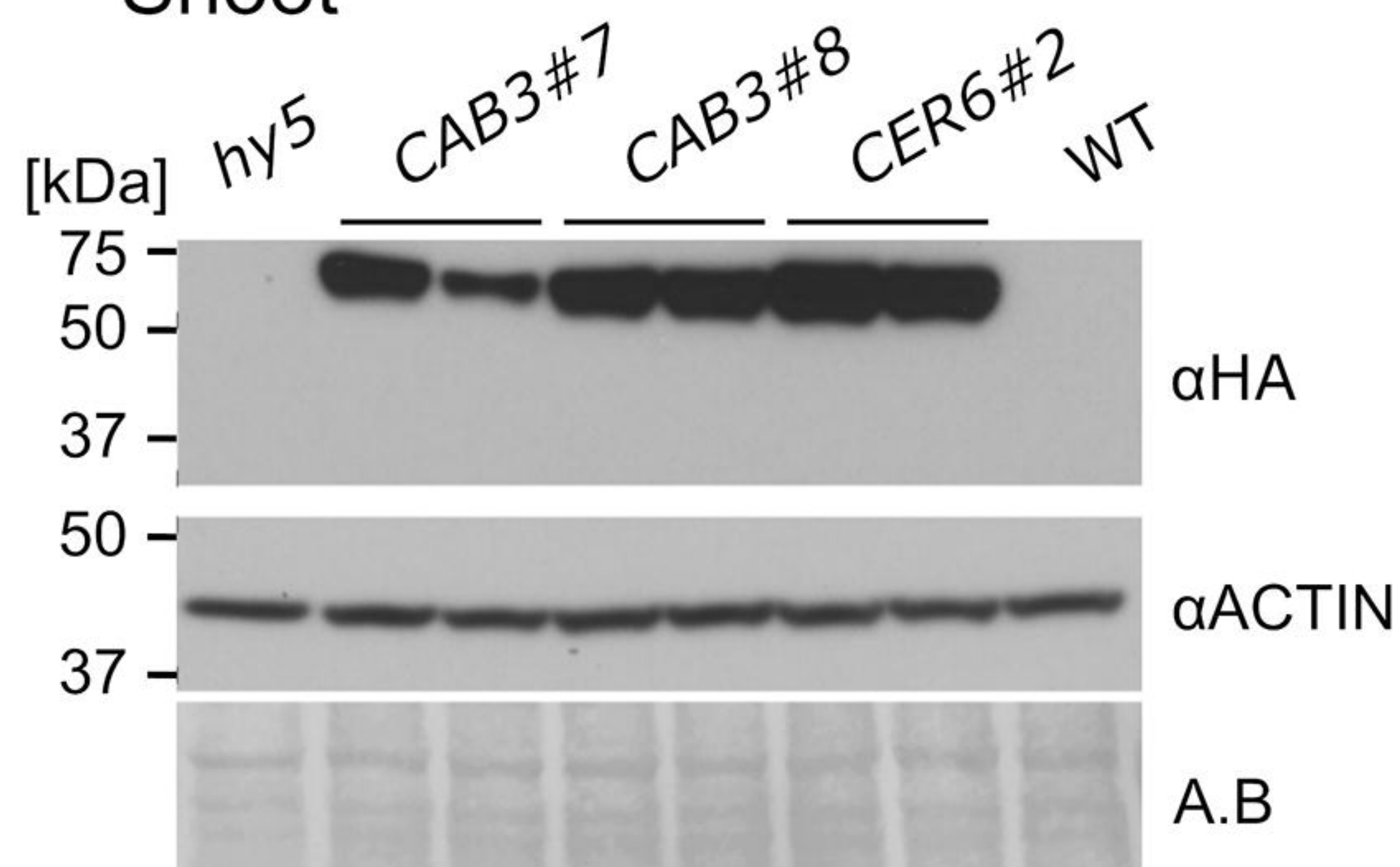
*pCAB3:DOF-HY5* in *hy5*
Line #7

C

*pCAB3:DOF-HY5* in *hy5*
Line #8

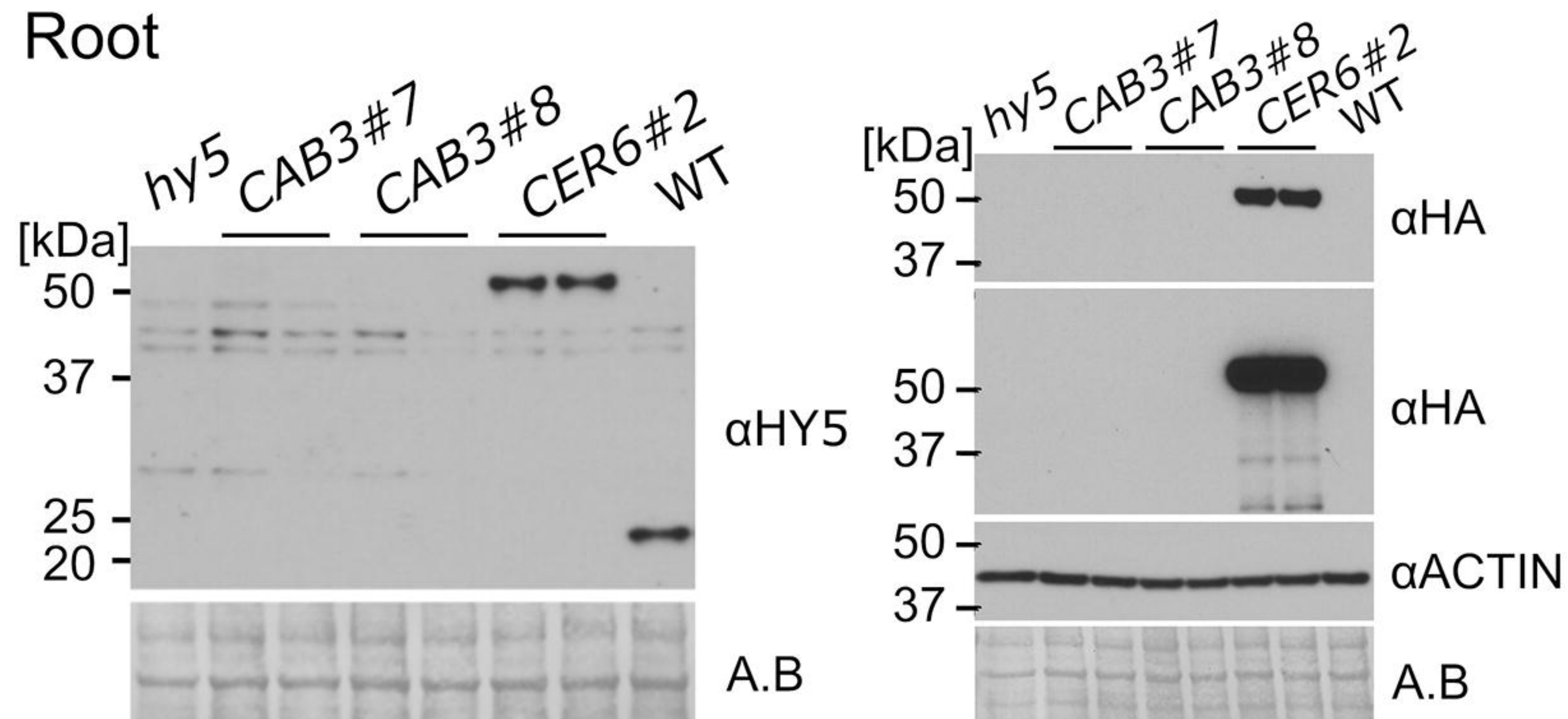
D

Shoot

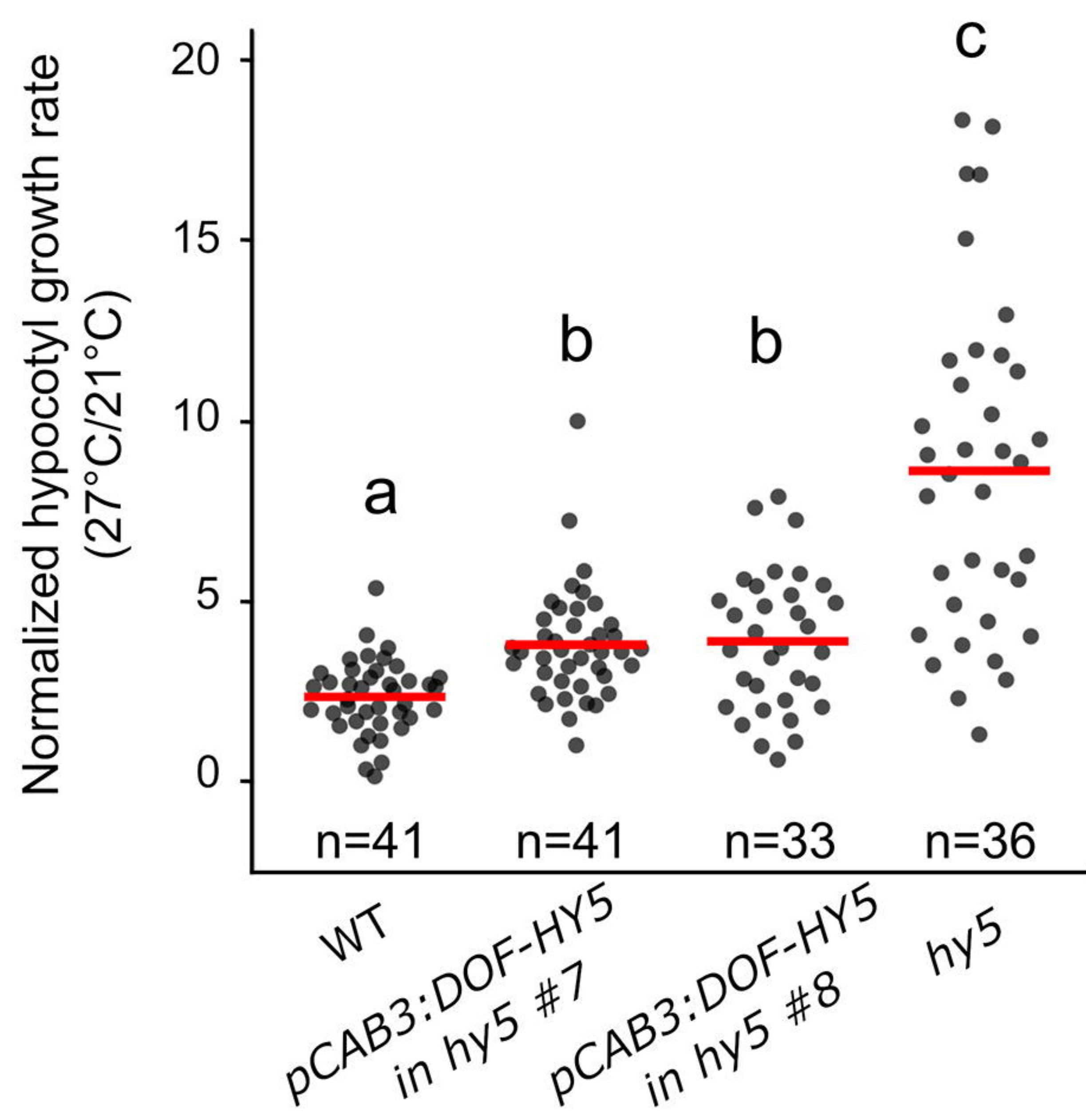


E

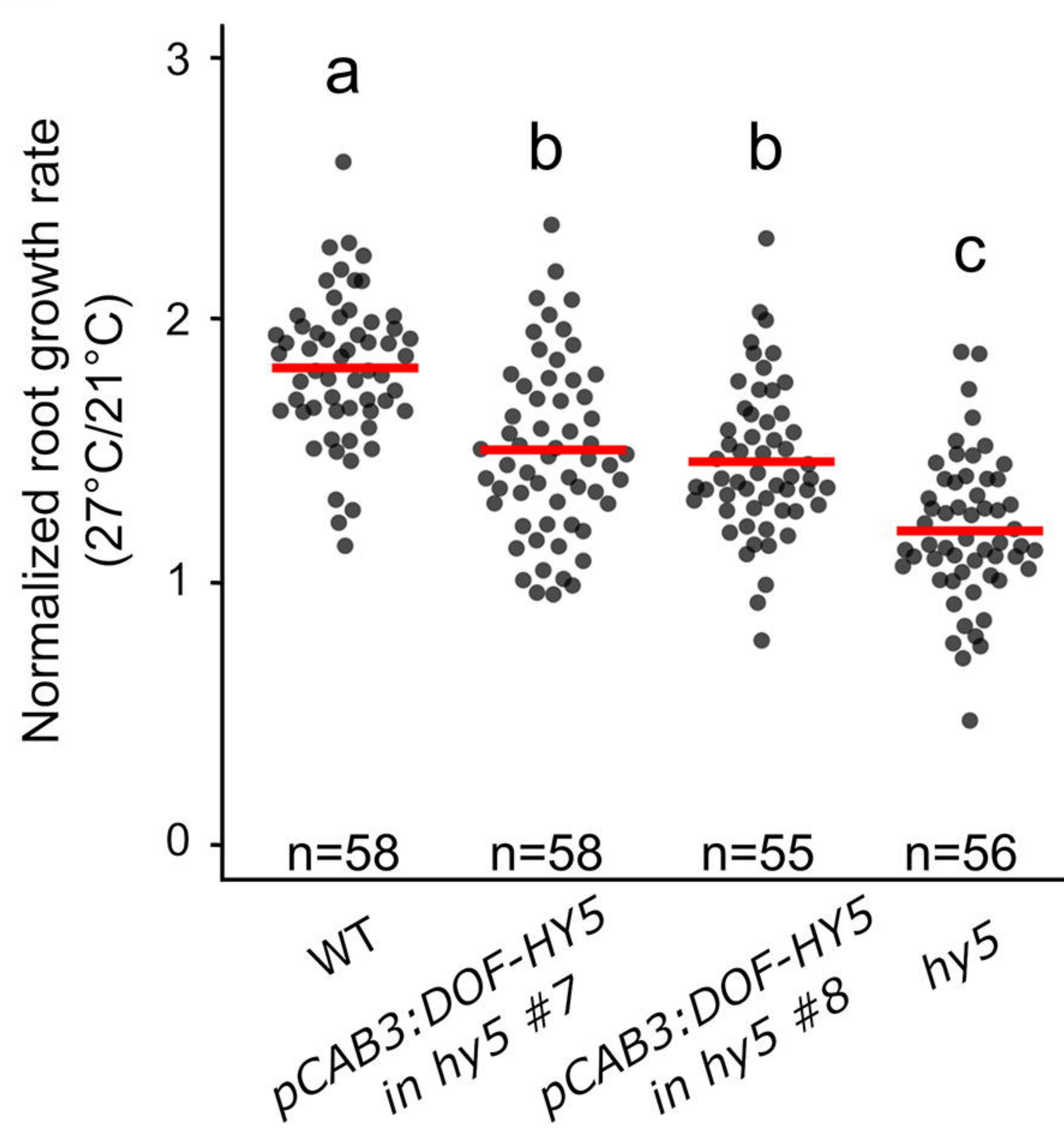
Root



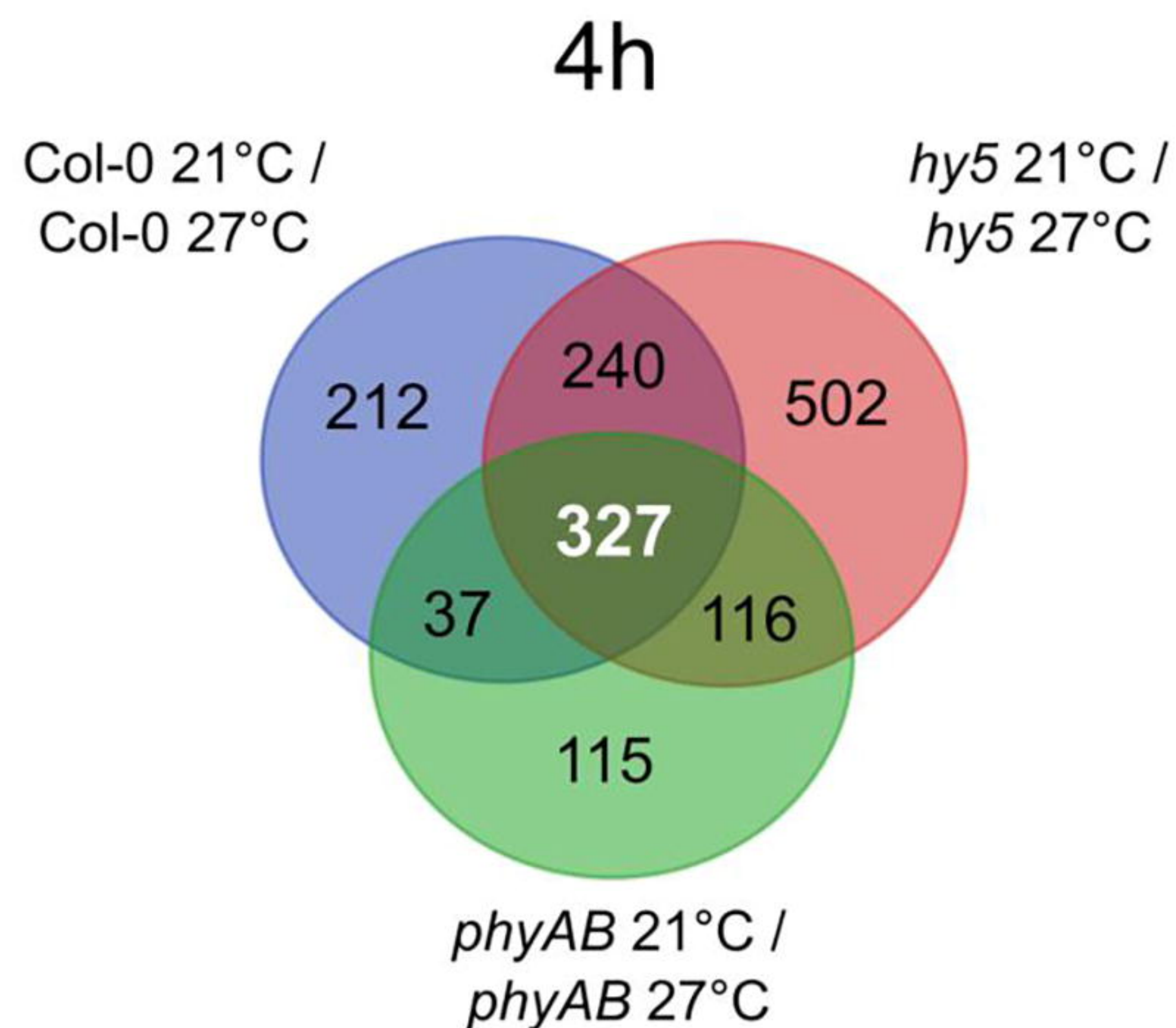
F



G

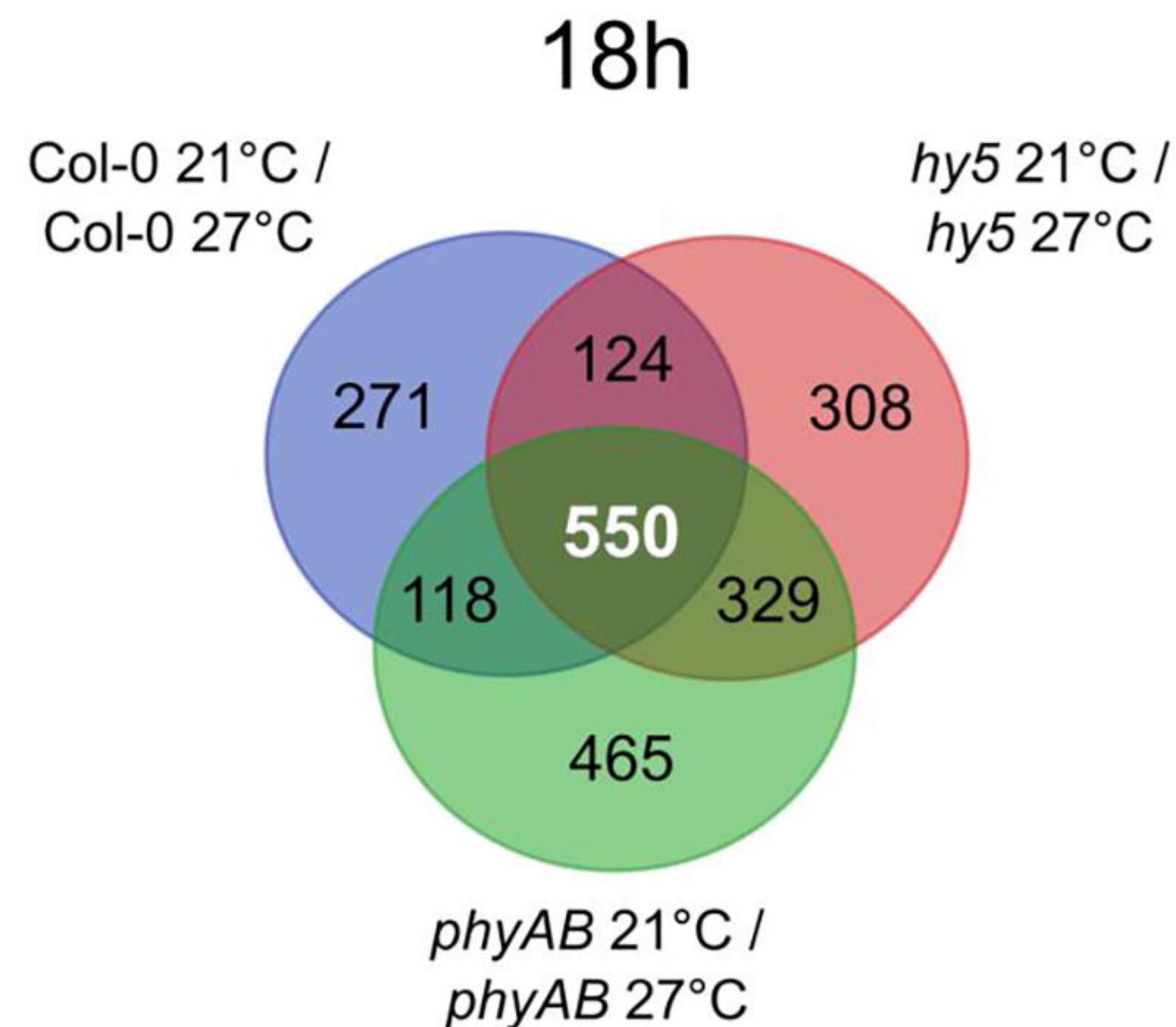


A



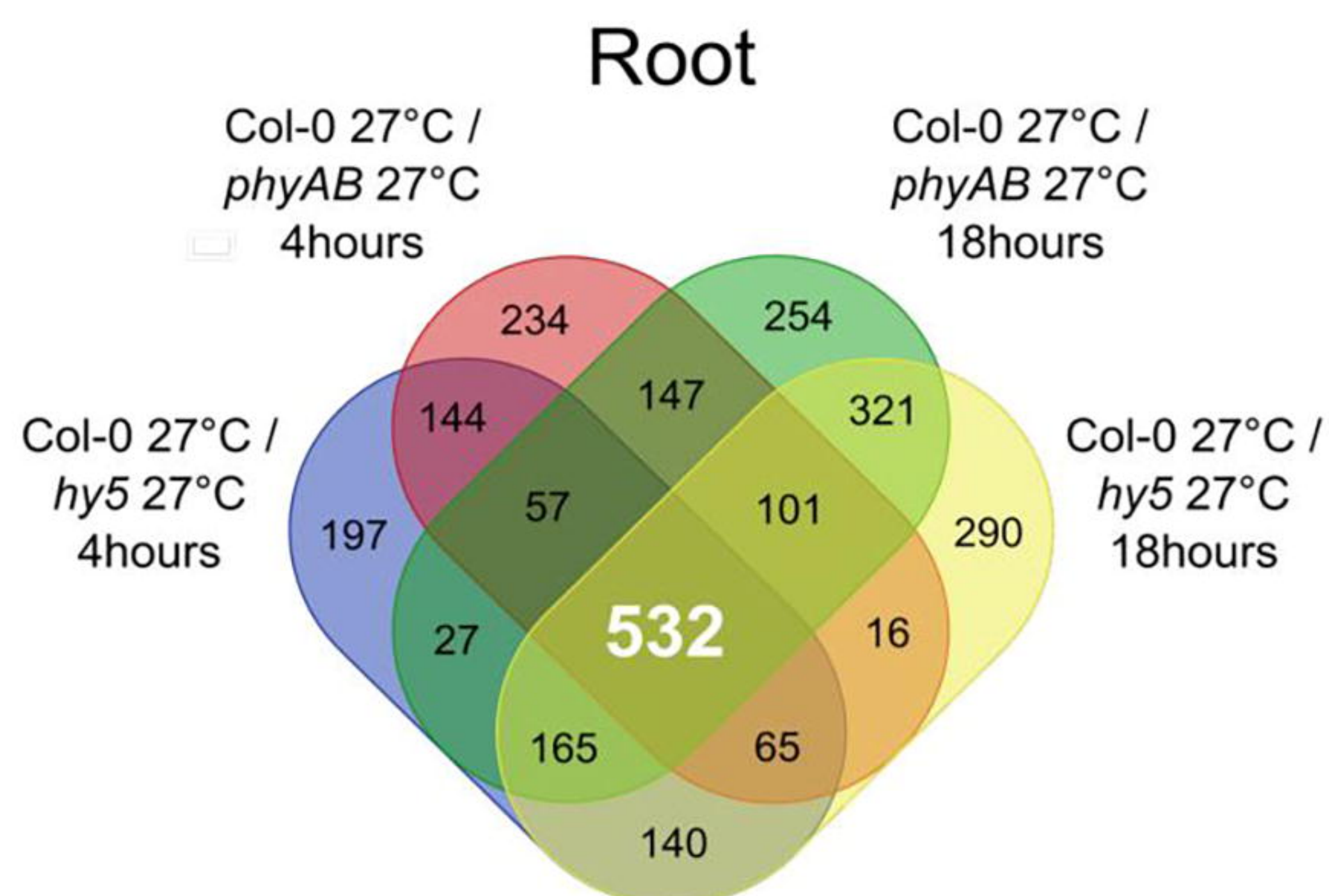
GO category	p-value
Response to heat	9.30e-18
Response to hydrogen peroxide	5.30e-15
Glucosinolate biosynthetic process	5.80e-14
Response to high light intensity	2.40e-11

B



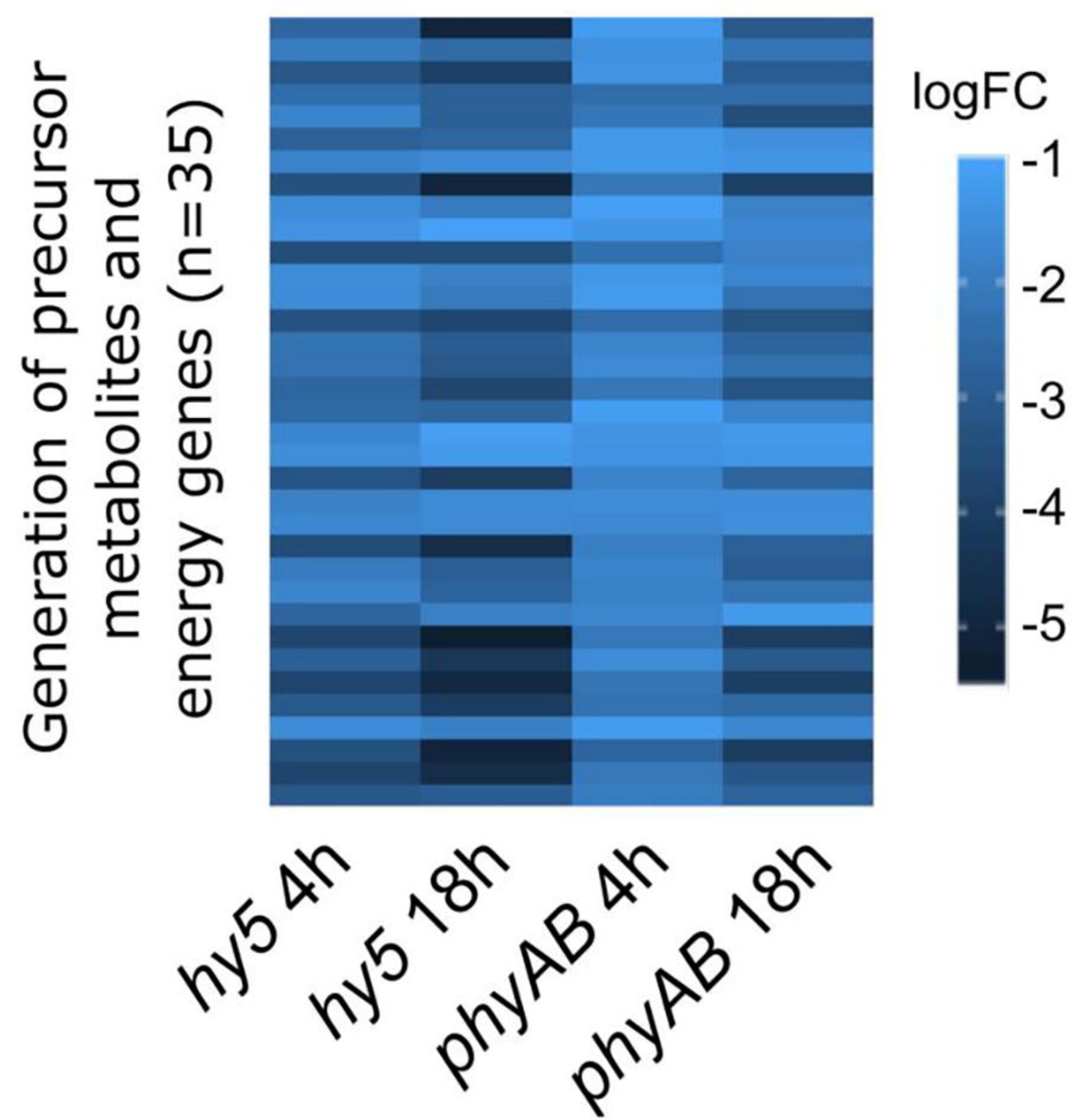
GO category	p-value
Oxidation-reduction process	1.3e-16
Secondary metabolite biosynthetic process	5.4e-16
Glucosinolate biosynthetic process	4.1e-10
Response to sucrose transport	5.60e-5

C

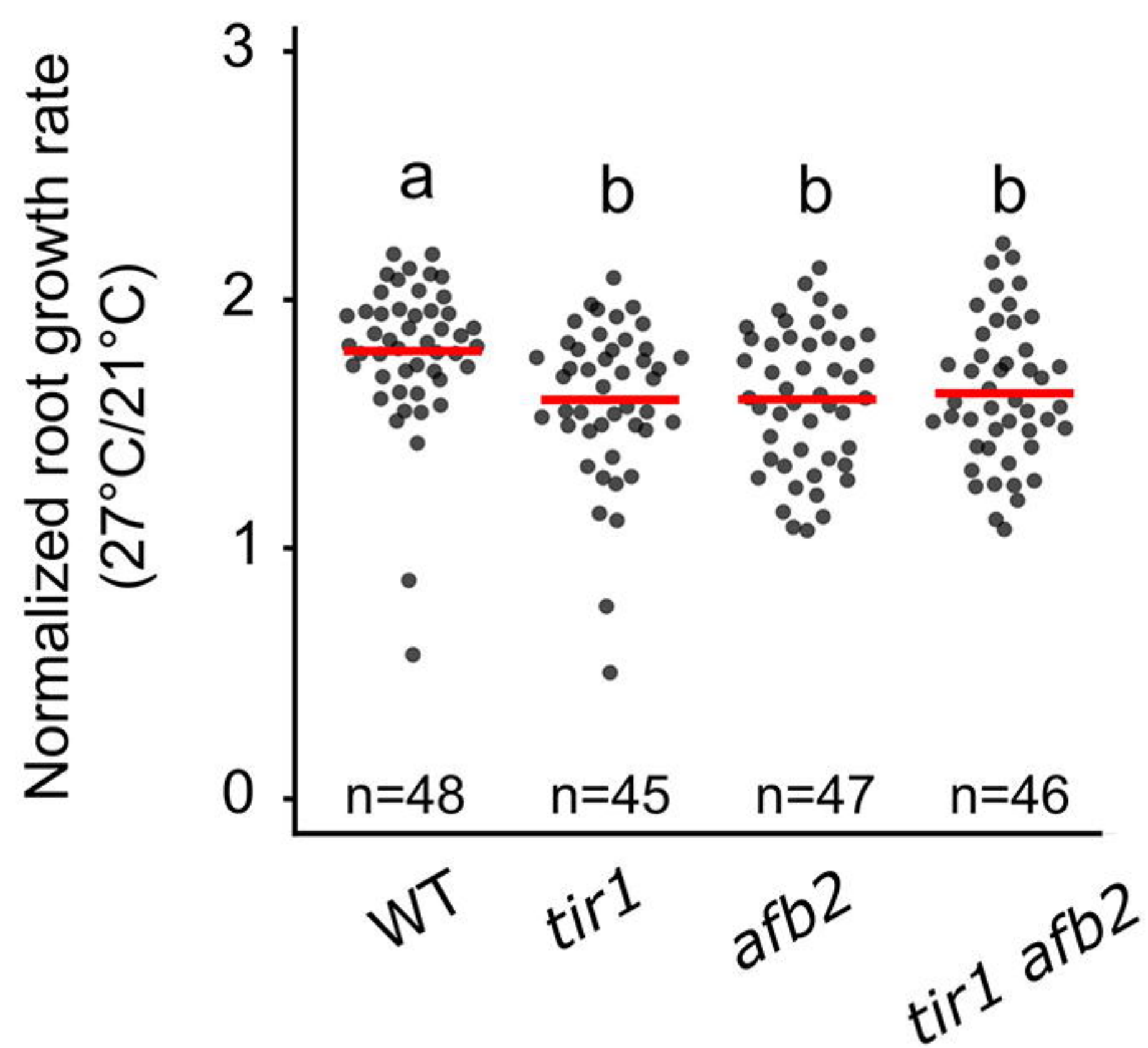


GO category	p-value
Photosynthesis	1.20e-34
Response to abiotic stimulus	1.90e-23
Generation of precursor metabolites and energy	2.60e-14

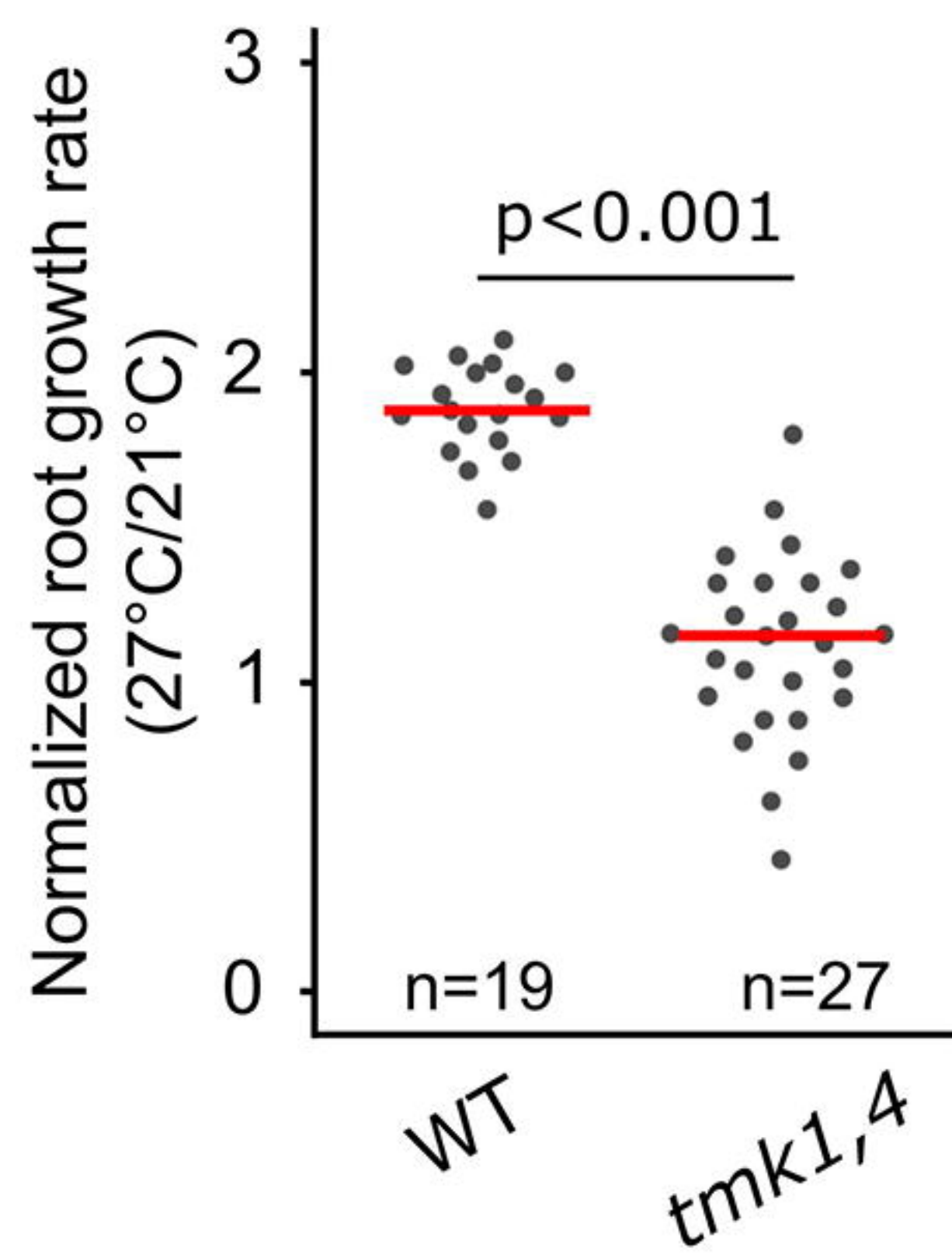
D



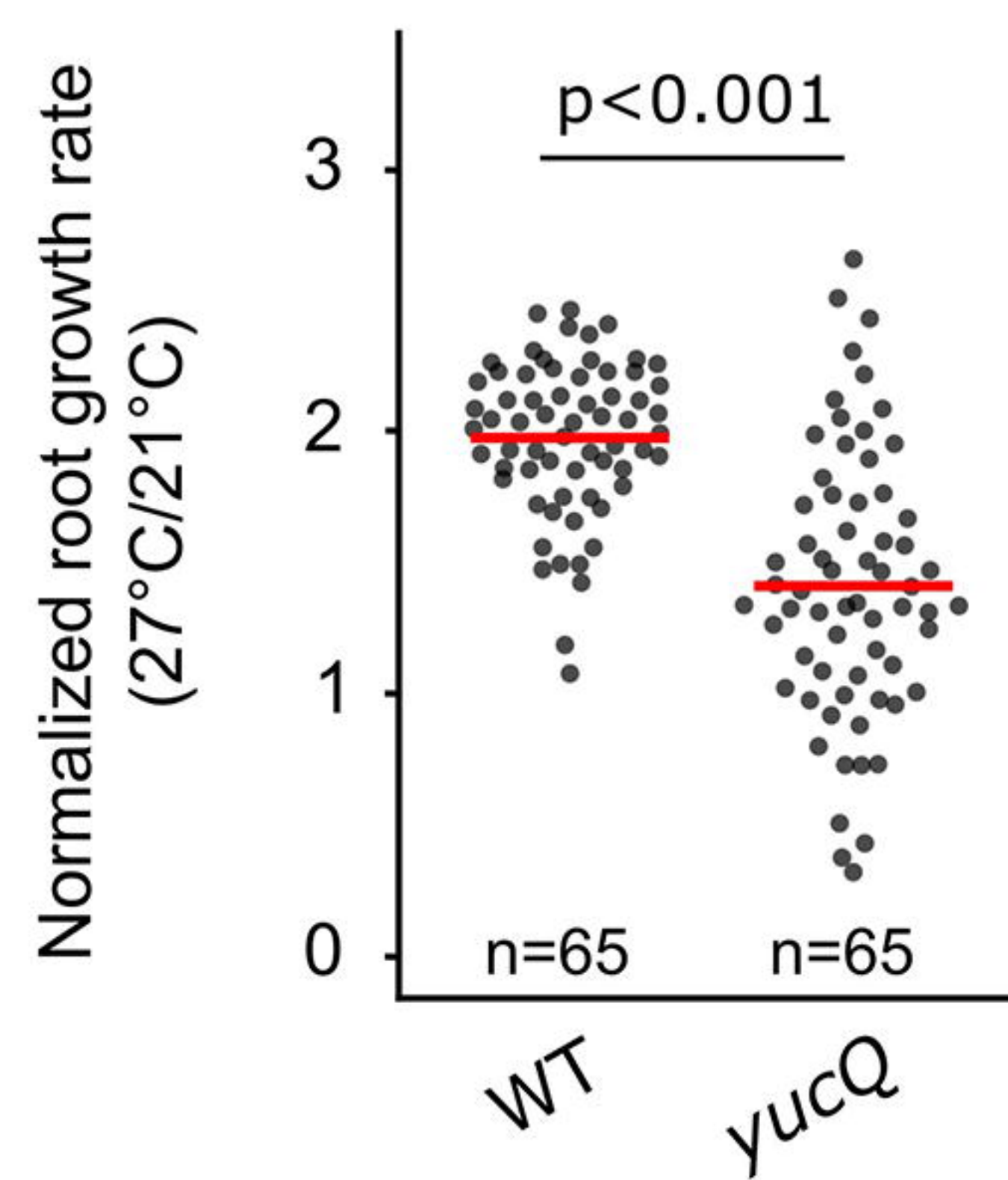
A



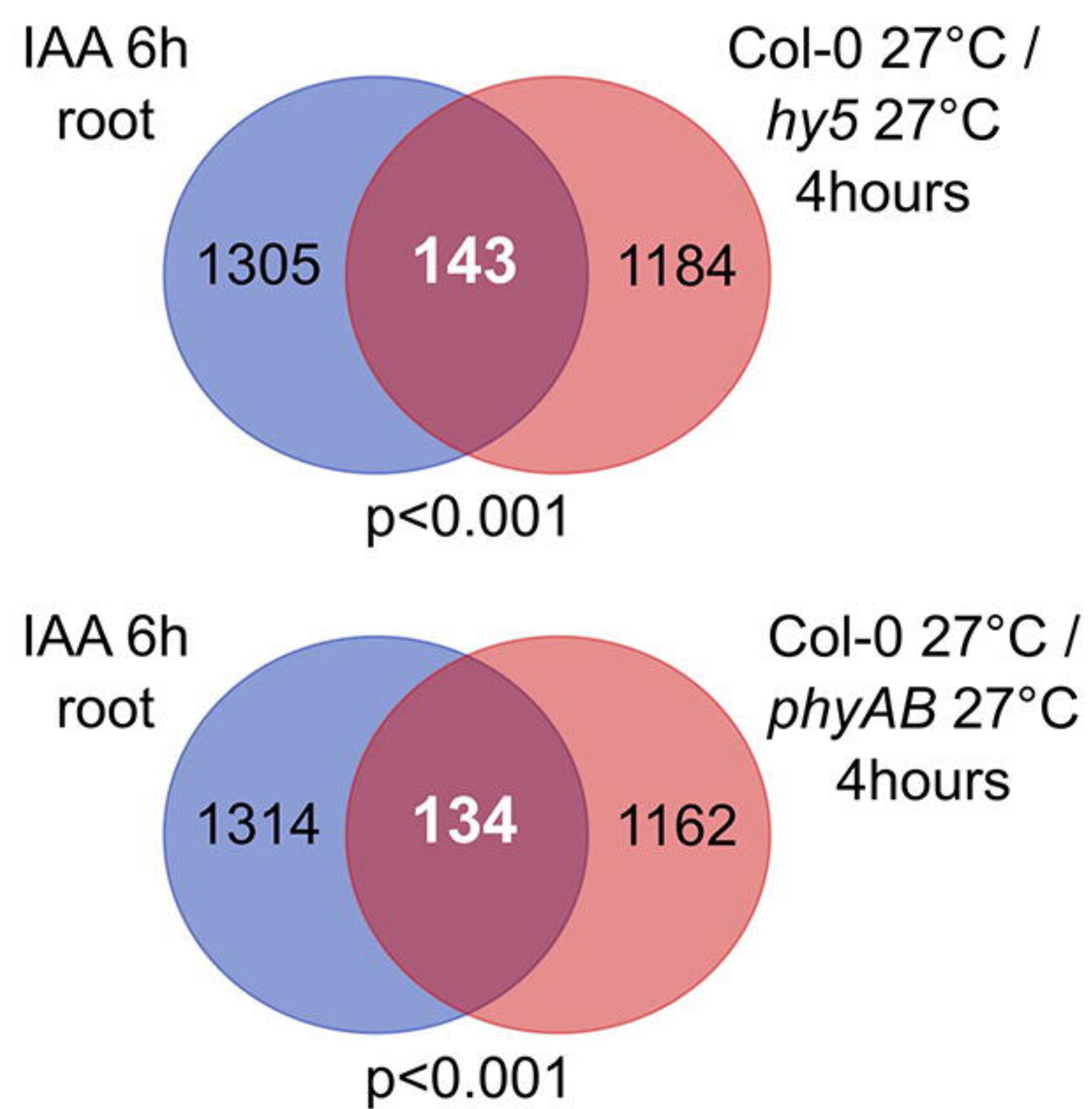
B



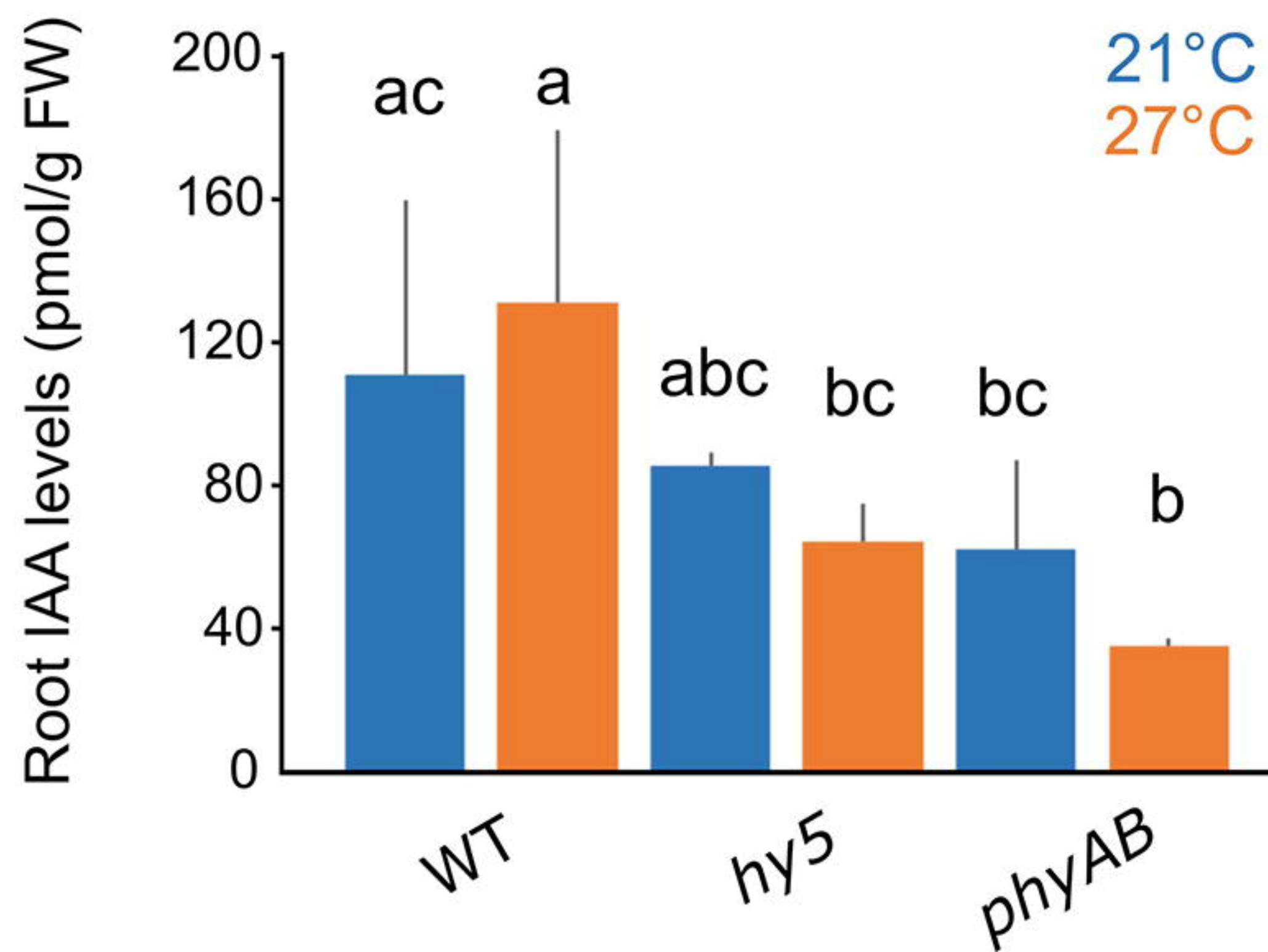
C



D



E



F

